DNA 4246F

TACTICAL IMPLICATIONS OF AIR BLAST VARIATIONS FROM NUCLEAR WEAPON TESTS

Science Applications, Inc.
8400 Westpark Drive
McLean, Virginia 22101

30 November 1976

Final Report for Period 15 April 1976—30 November 1976

CONTRACT No. DNA 001-76-C-0284

APPROVED FOR PUBLIC RELEASE;
DISTRIBUTION UNLIMITED.

THIS WORK SPONSORED BY THE DEFENSE NUCLEAR AGENCY
UNDER RDT&E RMSS CODE B323075462 L37DAXYX97102 H2590D.

Prepared for
Director
DEFENSE NUCLEAR AGENCY
Washington, D. C. 20305

UNCLASSIFIED

SECURITY CLASSIFICATION OF THIS PAGE (When Data Entered)

(19) **REPORT DOCUMENTATION PAGE**

READ INSTRUCTIONS BEFORE COMPLETING FORM

1. REPORT NUMBER: DNA 4246F AD-E300 069	2. GOVT ACCESSION NO. (18) DNA SBIE
	3. RECIPIENT'S CATALOG NUMBER
(6) 4. TITLE (and Subtitle): TACTICAL IMPLICATIONS OF AIR BLAST VARIATIONS FROM NUCLEAR WEAPON TESTS	(9) 5. TYPE OF REPORT & PERIOD COVERED: Final Report for Period 15 Apr [redacted] — 30 Nov 76
(14)	6. PERFORMING ORG. REPORT NUMBER: SAI-76-677-WA
(10) 7. AUTHOR(s): J. E. Cockayne, E. V. Lofgren	(15) 8. CONTRACT OR GRANT NUMBER(s): DNA 001-76-C-0284
9. PERFORMING ORGANIZATION NAME AND ADDRESS: Science Applications, Inc., 8400 Westpark Drive, McLean, Virginia 22101	(16) 10. PROGRAM ELEMENT, PROJECT, TASK AREA & WORK UNIT NUMBERS: NWET Subtask L37DAXYX971-02 (17) X99Y
11. CONTROLLING OFFICE NAME AND ADDRESS: Director, Defense Nuclear Agency, Washington, D.C. 20305 (12) 160 p. (11)	12. REPORT DATE: 30 Nov [redacted]76
	13. NUMBER OF PAGES: 166
14. MONITORING AGENCY NAME & ADDRESS (if different from Controlling Office)	15. SECURITY CLASS (of this report): UNCLASSIFIED
	15a. DECLASSIFICATION DOWNGRADING SCHEDULE

16. DISTRIBUTION STATEMENT (of this Report)

Approved for public release; distribution unlimited.

17. DISTRIBUTION STATEMENT (of the abstract entered in Block 20, if different from Report)

18. SUPPLEMENTARY NOTES

This work sponsored by the Defense Nuclear Agency under RDT&E RMSS Code B323075462 L37DAXYX97102 H2590D.

19. KEY WORDS (Continue on reverse side if necessary and identify by block number)

Blast	Uncertainty
Overpressure	Analysis of Variance
Dynamic Pressure	Error Factor
Lognormal	

20. ABSTRACT (Continue on reverse side if necessary and identify by block number)

The objective was to assess the rationale for additional nuclear tests which would produce a better predictive capability for tactical blast environments. The work described herein includes the following:

- Refinement and concise synopsis of the theoretical and empirical basis for the rationale assessment;

DD FORM 1 JAN 73 1473 EDITION OF 1 NOV 65 IS OBSOLETE

UNCLASSIFIED

SECURITY CLASSIFICATION OF THIS PAGE (When Data Entered)

408 404

20. ABSTRACT (Continued).

- Testing of the assumption of a lognormal distribution for the measurements which implies an uncertainty proportional to the measurements; this assumption simplifies the methodology, and
- An analysis of variance for some blast data to ascertain if systematic errors (biases) could exist which might require additional measurements of a weapon produced environment to resolve.

TABLE OF CONTENTS

LIST OF FIGURES

LIST OF FIGURES (cont.)

LIST OF FIGURES (cont.)

LIST OF FIGURES (cont.)

LIST OF FIGURES (cont.)

LIST OF TABLES

Section 1

INTRODUCTION

This report is the final documentation describing work completed under Contract DNA 001-76-C-0284. The objective of this analysis was to assess the rationale for additional underground tests (UGT) to produce an air blast environment. To accomolish this objective, measures relating to the tactical utility of achieving increased accuracy in predicting nuclear weapon produced environments were developed and applied to existing environments data (blast and radiation). This work was accomplished in two phases. The first phase resulted in development of the methodology to assess the rationale for additional tactical nuclear underground environments testing, and a preliminary application of this methodology to selected weapon produced environment data. The second phase was oriented toward strengthening and broadening the theoretical and empirical basis for the methodology, testing some of the assumptions upon which the initial applications were based, and additional applications of the methodology for a more complete assessment of the UGT rationale.

This report summarizes work performed in phase 1, and presents a detailed description of the analysis completed in phase 2. The work completed in phase 2 and described herein includes the following:

- Refinement and concise synopsis of the theoretical and empirical basis for the rationale assessment.
- Testing of the assumption of a lognormal distribution for the weapon produced environments, which is an issue in the application of the methodology.
- An analysis of the nuclear blast data to attempt to ascertain if systematic errors, or biases, could exist which would require additional measurements of weapon produced environment to resolve.
- An analysis of the peak dynamic pressure blast data to assess possible testing rationale based on this blast phenomenon.

In assessing the rationale for continued tactical nuclear underground environments testing, it is important to distinguish in the analysis between assuming that the weapon produced environment data are randomly distributed, and assessing the rationale based on that assumption and recognizing the possibility of the existence of systematic errors, or biases, in the environment test data that could have ramifications for the tactical utility of the weapons.

In an operational context, the effects of these two kinds of errors are quite different. If the probability of kill (P_k) is simplistically viewed as a specified weapon produced environment being produced at a given range 95 times out of 100, then this notion can be easily interpreted in terms of random shot-to-shot variation in the weapon produced environment. However, if a systematic error causes a bias between the predicted and true weapon produced environments, all operational shots could be systematically different from predictions. Thus, instead of a specified effect occurring at a calculated range 95 percent of the time, the effect could never occur at the predicted range in an operational environment if there was an unmodeled bias.

Alternatively, the choice of yields estimated to accomplish a specified objective could be systematically too large or too small because of such a bias. Thus, this assessmen proceeded along two parallel paths with regard to analysis of the nuclear blast data, namely:

- An assessment of the rationale for tactical nuclear underground effects testing based on the assumption that variations observed in the blast data are randomly distributed.
- A preliminary analysis of the existing blast data with the objective of attempting to identify possible biases (systematic errors).

The blast data variations would be classified as random if the statistical nature of variations observed in the blast test data were

assumed to be the same as the variations that one would observe during deployment of the weapons. On the other hand, biases between the statistical characteristics of the variations observed from the test data and during weapon employment would represent a case where the predictive models are either under-specified or mis-specified. Obviously, large biases could adversely impact the tactical utility of the weapons.

To strengthen the random error analysis, an assessment was made to ascertain if the assumption of a lognormal distribution for the weapon produced blast environment is a reasonable one. The random error methodology is based on this assumption. This approach involved an analysis of the relationship between the error in estimating the range to a specified nuclear produced environment, and the range for peak overpressure and overpressure impulse. An approximately linear relationship between the error in range and range would suggest that the assumption of lognormal distribution for the error is a reasonable one, since this is a characteristic of data that are lognormally distributed. This analysis and the results are described in Section 4.2.

Section 2

SUMMARY OF RESULTS AND CONCLUSIONS

The results of this uncertainty analysis indicate that the justification for improving the predictive capability of the nuclear produced blast environment is marginal provided the variations in the existing blast data from nuclear bursts are treated as random. The quantitative basis for this result is that the target vulnerability and weapon emplacement uncertainties essentially dominate the weapon produced environment uncertainty. (Conclusion 1)

On the other hand, it has been found that there are non-trivial systematic errors (biases) in some blast data which could be included in the predictive models of the blast environment if the causal physics of these biases were better understood. The impact on this uncertainty of one or more additional nuclear tests has not been quantitatively evaluated because this result came from a secondary task.

The general methodology, developed in Section 3 for this random uncertainty analysis, is based on the assumption that the randomness in the nuclear produced environment which would be experienced during employment of the tactical nuclear weapons is statistically the same as the deviations observed among past weapons tests. The methodology relates the magnitude of this environmental uncertainty (potentially reducible through additional underground testing of nuclearly produced environments) to a measure of the tactical utility of the weapon (i.e., yield change). Thus the direct payoff from continued underground detonations of tactical nuclear weapons in order to more accurately predict the environment, is related to the tactical utility gained from this improvement.

To obtain closed-form expressions for the relationships between the measure (yield) and the environment predictive capability, it was assumed that the uncertainty in the nuclear produced environment was

proportional to the measurements which are then implied to be distributed lognormally. This hypothesis was tested in Section 4.2, and the characteristics of the uncertainty in the blast data were found to support the assumption of lognormality. (Conclusion 2)

Using the above mentioned methodology (which assumes that there are no biases between the weapon produced environments observed during testing and during employment of the weapons), the maximum possible reduction in yield (average is also available in Section 4.1) is:

- Peak Overpressure: 21 percent
- Peak Dynamic Pressure: 9 percent
- Overpressure Impulse: 15 percent

It is concluded that only a tenuous rationale exists for underground testing of tactical nuclear environments, based on the assumptions upon which the rationale was assessed (no biases). The dynamic pressure impulse data are probably too sparse and too uncertain to be statistically analyzed. Therefore, in cases where the dynamic pressure impulse totally dominates the target damage mechanisms, there is a rationale for additional underground testing of tactical nuclear environments.

The analysis in Section 5 for the existence of systematic errors (biases) was conducted for scaled ranges to 10, 30 and 100 psi peak overpressure data from tests between 0 and 11 $ft/kt^{1/3}$ scaled height of burst (SHOB). Such biases, if found, would represent blast predictive modeling under-specification or mis-specification, and would require an attempt to adjust or improve the predictive models to remove the bias. Since part of the objective of this bias analysis was to assess the degree to which the Johnie Boy (negative SHOB) test results differ from surface test results, the analysis was limited to surface and very low SHOB tests.

The conclusion from this limited bias analysis is that, for scaled range to 100 psi and 30 psi peak overpressure, there are statistically significant deviations from the $W^{1/3}$ scaling law over the yield range between 15 t and 15 Mt, a factor of one million. More precisely, the low yield data shows a deviation from cube-root scaling of high-yield data due most likely to a mass-to-yield effect. This range bias is relatively small but not insignificant when translated into a potential yield mis-specification. For instance, if the medium and high yield data were used to estimate scaled range to 30 psi for small yield weapons (or vice versa), a yield under-estimate (or over-estimate) of approximately 25 percent would occur. (Conclusion 3)

This yield under-estimation for sub-kiloton weapons is more severe when using the expression from DASA 2506 (Reference 2). Even though the author of the report did not provide an explicit caveat against sub-kiloton application, we believe one is implied. Nevertheless, the empirical equation of that report is more widely available than the graphical results in appropriate classified reports and thus frequently used. For range to 30 psi peak overpressure, the calculated range is 15 percent too large so the yield would be a factor of 1.5 too small. Modifying the analytical expression to use only 1.65 versus a 2.0 multiplier for surface reflection enhancement, the calculated range is 7.5 percent too large for a yield factor of approximately 1.25 too small.

Another conclusion is that, for scaled range to 10 psi peak overpressure, there are statistically significant differences among the BRL, NOL and SC/SRI instrumentation types. For the two higher pressures, instrumentation type and the interaction between yield and instrumentation type were not significant contributors to the total variance of the data. (Conclusion 4)

The bias analysis of near-ideal waveform (type V) versus precursor-associated waveform types for 30 psi peak overpressure from surface bursts did not produce a statistically significant result. Recognizing the subjective nature of the waveform parameter, this conclusion is also considered more subjective than objective despite its interesting implications.

Section 3

RANDOM ERROR METHODOLOGY

This section describes the methodology developed to assess a rationale for underground environment testing of tactical nuclear weapons, based on the assumption that variations observed during testing are statistically the same as variations that would be experienced during deployment of the weapons.

The measure developed in Section 3.1 and applied in later sections to assess the requirements for underground testing of tactical nuclear weapons, is the ratio of the yield required to achieve a specified probability of kill against a particular target assuming an improved predictive capability, to the yield required to achieve the same probability of kill with the present predictive capability. This measure is developed for both air blast and nuclear radiation effects on a point target existing alone or in a cluster constituting a distributed target. The approach taken throughout attempts to obtain closed-form expressions for the measure when that is possible; this necessitated making assumptions about the distributions of weapon produced environments and target vulnerability. These assumptions were made on the basis of reasonableness: work has been completed to ascertain the validity of the assumption concerning the distribution of the weapon produced blast environment, and is reported in Section 4.2. The development can, of course, be generalized to include any assumptions about these distributions, but numerical solutions rather than closed-form solutions might be required or convenient.

Section 3.2 describes the relationship between the yield ratio measure and the tactical utility associated with increased knowledge of the nuclear produced environment.

3.1 METHODOLOGY DEVELOPMENT

This section builds the theoretical framework for assessing a rationale for underground testing of tactical nuclear weapons based on the assumption that the weapon produced environment variabilities observed during testing are random and will be statistically the same as the variabilities observed during weapon employment. In particular, expressions are derived for yield changes to ensure a given damage level that would result from changes in the predictive capability for weapon produced environments.

To facilitate the development of the expressions for yield ratio, a damage function is derived which is based on the distributions for the weapon created environment and the target vulnerability. This function is written for convenience in terms of a median weapon radius, defined as the range at which the median weapon produced environment equals the median target vulnerability. The median weapon radius thus becomes a parameter of the expressions to be developed for the yield ratio. The damage function is generalized to include the effects of the weapon CEP, and the median weapon radius is expressed as a function of all sources of uncertainty (i.e., the uncertainty in the weapon produced environment, the uncertainty in the target vulnerability, and the weapon CEP) the offset distance, and the kill probability. The requisite ratio of yields is then expressed as the ratio of the above functions with a specified kill probability ($P_k = 0.9$), where the numerator contains the required uncertainty in the weapon produced environment and the denominator contains the existing uncertainty in the weapon produced environment. This is the measure used to assess the effects of hypothesized changes in the uncertainty of weapon produced environments on the yield estimated to achieve a given kill probability. Each of the following subsections treats some pertinent aspect of the above development.

3.1.1 Derivation of the Damage Function

The damage function relates the probability of damage at a given range to the distribution of the weapon produced environment, and the distribution of target vulnerability. For the purposes of this development, lognormal distributions were assumed for both the weapon produced environment and the target vulnerability. In the case of target vulnerability, Reference 1 indicates that for blast damage the response of the target is lognormal. These data are based on both weapons tests and response tests in controlled environments. The blast response data have been collated and reviewed by the Defense Intelligence Agency and are the basis of the so-called "VN" (Vulnerability Number) system (Ref. 1). The radiation produced effects of interest are prompt effects; the information used in this analysis comes from the primate studies reported by the Armed Forces Radiobiology Research Institute (AFRRI) (Reference 3).

In the case of the weapon produced environments, no existing source of information is known to the authors concerning analysis to indicate the exact distribution of environments. However, a lognormal assumption is not unreasonable. This hypothesis is addressed in Section 4.2. Although the specific closed-form derivations presented herein depend upon assumptions about distributions, the general approach is not, and could be worked out numerically with any choice of distribution.

To derive an expression for the damage function, let I represent the random variable for the nuclear created environment and V represent the random variable for the target vulnerability, expressed in the same units as I. The random variable I is a function of ground range R from the point of detonation, and both the measure of centrality of I (e.g., mean or median) and the variation of I (e.g., variance) could change with R. Target damage occurs when I is greater than V

(i.e., when the weapon produced environment is greater than the target vulnerability). Defining a new random variable Z:

$$Z = I/V \quad , \tag{3.1-1}$$

The probability of target damage at some arbitrary range R is:

$$P(R) = \int_1^\infty f\,(Z|_R)\, dZ \tag{3.1-2}$$

where:

$P(R)$ = damage probability

$f\,(Z|_R)$ = the probability density function of Z at the range R.

The integration of $f(Z_R)$ is over the range where I is greater than V, yielding the probability of target damage. If I and V are lognormally distributed (with medians I_o and V_o, and variances s_i^2 and s_v^2), then Z is lognormally distributed with median $Z_o = I_o/V_o$ and variance $s_z^2 = s_i^2 + s_v^2$. Thus, in terms of normal deviates the probability of damage at range R is the result of integrating Equation 3.1-2.

$$\begin{aligned} P(R) &= 1 - F\left[\frac{\ln(1/Z_o)}{s_z}\right] \\ &= F\left[\frac{\ln(Z_o)}{s_z}\right] \\ &= F\left[\frac{\ln I_o(R\ \ V_o)}{s_z}\right] \end{aligned} \tag{3.1-3}$$

A convenient parameter, useful in the derivation of the expression for the yield ratio measures, is the median weapon radius, R_o, defined as that range where:

$$I_o\,(R_o) = V_o \quad , \tag{3.1-4}$$

i.e., where the median weapon produced environment equals the median target vulnerability.

The next two subsections derive explicit expressions for the damage function for blast and radiation targets.

3.1.2 Blast Damage Function

For the case of blast environments (peak overpressure, overpressure impulse, peak dynamic pressure), the median intensity of the weapon produced environment can be assumed to follow an approximate power law,

$$I_o(R) = I_o(R_o)\,(R/R_o)^{-k} \quad , \tag{3.1-5}$$

for ranges close to R_o. Thus, it is assumed that $I_o(R)$ can be adequately represented by piecewise power laws, where the exponent k could be different for each section. Using Equation 3.1-4, Equation 3.1-5 becomes:

$$I_o(R) = V_o\,(R/R_o)^{-k} = V_o\,(R_o/R)^k. \tag{3.1-6}$$

The damage function for blast targets, becomes, on substituting Equation 3.1-6 into Equation 3.1-3:

$$P(R) = F\left[\frac{k \ln (V_o(R_o/R)/V_o)}{s_z}\right]$$

$$= F\left[\frac{\ln(R_o/R)}{s_z/k}\right]$$

$$= F\left[\frac{\ln(R_o/R)}{\Sigma}\right] \tag{3.1-7}$$

where: $\Sigma = s_z/k$, the standard deviation of a lognormal distribution

R_o = the median of a lognormal distribution.

Thus the damage function in range for blast targets is a lognormal distribution with variance Σ and median R_o.

3.1.3 Radiation Damage Function

For the case of the nuclear radiation environment, the dose at range, including exponential attenuation in air, can be written:

$$I_0(R) = I_0(R_0)\exp[-a(R-R_0) - 2\ln(R/R_0)] \qquad (3.1\text{-}8)$$

where a is a range-dependent inverse absorption length. Equation 3.1-8 is valid for intervals around the median range, R_0, for a given value of a. By Equation 3.1-4, this equation becomes:

$$I_0(R) = V_0 \exp[a(R_0-R) - 2\ln(R/R_0)] \qquad (3.1\text{-}9)$$

Using Equation 3.1-9, the damage function, Equation 3.1-3, becomes:

$$P(R) = F\left[\frac{\ln(V_0\exp[a(R_0-R) - 2\ln(R/R_0)]/V_0)}{s_z}\right]$$

$$= F\left[\frac{R_0 - R - (2/a)\ln(R/R_0)}{s_z/a}\right]$$

$$= F\left[\frac{R_0 - R - (2/a)\ln(R/R_0)}{\Sigma}\right] \qquad (3.1\text{-}10)$$

where: $\Sigma = s_z/a$; the standard deviation of a lognormal distribution

R_0 = the median of a lognormal deviation

A good approximation to Equation 3.1-8 for the dose at ranges somewhat larger than the median range (e.g., distances on the order of 1 Km for many tactical weapons) is obtained by neglecting the R-squared decrease:

$$I_0(R) = I_0 \exp(-aR) \qquad (3.1\text{-}11)$$

This regime is of significant interest for the tactical nuclear case. The radiation damage function assuming Equation 3.1-11 is derived analogously to the above, and the result is:

$$P(R) = F\left[\frac{R_0-R}{\Sigma}\right] \qquad (3.1\text{-}12)$$

where Σ is as previously defined for Equation 3.1-10; Equation 3.1-12 cannot be used near the weapon detonation point since P(R=o) is less than one for all R_o.

3.1.4 Derivation of Damage Probability

The damage function for point targets can be generalized to a probability of damage if offset targeting and the effects of weapon CEP are included. The case presented here assumes a circular bivariate normal distribution for weapon targeting error (containing both target acquisition uncertainties and weapon impact uncertainties due to guidance, survey, etc.).

The damage probability for a given CEP, where the CEP defines a standard deviation for the bivariate normal probability density function (pdf), where the aimpoint is offset a distance d from the target is:

$$P_k = \frac{1}{2\pi\sigma^2} \int \exp[-(\bar{R}-d)^2/2\sigma^2] \; P(R)dA \qquad (3.1\text{-}13)$$

where:

$\bar{R}$ = range; burst to target

P(R)= damage function

σ^2 = variance of the targeting pdf; by definition of the CEP this variance is:

$\sigma = CEP/\sqrt{2\ln(2)} = 0.8493\ CEP$

dA implies the integration is over area (centered at the point of weapon impact).

Appendix A presents the rather complex integration of this function. The results indicate that, for offset distance $d \geq \pi(CEP)$

$$P_k = P(d) \qquad (3.1\text{-}14)$$

is an adequate approximation for the damage probability. Thus, for offset distances greater than approximately three times the CEP, and for P_k between .05 and .95, evaluation of the damage function at the

offset distance is a valid approximation to P_k. For offset distances $d \leq \pi$ CEP, Figure 3-1 shows scaled median radius versus Σ (or versus damage sigma, σ_d) for a given offset, for $P_k = 0.9$. In functional notation, then, the scaled median radius can be expressed as:

$$R_o/CEP = g\ (\Sigma,\ d/CEP,\ P_k) \qquad (3.1\text{-}15)$$

For $P_k = .9$, this function can be written as:

$$g\ (\Sigma,\ d/CEP,\ .9) = g\ (o,\ d/CEP,\ .9)\exp(\Sigma^2)\ (1\text{-}G(\Sigma)) \qquad (3.1\text{-}16)$$

where $G(\Sigma)$ is small compared to one. Thus, an approximation to the curves of Figure 3-1 is:

$$R_o\ (\Sigma) \cong R_o(o)\exp(\Sigma^2) \qquad (3.1\text{-}16a)$$

or $$R_o\ (\Sigma) \cong R_o(o)/(1\text{-}\sigma_d^2)\ , \qquad (3.1\text{-}16b)$$

where σ_d is the so-called damage sigma of the VN system (Reference 1) and is related to Σ by the expression:

$$\sigma_d^2 = 1\text{-}e^{-\Sigma^2}$$

The next subsections utilize the above derived results to obtain measures in the form of yield ratios that would indicate a requirement for underground testing of tactical nuclear weapons for those cases where large yield adjustments could be possible.

3.1.5 Yield Ratio Measure

The measure to be utilized to determine a rationale for underground testing of tactical nuclear weapons is the potential percent change in yield by which one would predict a given probability of target damage or a given level of collateral damage, if the weapon produced environment were better known. An alternative statement of the measure is that it is a measure of the compensation in yield required because the weapon produced environment is not as well known

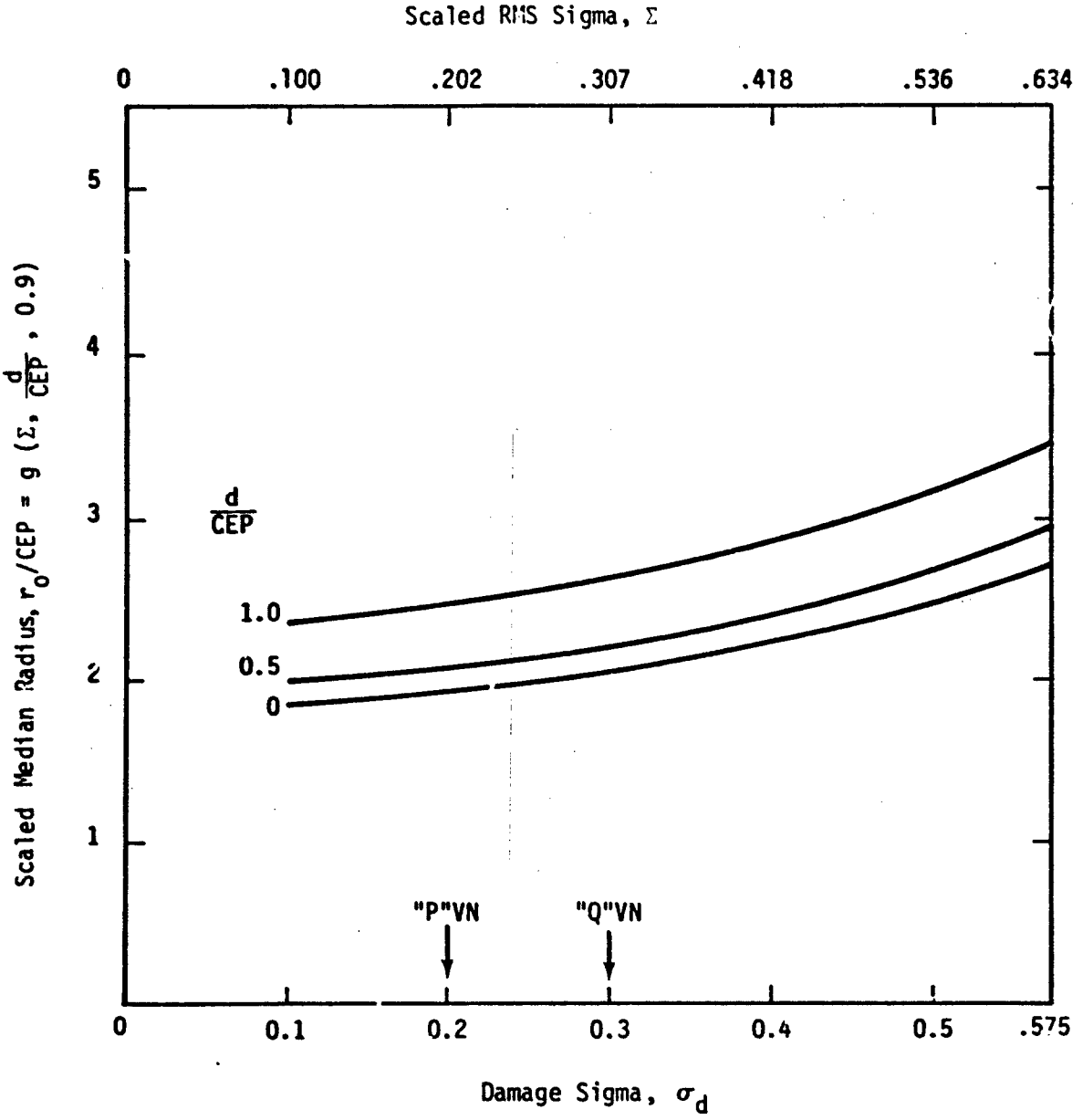

Figure 3-1. Scaled Median Radius for Given Offset, P_k = 0.9, Blast Targets

as it could be. An analytical formulation of this measure, applicable to point targets, is the ratio of the yield, W, required to achieve a given probability of damage (90%) assuming the weapon produced environment were perfectly known, to the yield, W_{EPC}, required to achieve the same kill probability with the present degree of accuracy in the weapon produced environment.

To achieve a significant* reduction in the yield predicted to achieve a 90 percent kill probability, the ratio W/W_{EPC} must be in the range 0.75 to 0.5, corresponding to a 25 percent to 50 percent reduction in yield. The maximum improvement possible through UGT is, of course, when the variance in the weapon produced environment is set to zero. To show how the variance in the weapon produced environment would affect the yield selection to achieve a given probability of damage, reference to Equation 3.1-4 indicates that the median weapon radius is a function of yield, i.e.,

$$R_o = f(W) \qquad (3.1\text{-}17)$$

For many weapon produced environments (i.e., blast) R_o is very nearly proportional to $W^{1/3}$. Also, Equation 3.1-15 shows that R_o is a function of Σ, the damage function standard deviation, where:

$$\Sigma = s_z/k \text{ for blast}$$

$$\Sigma = s_z/a \text{ for radiation}$$

$$s_z^2 = s_i^2 + s_v^2$$

Thus, for those weapon produced environments where R_o is proportional to $W^{1/3}$, the ratio of yields becomes:

$$\frac{W}{W_{EPC}} = \left(\frac{R_o}{R_{o,\,EPC}}\right)^3$$

$$= \left[\frac{g(\Sigma,\, d/CEP,\, .9)}{g(\Sigma_{EPC},\, d/CEP,\, .9)}\right]^3 \qquad (3.1\text{-}18)$$

*Subjective definition.

for a P_k of 0.9. The value of s_i^2 that will cause Equation 3.1-18 to have a value 0.75 or smaller indicates the required predictive capability potentially achievable through environmental testing. Of course, there may be no positive (or zero) value of s_i^2 that will result in a solution in this range. This implies one of two conditions for UGT:

- No significant gains in predictive capability can be achieved through UGT if both s_i^2 and s_v^2 are small, or;
- Simultaneous reduction in both s_i^2 and s_v^2 is indicated, if both s_i^2 and s_v^2 are large.

The definition of "large" and "small" is, of course, subject to interpretation. Thus, the measure would clearly indicate a rationale for UGT if the required significant yield change is computed, but would not necessarily indicate no rationale if the maximum yield change is not significant; this later case would require further analysis.

The remaining subsection derives explicit expression for the ratio of yields for blast environment on point targets.

3.1.6 Yield Ratio for Point Blast Targets

For point targets, Equation 3.1-16 can be used to express the weapon radius as a function of Σ:

$$R_o(\Sigma) \cong R_o(0)\ \exp(\Sigma^2) \quad . \tag{3.1-16}$$

The ratio of R_o for the required predictive capability to R_o for the existing predictive capability is:

$$\frac{R_o}{R_{o,\,epc}} \cong [R_o(0)\ \exp(\Sigma^2)] \,/\, [R_o(0)\ \exp(\Sigma^2_{epc})]$$

$$\cong \exp[\Sigma^2 - \Sigma^2_{epc}]$$

$$\cong \exp\left[\frac{s_i^2 + s_v^2}{k^2} - \left(\frac{s_{i,\,epc}^2 + s_v^2}{k^2}\right)\right]$$

$$\cong \exp\left[\frac{s_i^2 - s_{i,\,epc}^2}{k^2}\right] \quad , \qquad (3.1\text{-}19)$$

so that the vulnerability variance, s_v^2, cancels out of the expression. Thus, this measure does not contain the target vulnerability when P_k is fixed and defined in terms of the median weapon radius.

A general expression for the median weapon radius for blast targets that encompasses peak overpressure and dynamic pressure and overpressure impulse is:

$$R_o = (A_o/V_o)^{1/k} W^{(1+b)/3} \qquad (3.1\text{-}20)$$

where: b = 0 for peak overpressure or dynamic pressure,
b = 1/k for impulse.

Inverting Equation 3.1-20 to solve for W:

$$W = \left[R_o \left(\frac{A_o}{V_o}\right)^{-1/k}\right]^{\frac{3}{1+b}} \qquad (3.1\text{-}21)$$

Thus, the ratio of yields becomes:

$$\frac{W}{W_{epc}} = \left[\frac{R_o}{R_{o,\,epc}}\right]^{\frac{3}{1+b}} \qquad (3.1\text{-}22)$$

From Equation 3.1-19, the expression for the ratio of median weapon radii is inserted into Equation 3.1-22:

$$\frac{W}{W_{epc}} = \exp\left[\frac{3}{1+b}\left(\frac{s_i^2 - s_{i,epc}^2}{k^2}\right)\right] . \qquad (3.1\text{-}23)$$

It can be shown that the error factor in intensity, f, is related to the error factor in range, f_R, as:

$$f = f_R^k . \qquad (3.1\text{-}24)$$

Also, the error factor in intensity is defined:

$$f = e^{1.65\, s_i} . \qquad (3.1\text{-}25)$$

Equating Equations 3.1-24 and 3.1-25 results in the expression for s_i^2:

$$s_i^2 = \frac{1}{1.65}\, k \ln f_R . \qquad (3.1\text{-}26)$$

Substituting Equation 3.1-26 into Equation 3.1-23 results in:

$$\frac{W}{W_{epc}} = \exp\left[\frac{3}{(1+b)\ (1.65)^2}\left(\ln^2 f_R - \ln^2 f_{R,\,epc}\right)\right] . \qquad (3.1\text{-}27)$$

Equation 3.1-27 is not a function of target vulnerability or uncertainty in vulnerability. This expression clearly shows the relationship, for all blast phenomena on point targets, between the yield adjustment that one could make to accomplish an objective, and the improved accuracy in the weapon produced environment. The largest possible adjustment in yield would be the case where there is no error in the estimate of the weapon produced environment ($f_R = 1$). The value

of $f_{R,\ epc}$ that must exist so that a potentially significant reduction in yield could potentially result from environmental testing is defined as the critical value, $f_{R,\ CR}$, and is defined by rearranging Equation 3.1-27:

$$f_{R,\ CR} = \exp\left[1.65\sqrt{\frac{(1+b)}{3}\ \ln\left(\frac{W_{epc}}{W}\right)}\right], \qquad (3.1\text{-}28)$$

obtained by setting f_R=1 and inverting Equation 3.1-27. The significant change in yield is specified in Equation 3.1-28 by setting W_{EPC}/W equal to, say, 1.25, indicating a potential 25 percent reduction, and evaluating the expression. The result is then compared to $f_{R,\ epc}$.

3.2 MEASURE OF TACTICAL UTILITY

The tactical utility of a nuclear weapon would be related to the area that could be covered by a specified probability of kill, P_k, given the collateral constraints. For any weapon there may be a non-targetable excluded area defined by the difference in the ranges between the target-kill weapon produced environment and the collateral-damage weapon produced environment. If the target is to be killed with a given high probability (P_k = 0.9, for instance) and the collateral weapon produced environment is to be exceeded only with a given small probability (P_c = 0.1, for instance), then the excluded area will be a function of the uncertainty in these weapon produced environments -- knowing the weapon produced environment with a greater degree of certainty would allow (on the average) a smaller yield to be specified to achieve target kill, which would in turn allow deployment closer to a collateral asset, thus decreasing the excluded area. Figure 3-2 illustrates the decrease in excluded area that would result from improved weapon produced environment predictive capability.

To illustrate the relationship between this decrease in excluded area and the decrease in yield afforded by an improved predictive capability, consider the ratio of excluded areas for the existing and improved predictive capabilities:

$$\frac{A_{EPC}}{A_{IPC}} = \frac{C_{EPC}^2 - K_{EPC}^2}{C_{IPC}^2 - K_{IPC}^2} \qquad (3.2\text{-}1)$$

where:

A_{EPC}, A_{IPC} = The areas for the existing and improved predictive capabilities,

C_{EPC}, C_{IPC} = The ranges to the collateral damage weapon produced environment for the existing and improved predictive capabilities,

K_{EPC}, K_{IPC} = The ranges to the target kill weapon produced environment for the existing and improved predictive capabilities.

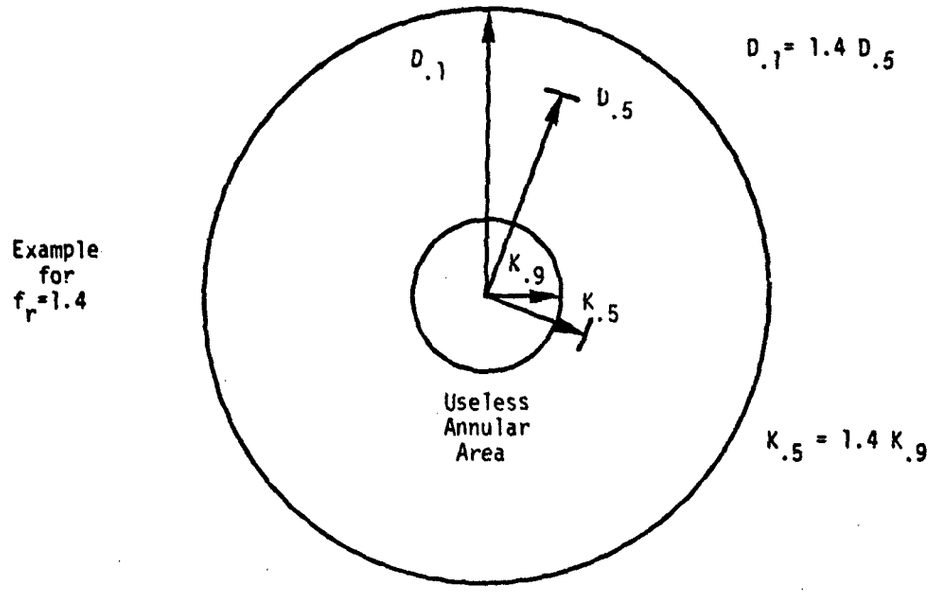

Figure 3-2(a). Schematic of Target Kill and Collateral Damage Areas

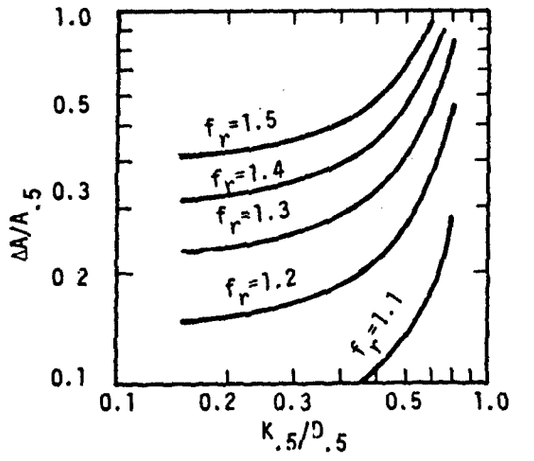

$$A_{.5} = \pi\left(D_{.5}^2 - K_{.5}^2\right)$$

$$A_{.5}+\Delta A \equiv \pi\left(D_{.1}^2 - K_{.9}^2\right)$$

$$f_r \equiv \frac{D_{.1}}{D_{.5}} = \frac{K_{.5}}{K_{.9}}$$

Figure 3-2(b). Fractional Uncertainty of Useless Area

The blast environment at a given range close to the median weapon radius was given by Equation 3.1-6 as:

$$I(R) = V_o(R/R_o)^{-k} \quad . \qquad (3.1\text{-}6)$$

Let I be some specified weapon produced blast environment. Solving Equation 3.1-6 for the range to this specified environment results in:

$$R_I = R_o(V_o/I)^{1/k} \quad . \qquad (3.2\text{-}2)$$

Thus the ranges to specified target and collateral environments are, respectively:

$$R = R_o(V_t/I_t)^{1/k} \qquad (3.2\text{-}3)$$

$$C = R_o(V_c/I_c)^{1/k} \quad . \qquad (3.2\text{-}4)$$

Equation 3.1-16a gives a conceptual form for R_o in terms of the weapon CEP, the specified P_k, and the weapon and target vulnerability uncertainties as:

$$R_o = g(o, d/CEP, P_k)e^{\Sigma^2} \quad . \qquad (3.1\text{-}16a)$$

Actually this expression is valid only for P_k's near 0.9; a more general expression, encompassing both target kill and collateral damage P_k's, would be:

$$R_o = g(o, d/CEP, P_k)f(\Sigma) \qquad (3.2\text{-}5)$$

where $f(\Sigma)$ would be different for target and collateral P_k's. On substituting Equation 3.2-5 into Equations 3.2-3 and 3.2-4, they become:

$$R = g(o, d/CEP, P_k) f_t(\Sigma) \qquad (3.2\text{-}6)$$

$$C = g(o, d/CEP, P_c) f_c(\Sigma) \quad . \qquad (3.2\text{-}7)$$

Equations 3.2-6 and 3.2-7 can now be used in Equation 3.2-1 to express the ratio of excluded areas in terms of the target and collateral P_k's and the existing and improved predictive capabilities. Equation 3.2-1 becomes:

$$\frac{A_{EPC}}{A_{IPC}} = \frac{g^2(o, d/CEP, P_k) f_c^2(\Sigma_{EPC}) \left(\frac{V_c}{I_c}\right)^{2/k}}{g^2(o, d/CEP, P_c) f_c^2(\Sigma_{IPC}) \left(\frac{V_c}{I_c}\right)^{2/k}} - \frac{g^2(o, d/CEP, P_k) f_T^2(\Sigma_{EPC}) \left(\frac{V_t}{I_t}\right)^{2/k}}{g^2(o, d/CEP, P_k) f_T^2(\Sigma_{IPC}) \left(\frac{V_t}{I_t}\right)^{2/k}} \quad . \qquad (3.2\text{-}8)$$

but the range to a particular nominal effect is related to the yield as:

$$R = k\, W^{1/3} \quad . \qquad (3.2\text{-}9)$$

Where k is the range to the effect for blast. Substituting Equation 3.2-9 into Equation 3.2-8, where the yields W_{EPC} and W_{IPC} have the relationship described in Section 3.1, results in:

$$\frac{A_{EPC}}{A_{IPC}} = \frac{k_c^2 W_{EPC}^{2/3} \left(\frac{V_c}{I_c}\right)^{2/k} - k_t^2 W_{EPC}^{2/3} \left(\frac{V_t}{I_t}\right)^{2/k}}{k_c^2 W_{IPC}^{2/3} \left(\frac{V_c}{I_c}\right)^{2/k} - k_t^2 W_{IPC}^{2/3} \left(\frac{V_t}{I_t}\right)^{2/k}} = \left(\frac{W_{EPC}}{W_{IPC}}\right)^{2/3} \quad . \qquad (3.2\text{-}10)$$

Thus, the ratio of the excluded areas for the existing and improved predictive capabilities is equal to the two-thirds power of the yield ratio.

Section 4
RANDOM ERROR RESULTS

This section describes the results of the assessment of a rationale for tactical UGT environment tests based on the assumption that the nuclear produced blast environments observed in the historical test data are random, and are statistically the same as the environments to be expected on deployment of tactical weapons. Section 4.1 presents the blast data, and the results for the rationale assessment based on analysis of peak overpressure data, overpressure impulse data, and peak dynamic pressure data. Section 4.2 presents the results of the investigation of the statistical distribution appropriate for these data.

4.1 RANDOM ERROR ANALYSIS OF BLAST DATA

This section presents the raw blast data and shows the results of applying the measure developed in Section 3 to assess a rationale for underground nuclear effects tests This methodology was developed in Section 3 in closed form under the assumption that errors in the scaled range to a specified environment are proportional to range. Section 4.2 examines the validity of that assumption in some detail (the conclusion is that the assumption of lognormality is a reasonable and adequate one for most nuclear blast data).

Figures 4.1-1 through 4.1-31 show the peak overpressure, overpressure impulse, and peak dynamic pressure data plotted versus scaled range for all ten ranges of scaled HOB. These plots show the scatter in the "raw" data, as well as the approximate linear relationship when plotted on a log-log scaled coordinate system, illustrating the approximate power-law relationship between these three blast effects and scaled range.

The measure previously developed applies to the scatter in the range to a specified environment, and is based on the range error factor at the specified environment. To compute the range error factors at specified environments, it is necessary to group the blast data into

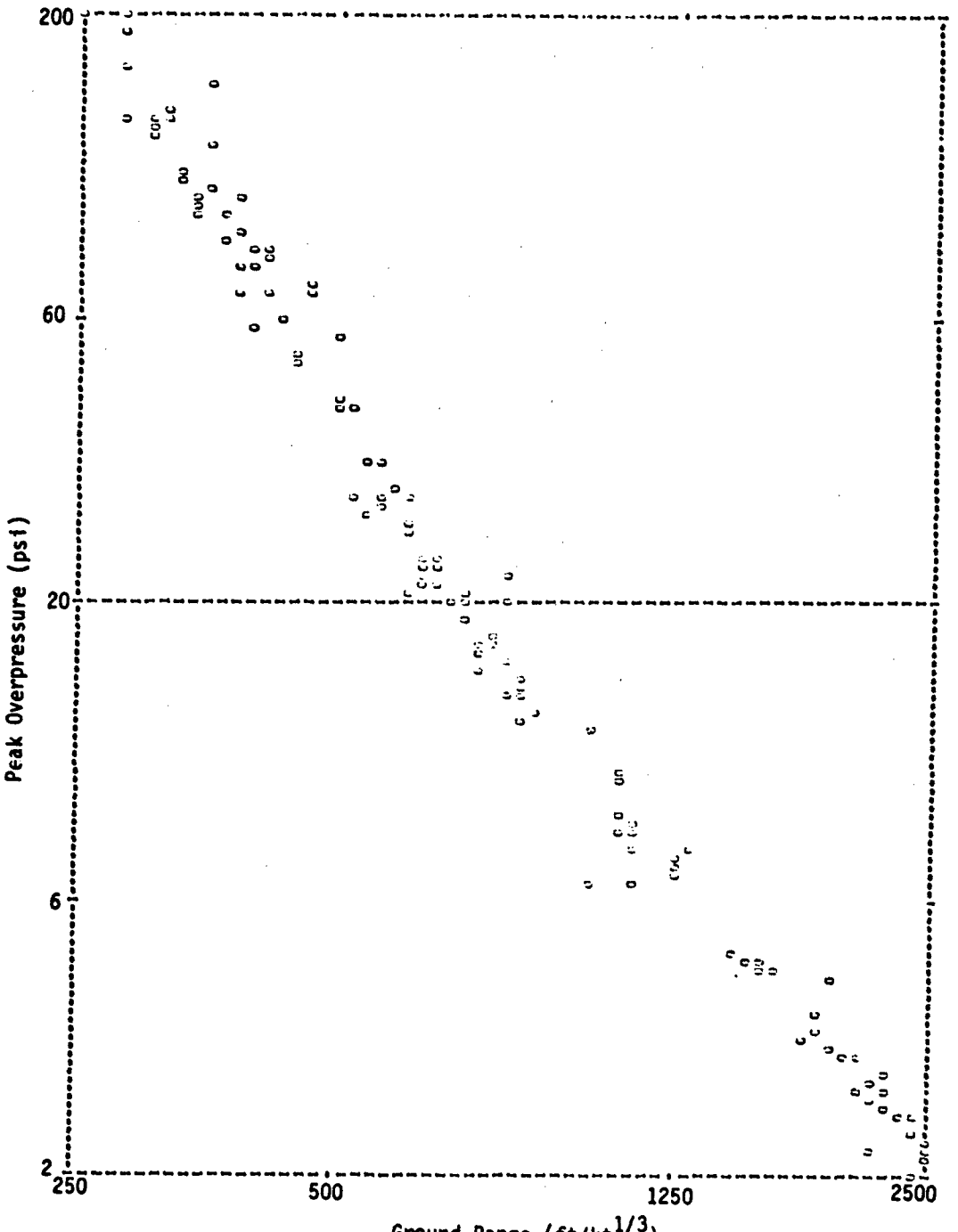

Figure 4.1-1. Peak Overpressures for 0 to 3 ft/kt$^{1/3}$ HOB

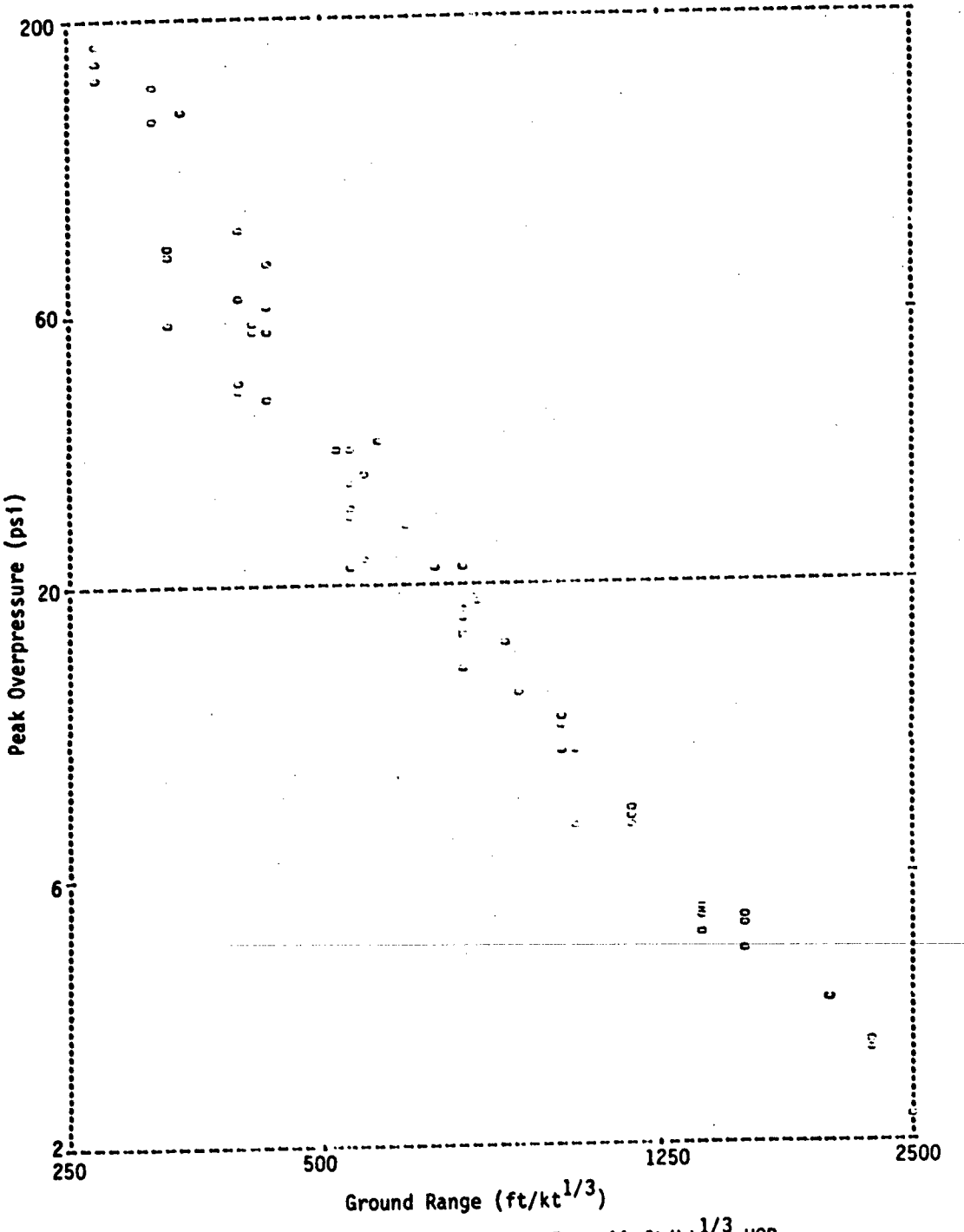

Figure 4.1-2 Peak Overpressures for 5 to 11 ft/kt$^{1/3}$ HOB

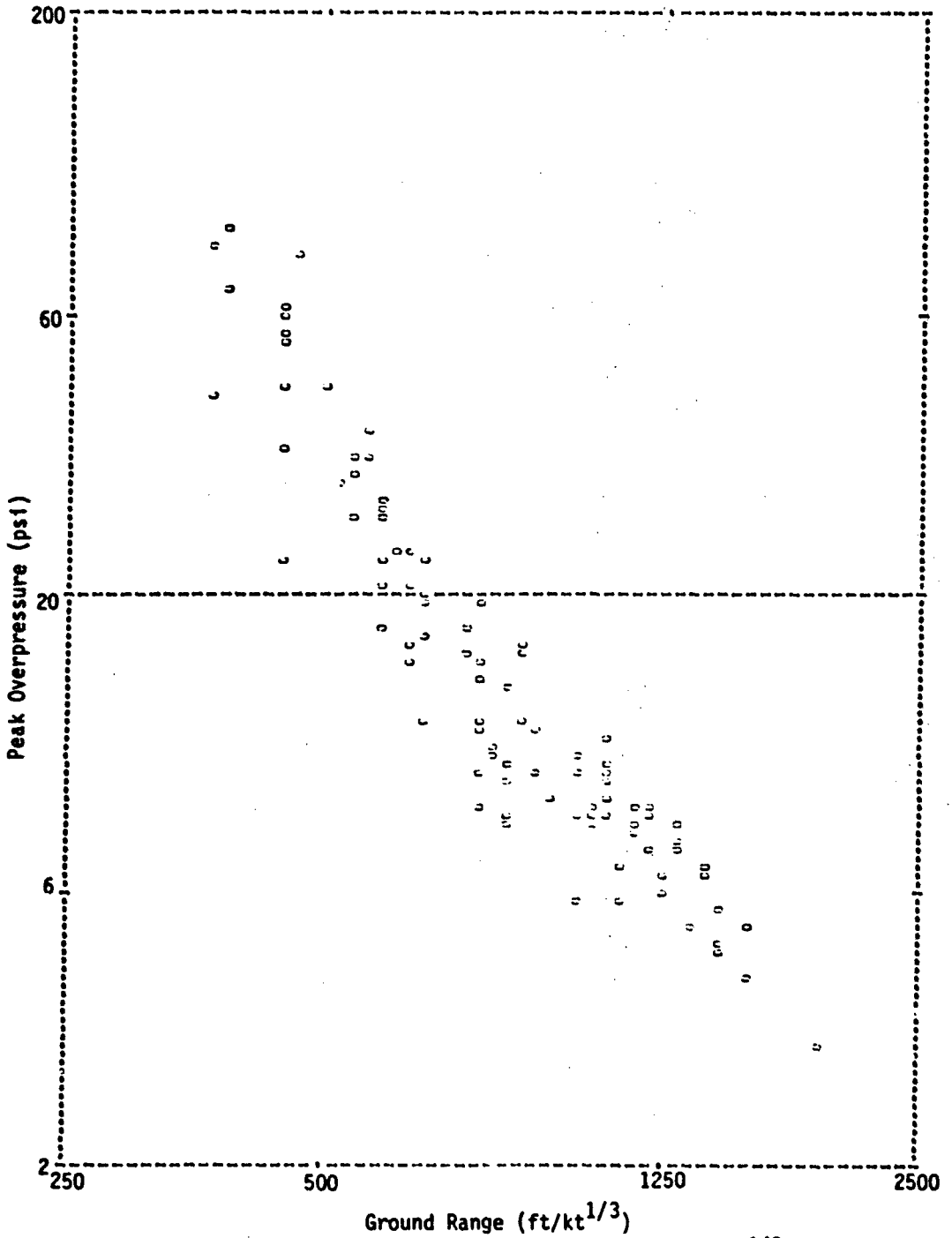

Figure 4.1-3. Peak Overpressures for 55 to 83 ft/kt$^{1/3}$ HOB

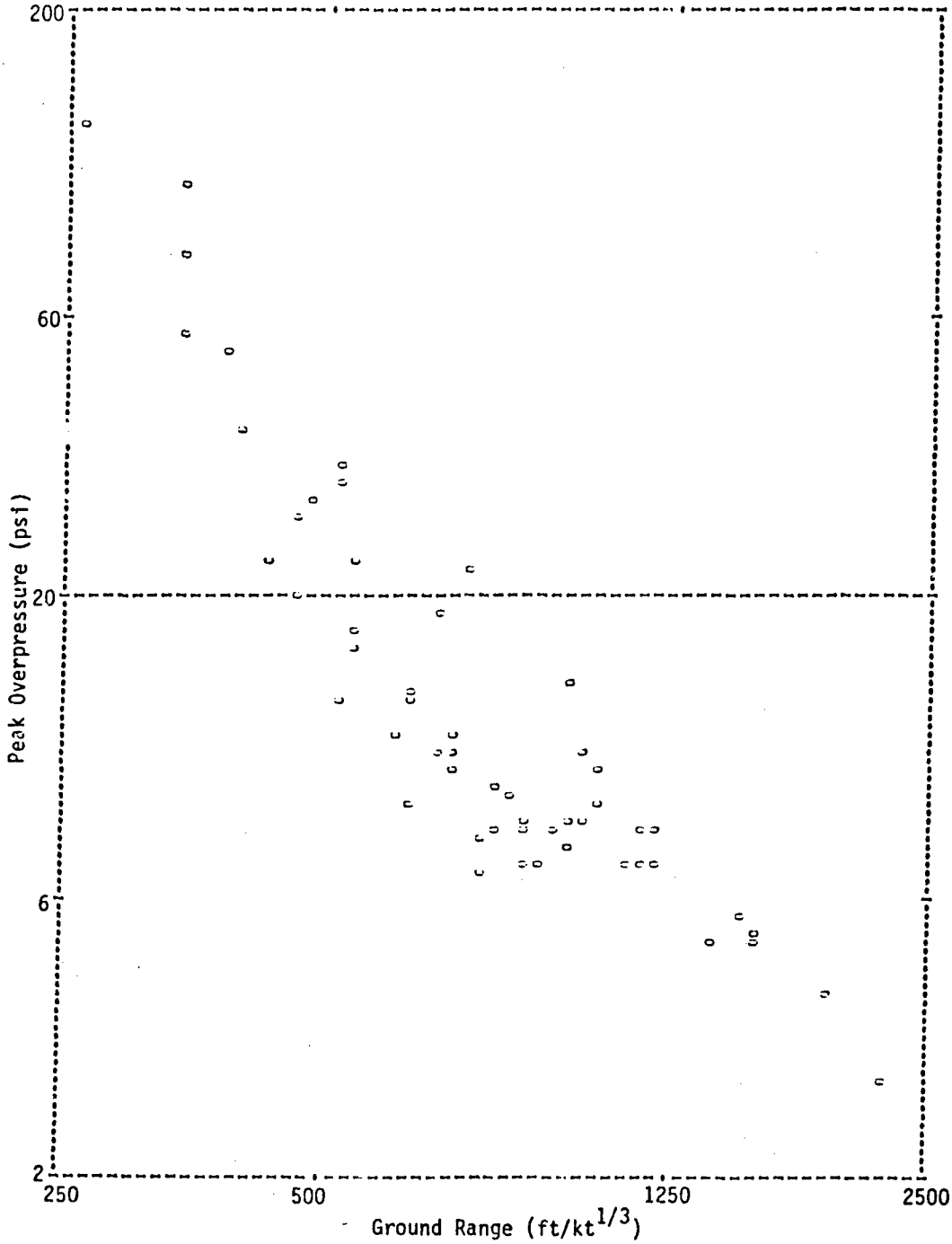

Figure 4.1-4. Peak Overpressures for 113 to 157 ft/kt$^{1/3}$ HOB

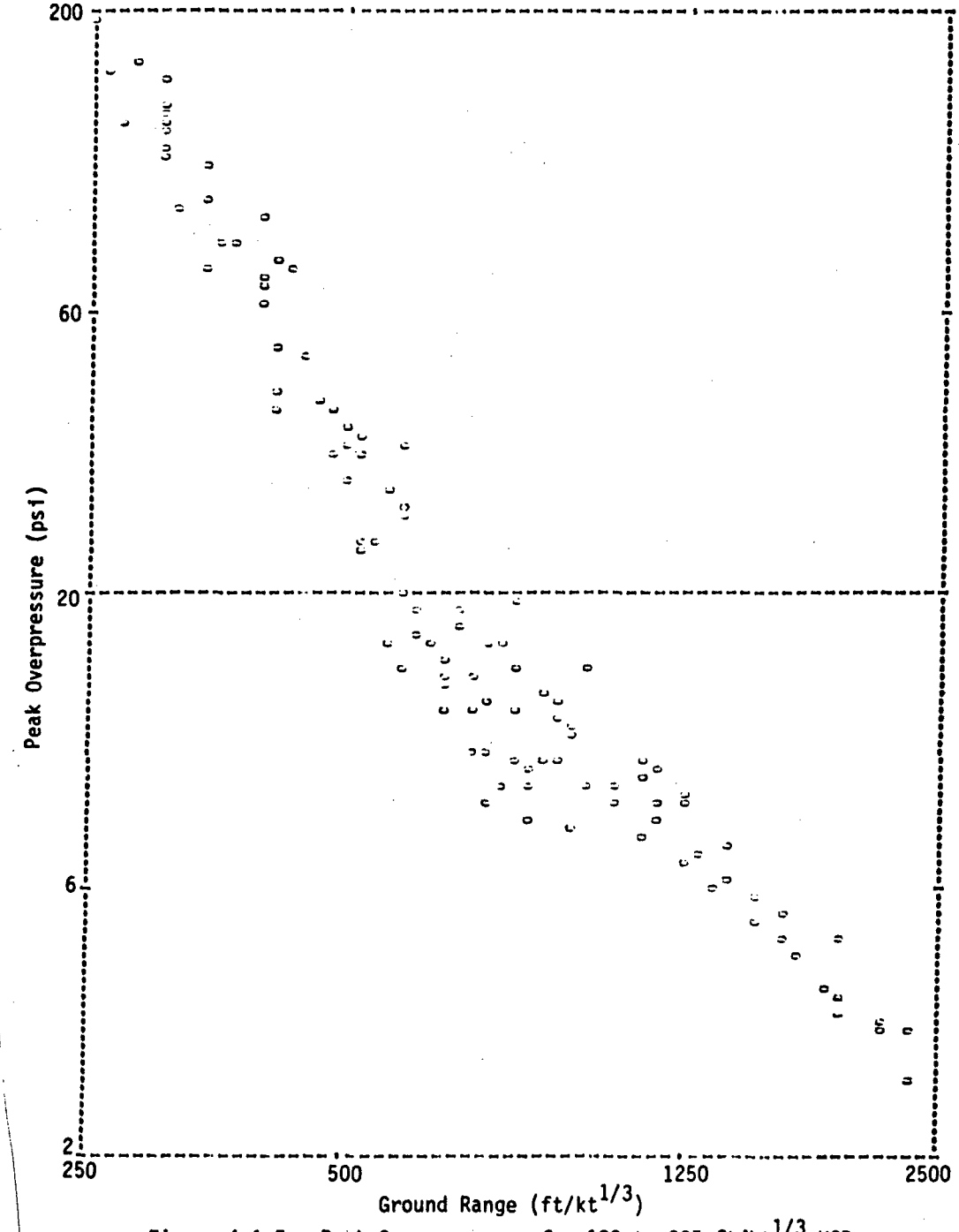

Figure 4.1-5. Peak Overpressures for 182 to 205 ft/kt$^{1/3}$ HOB

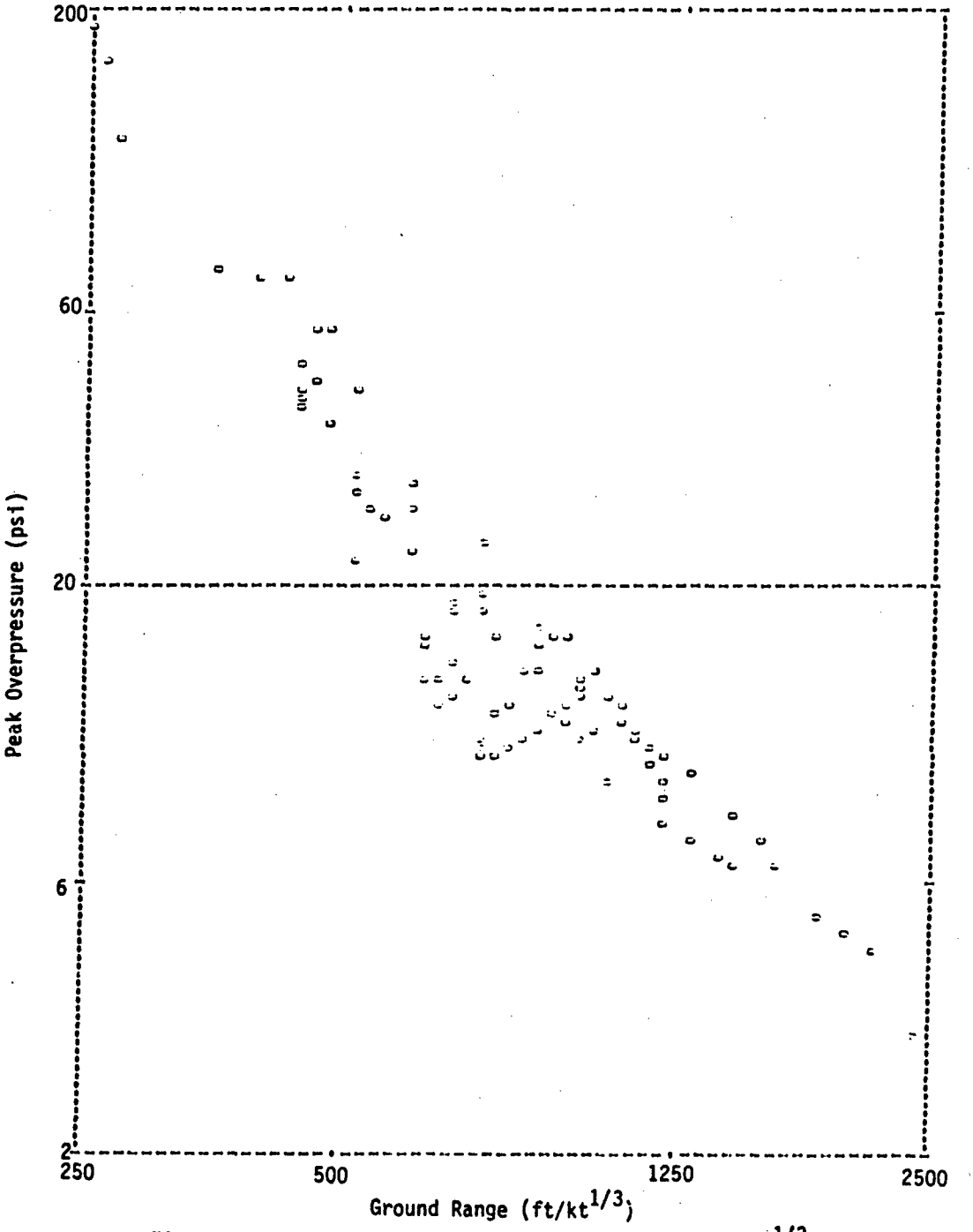

Figure 4.1-6. Peak Overpressures for 212 to 252 ft/kt$^{1/3}$ HOB

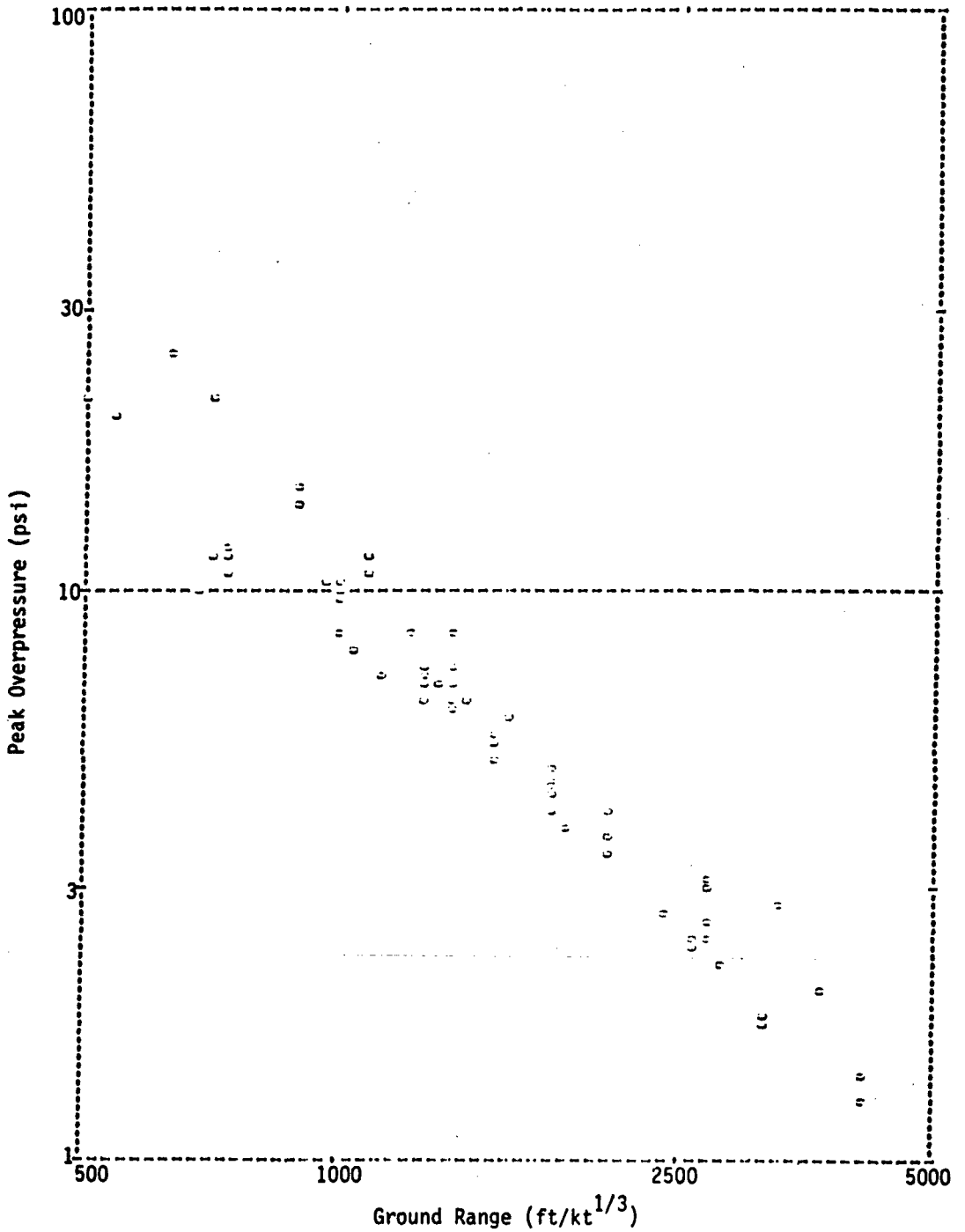

Figure 4.1-7. Peak Overpressures for 323 to 375 ft/kt$^{1/3}$ HOB

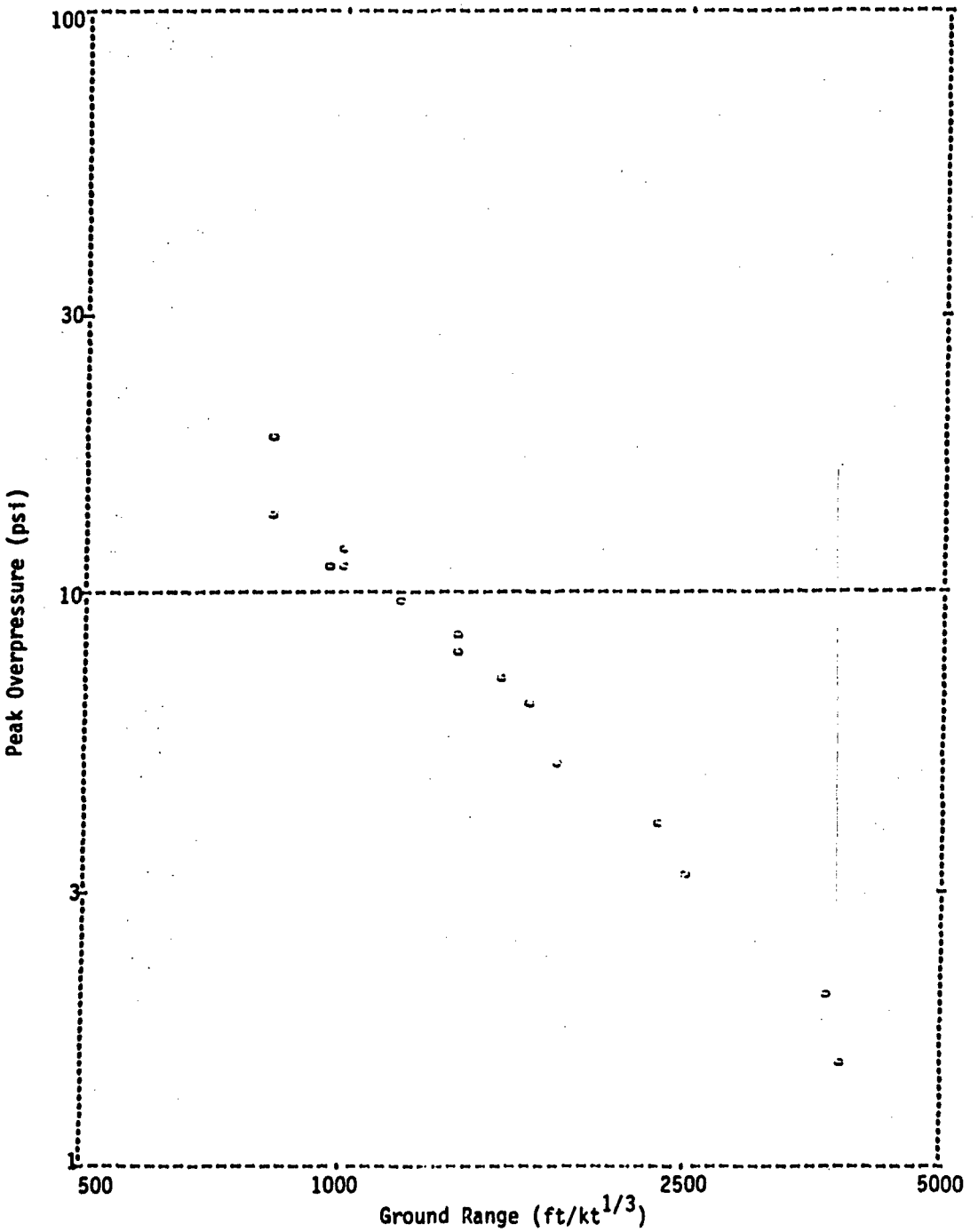

Figure 4.1-8. Peak Overpressures for 478 to 500 ft/kt$^{1/3}$ HOB

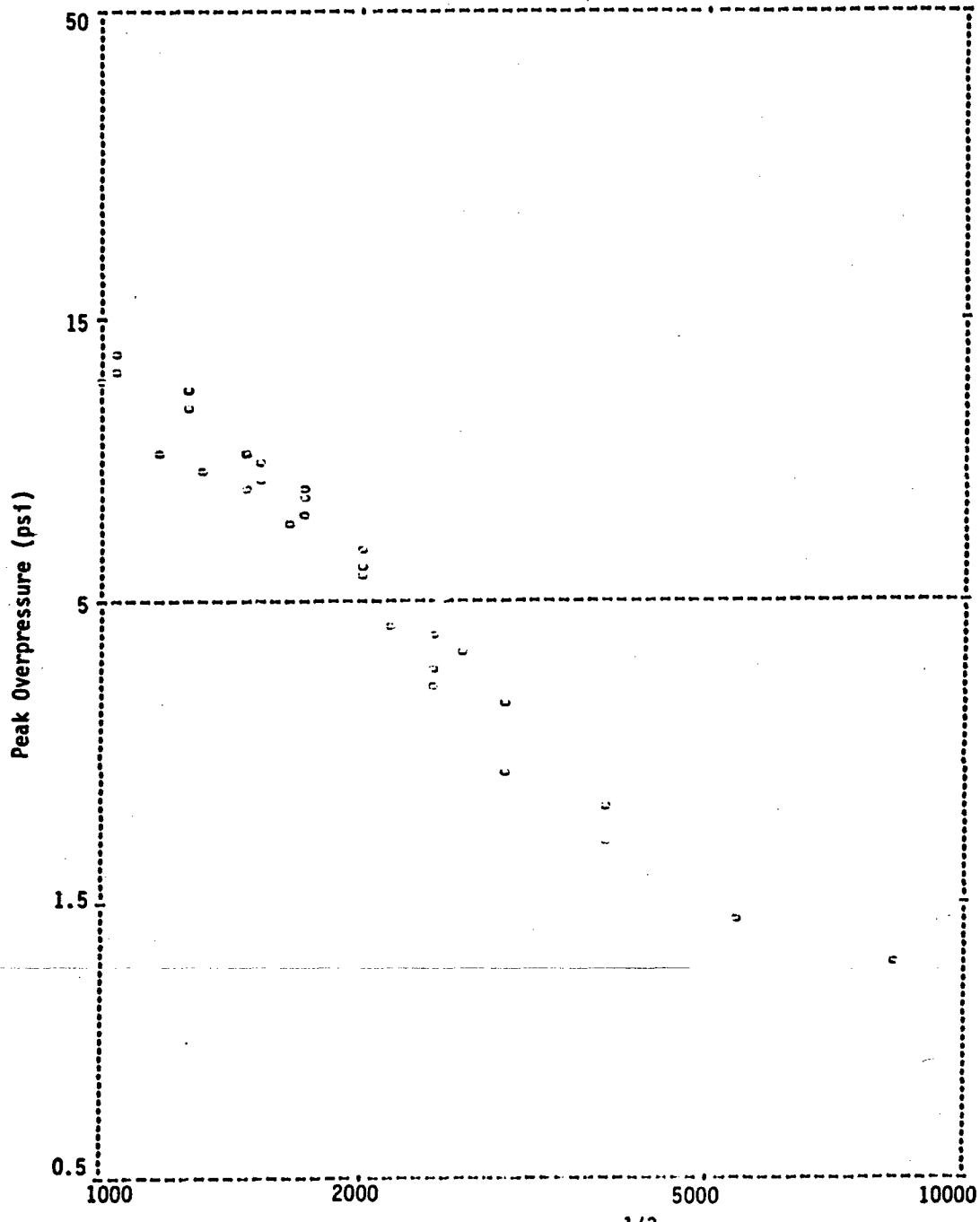

Figure 4.1-9. Peak Overpressures for 751 to 831 ft/kt$^{1/3}$ HOB

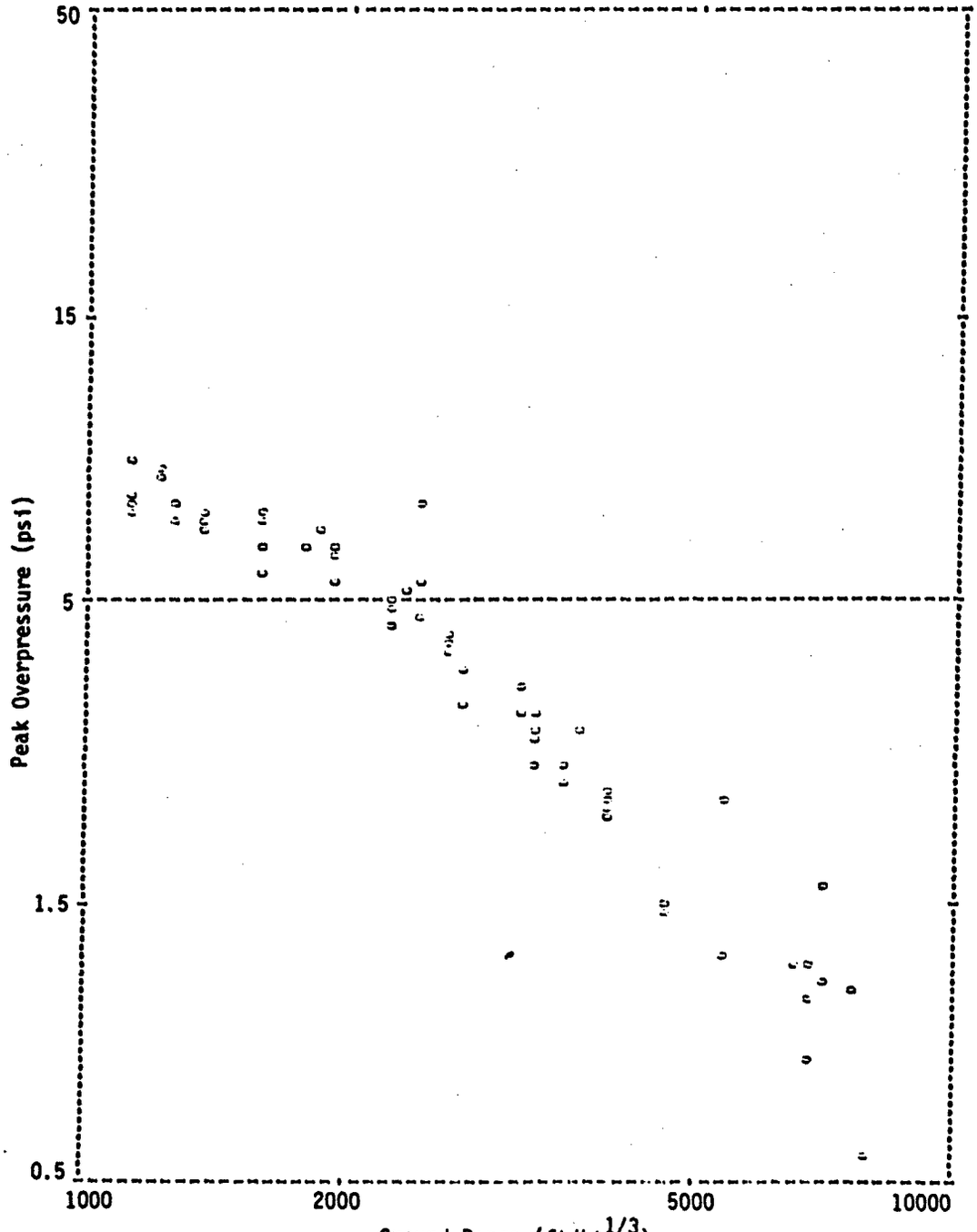

Figure 4.1-10. Peak Overpressures for 1003 to 1249 ft/kt$^{1/3}$ HOB

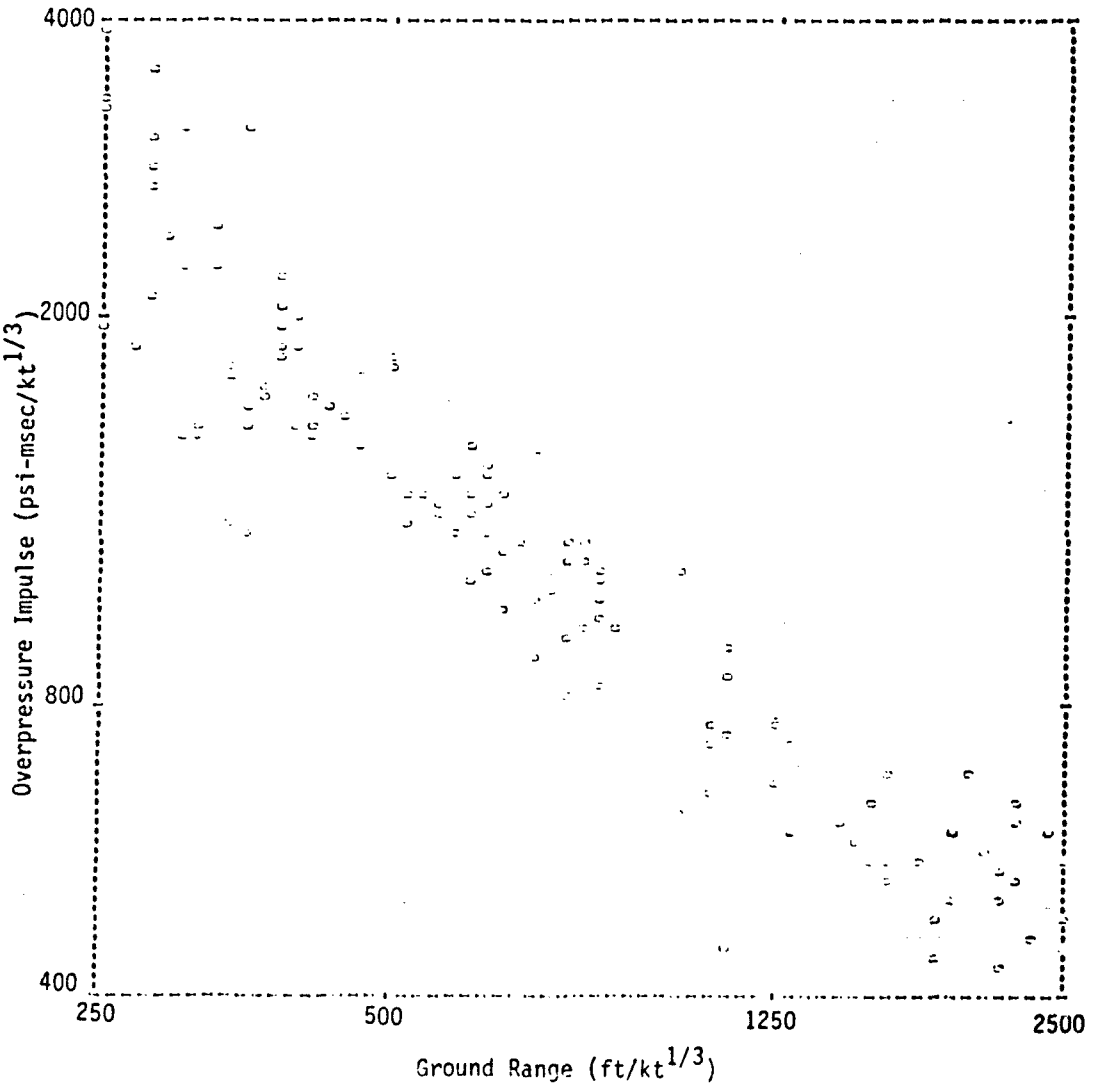

Figure 4.1-11. Overpressure Impulses for 0 to 3 ft/kt$^{1/3}$ HOB

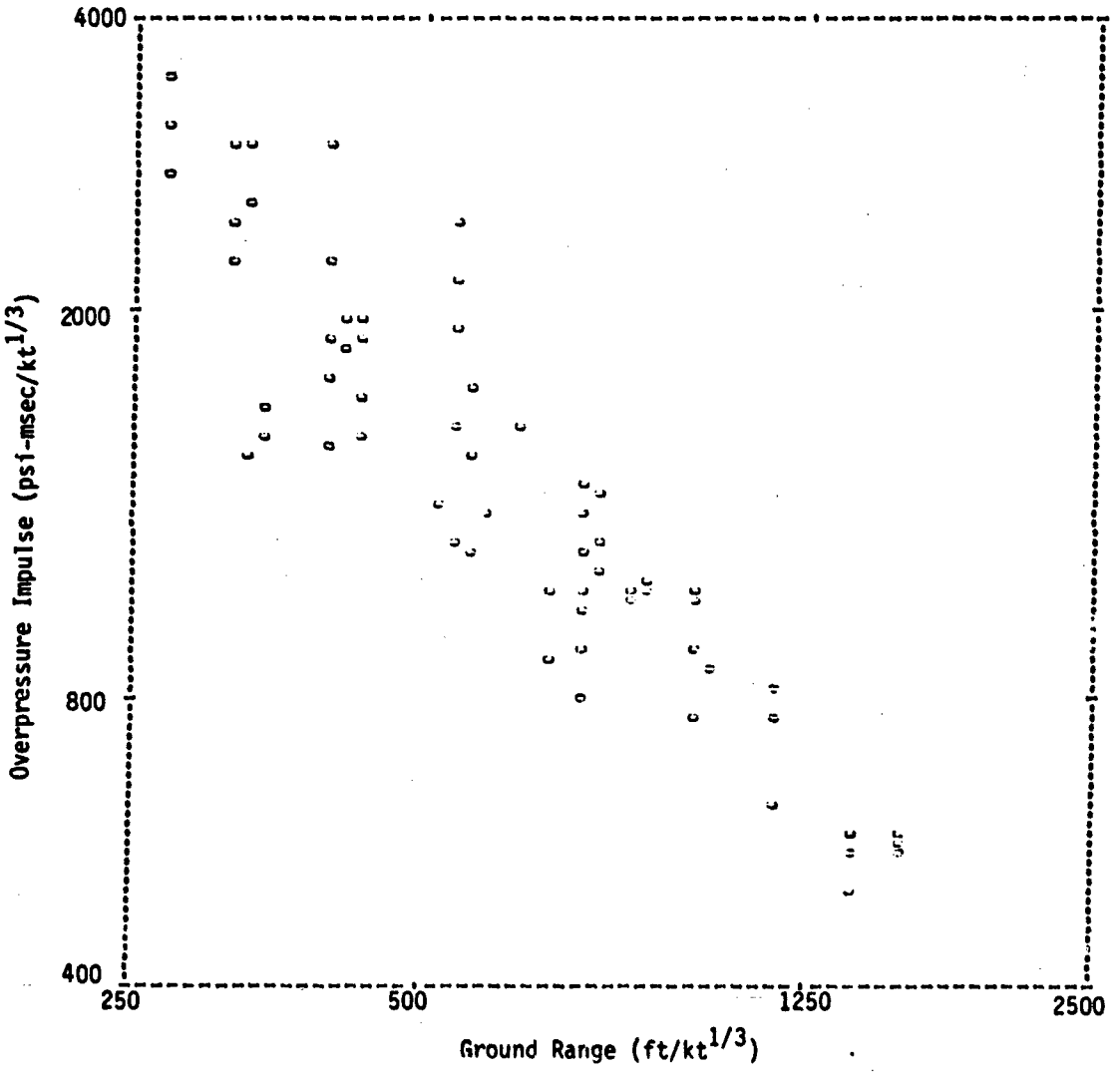

Figure 4.1-12. Overpressure Impulses for 5 to 11 ft/kt$^{1/3}$ HOB

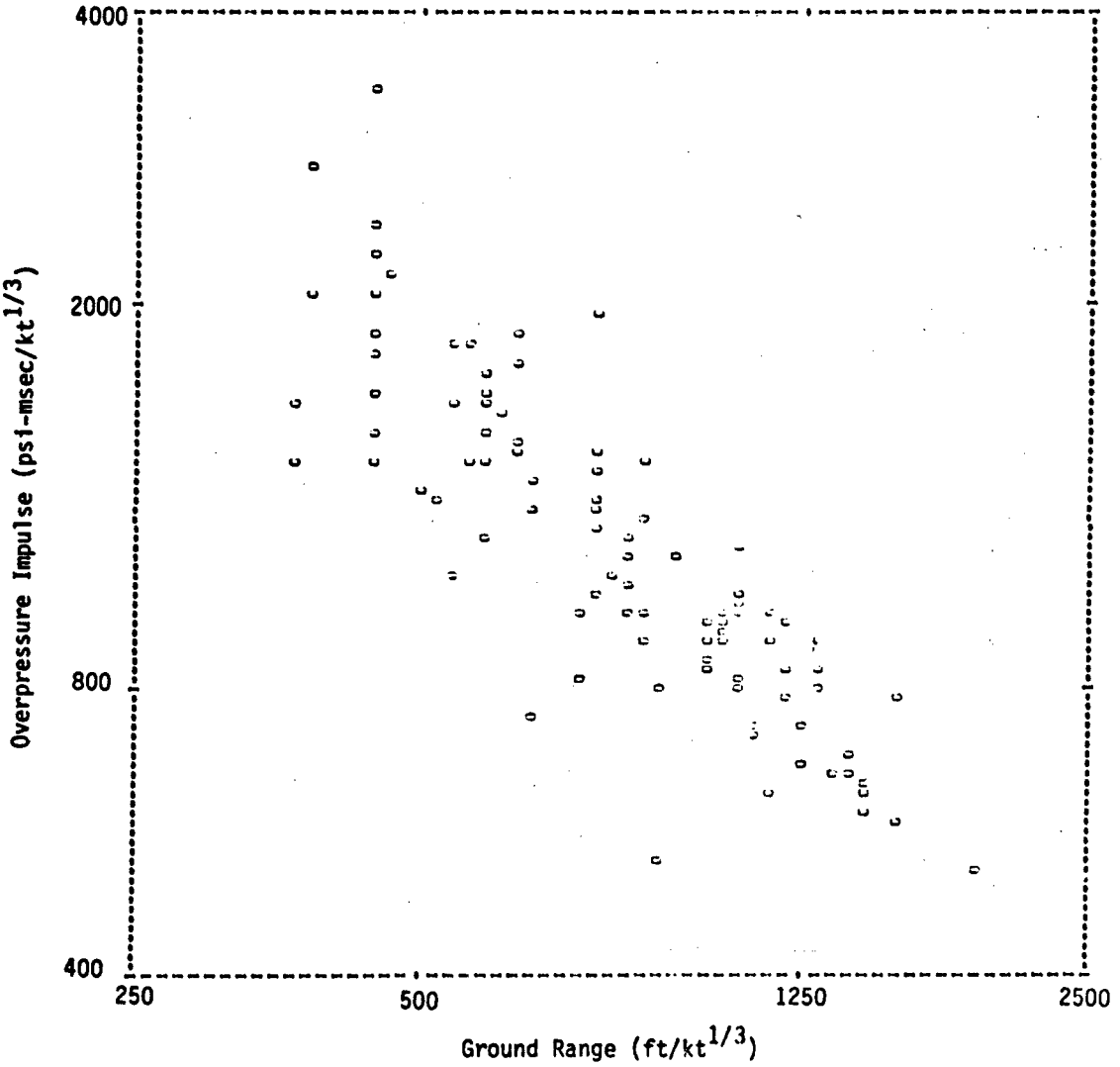

Figure 4.1-13. Overpressure Impulses for 55 to 83 ft/kt$^{1/3}$ HOB

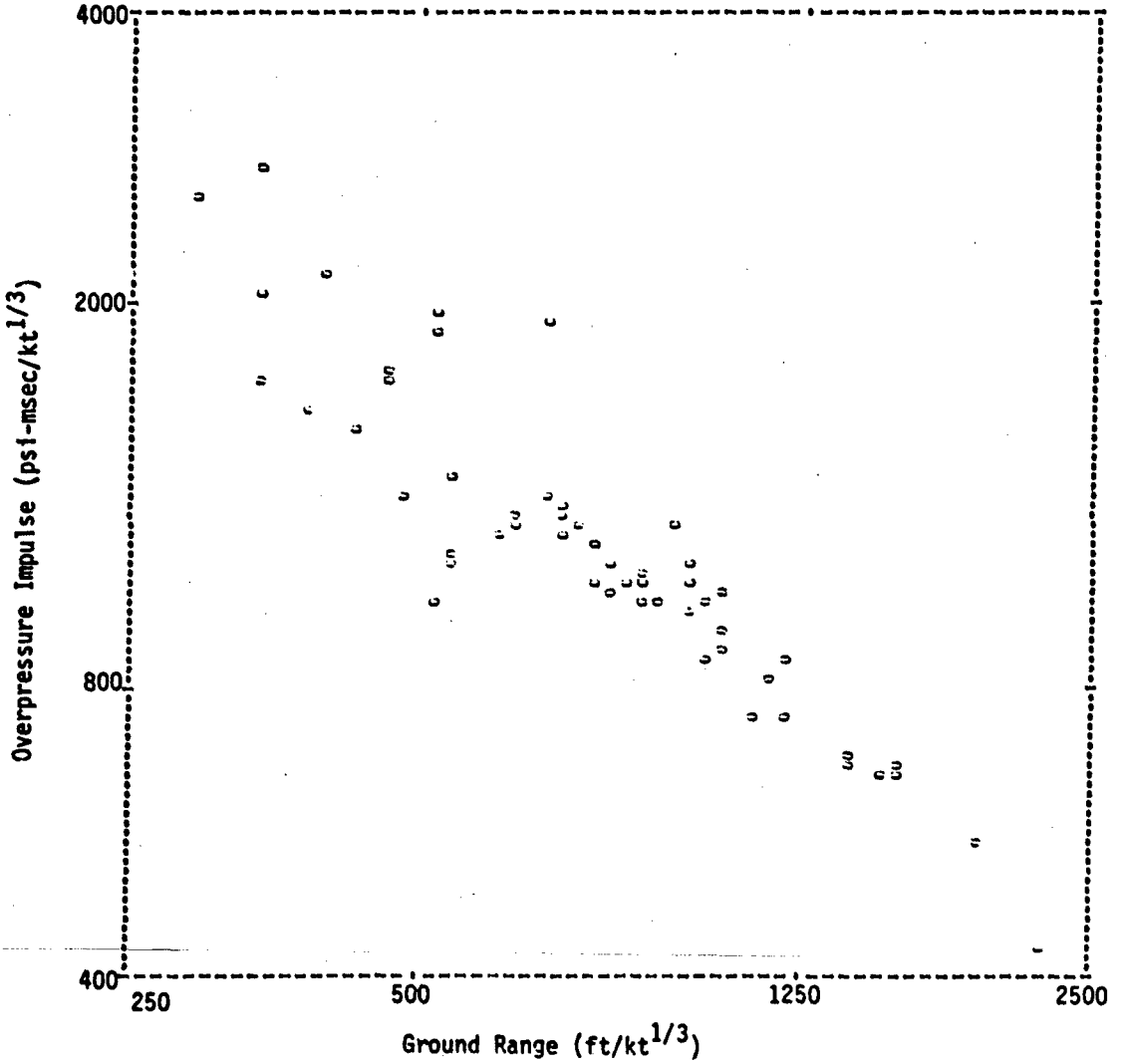

Figure 4.1-14. Overpressure Impulses for 113 to 157 ft/kt$^{1/3}$ HOB

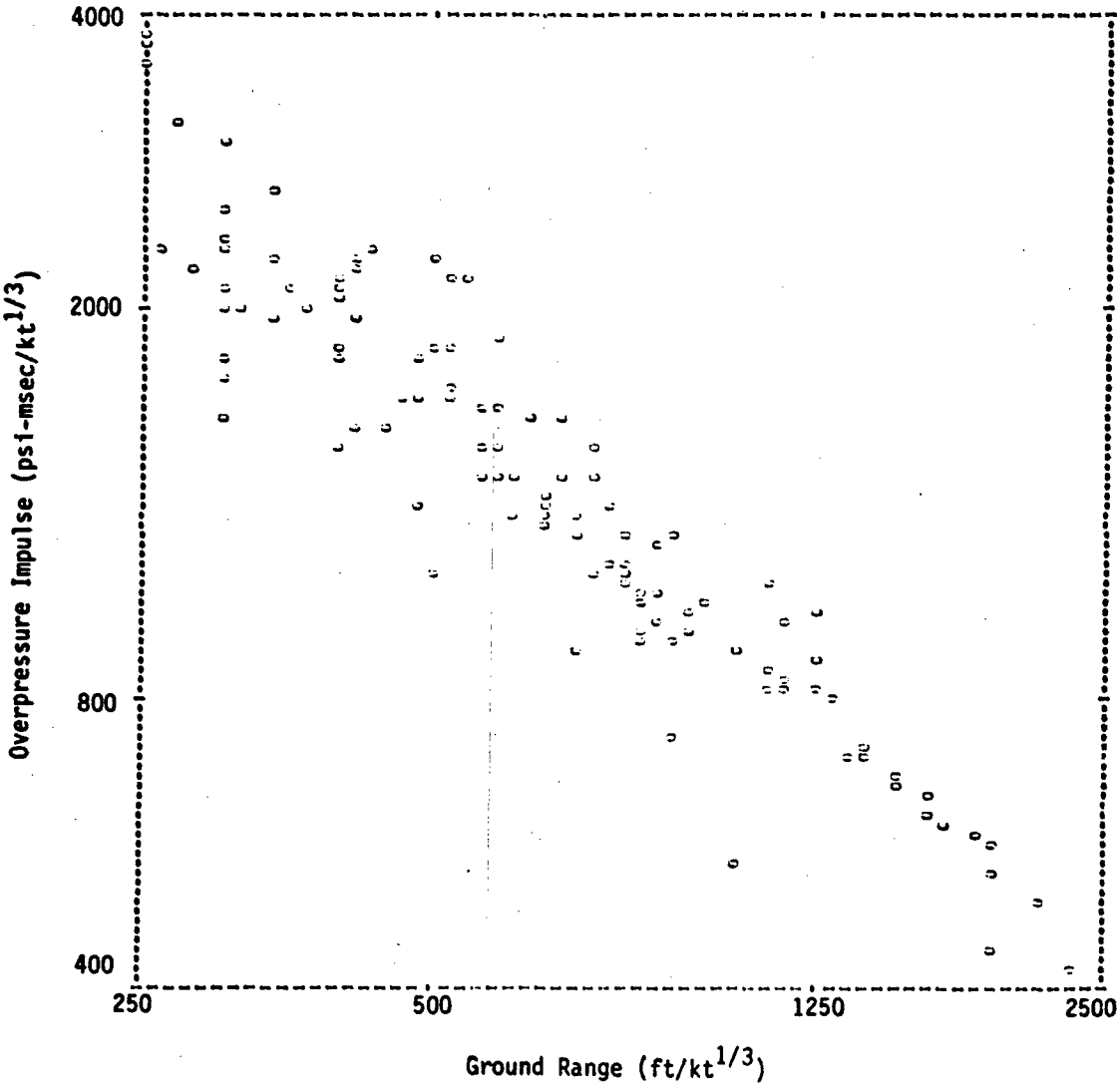

Figure 4.1-15. Overpressure Impulses for 182 to 205 ft/kt$^{1/3}$ HOB

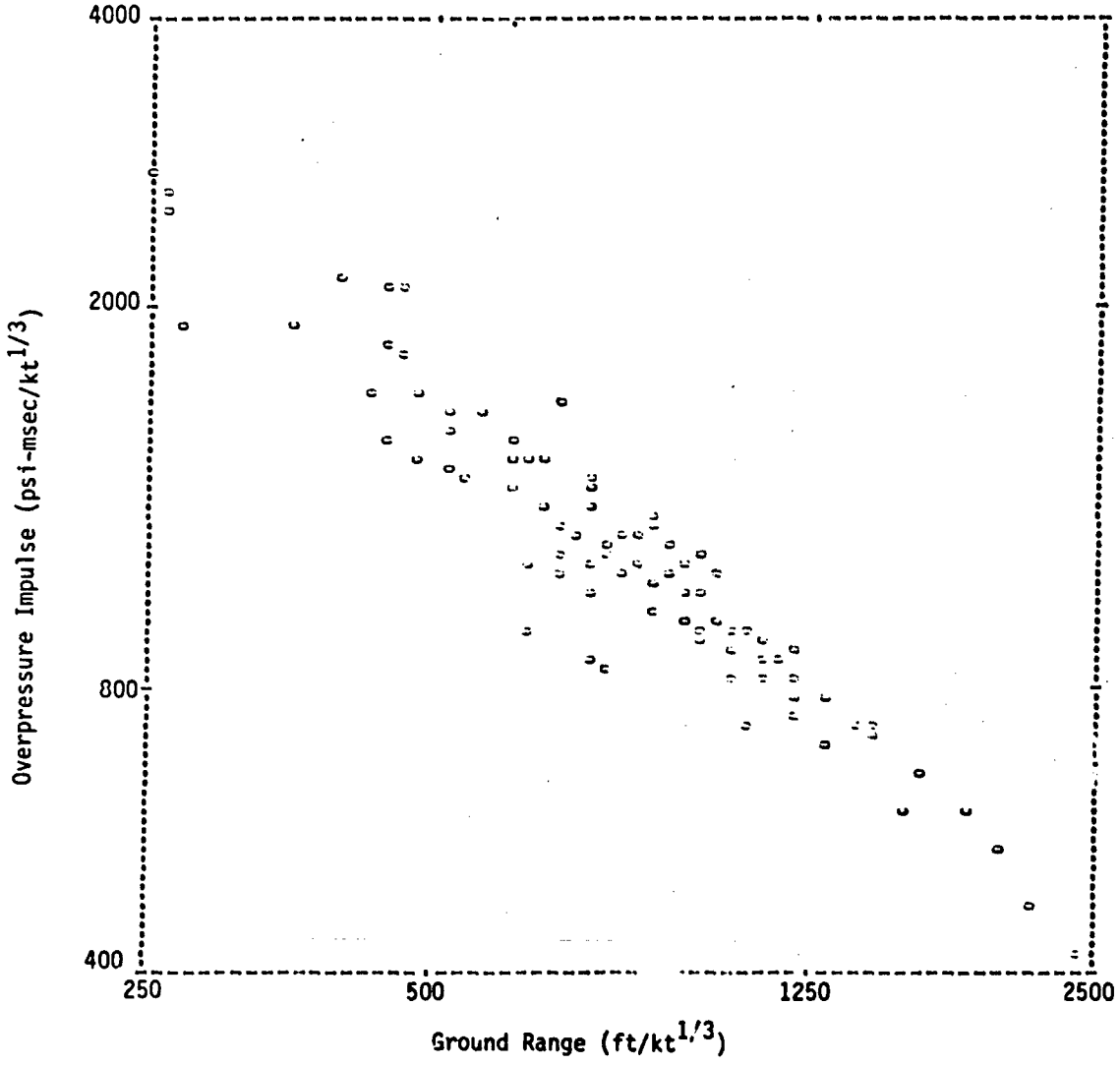

Figure 4.1-16. Overpressure Impulses for 212 to 252 ft/kt$^{1/3}$ HOB

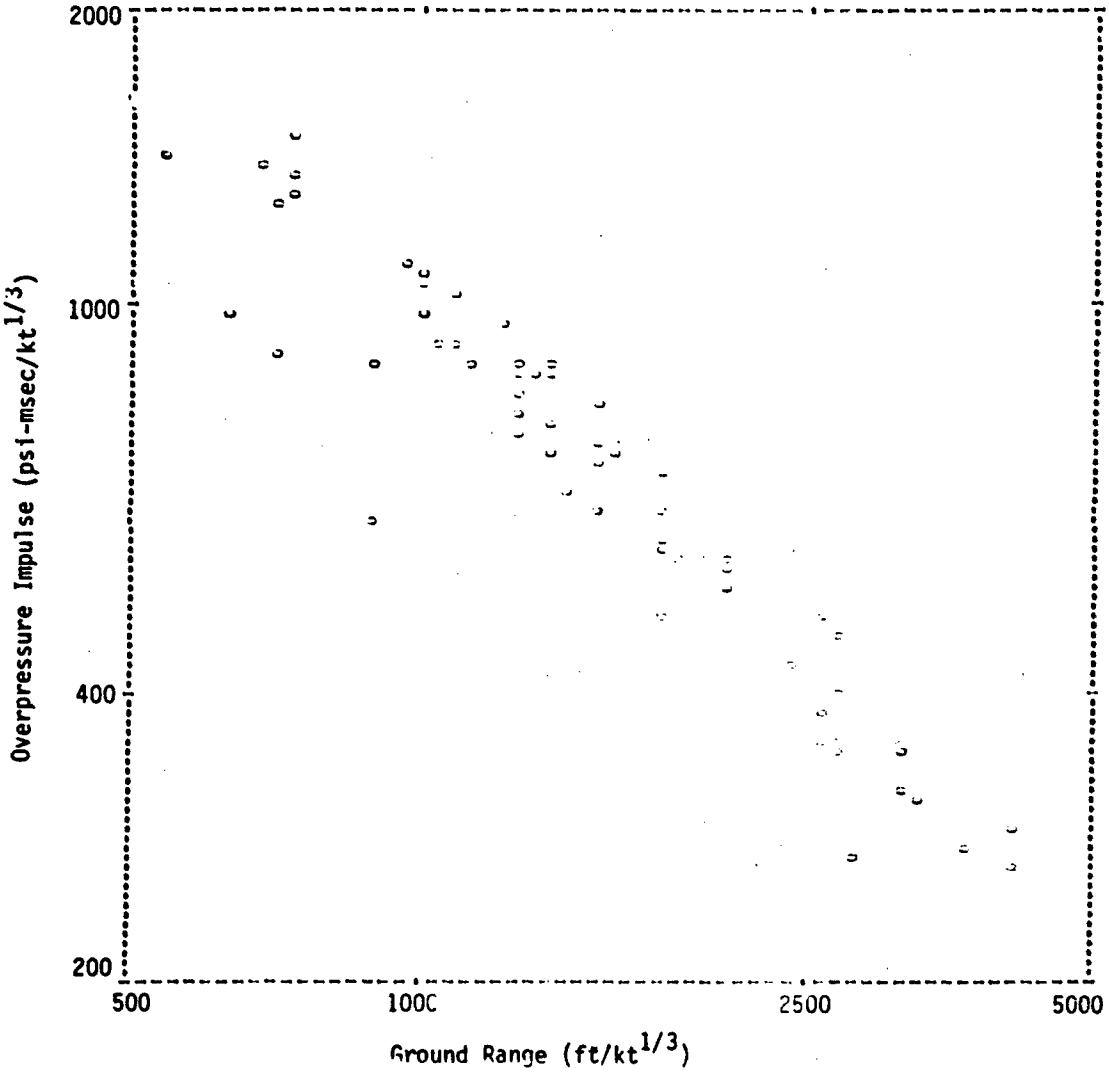

Figure 4.1-17. Overpressure Impulses for 323 to 375 ft, $kt^{1/3}$ HOB

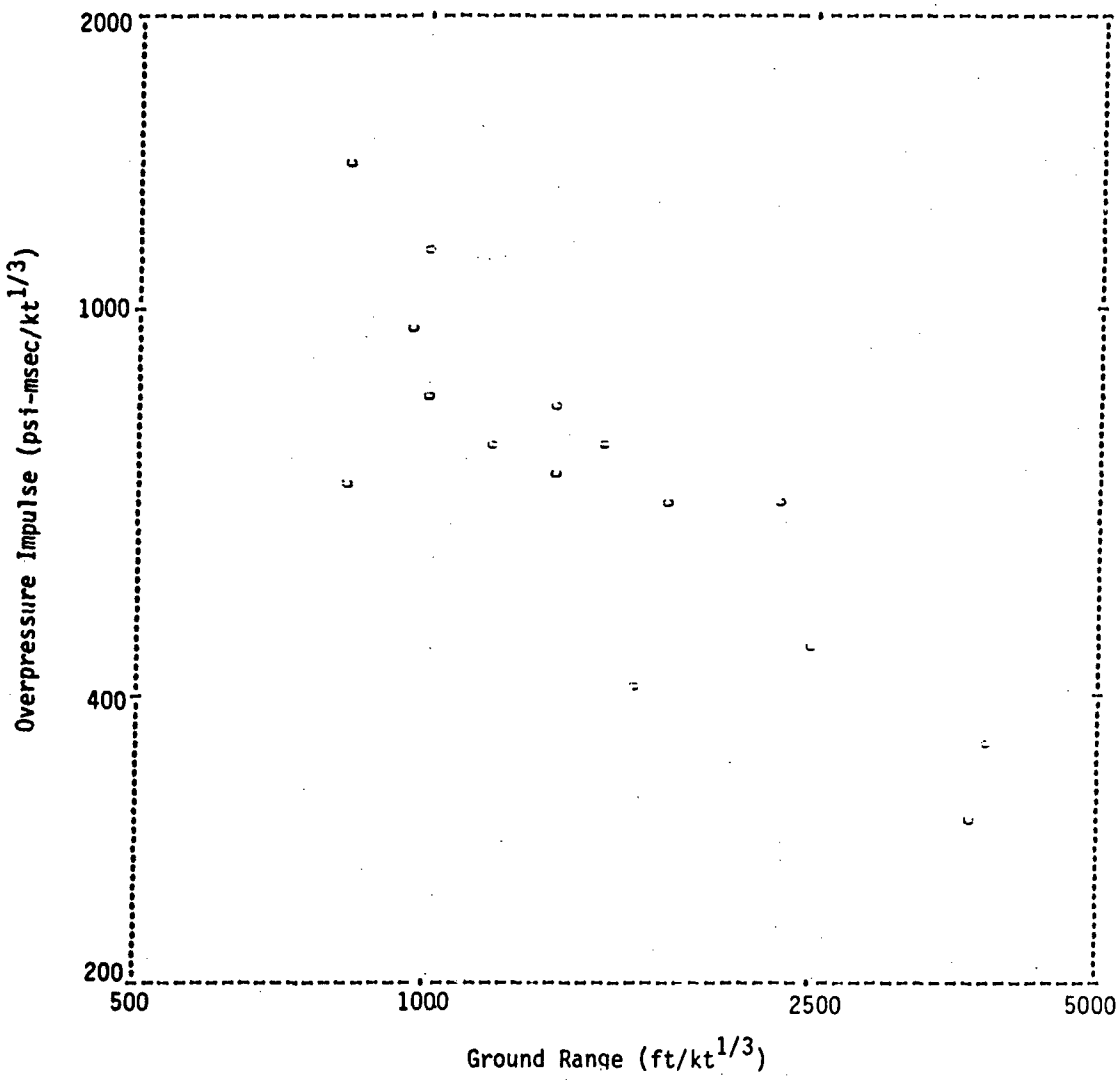

Figure 4.1-18. Overpressure Impulses for 478 to 500 ft/kt$^{1/3}$ HOB

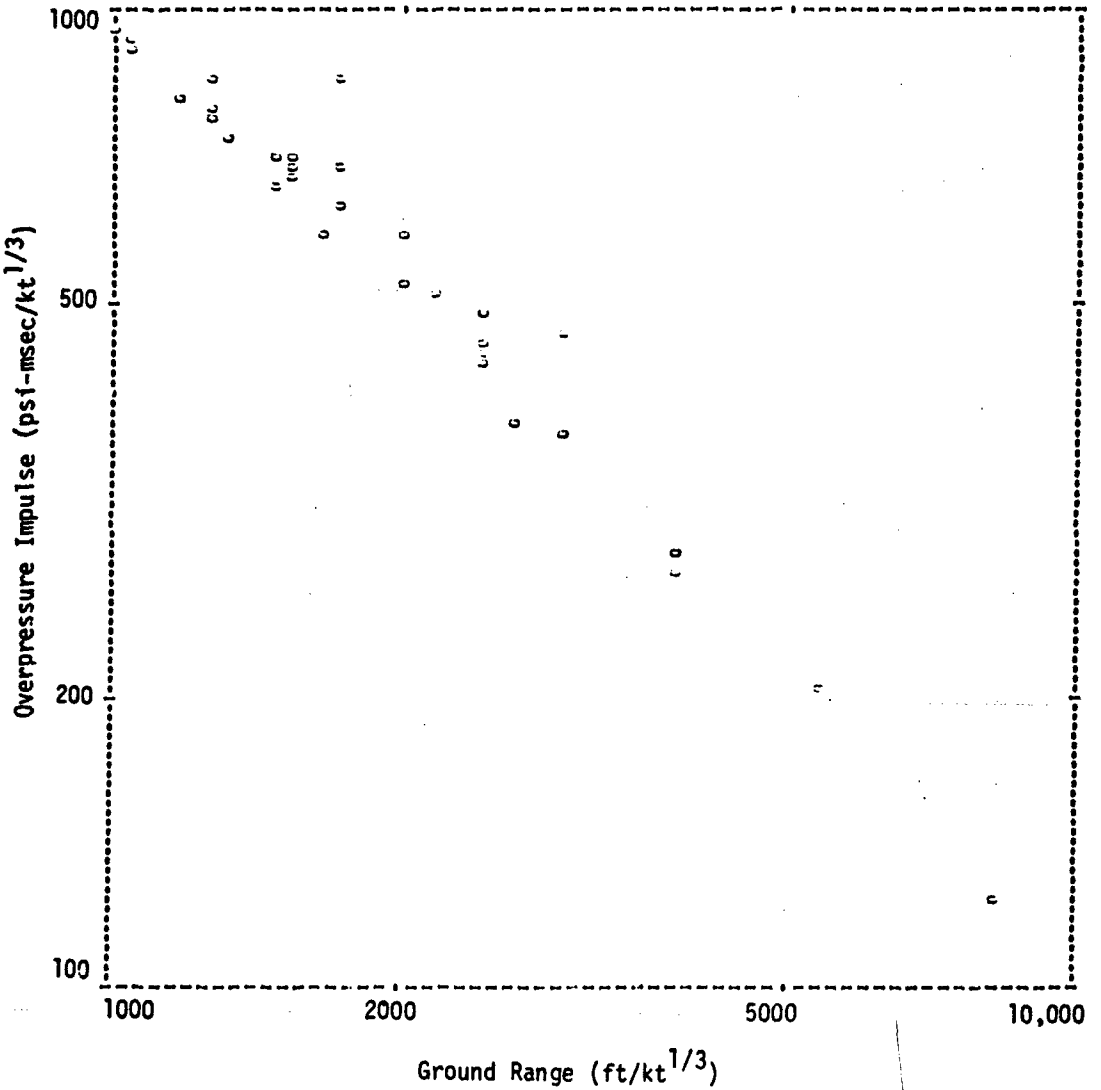

Figure 4.1-19. Overpressure Impulses for 751 to 831 ft/kt$^{1/3}$ HOB

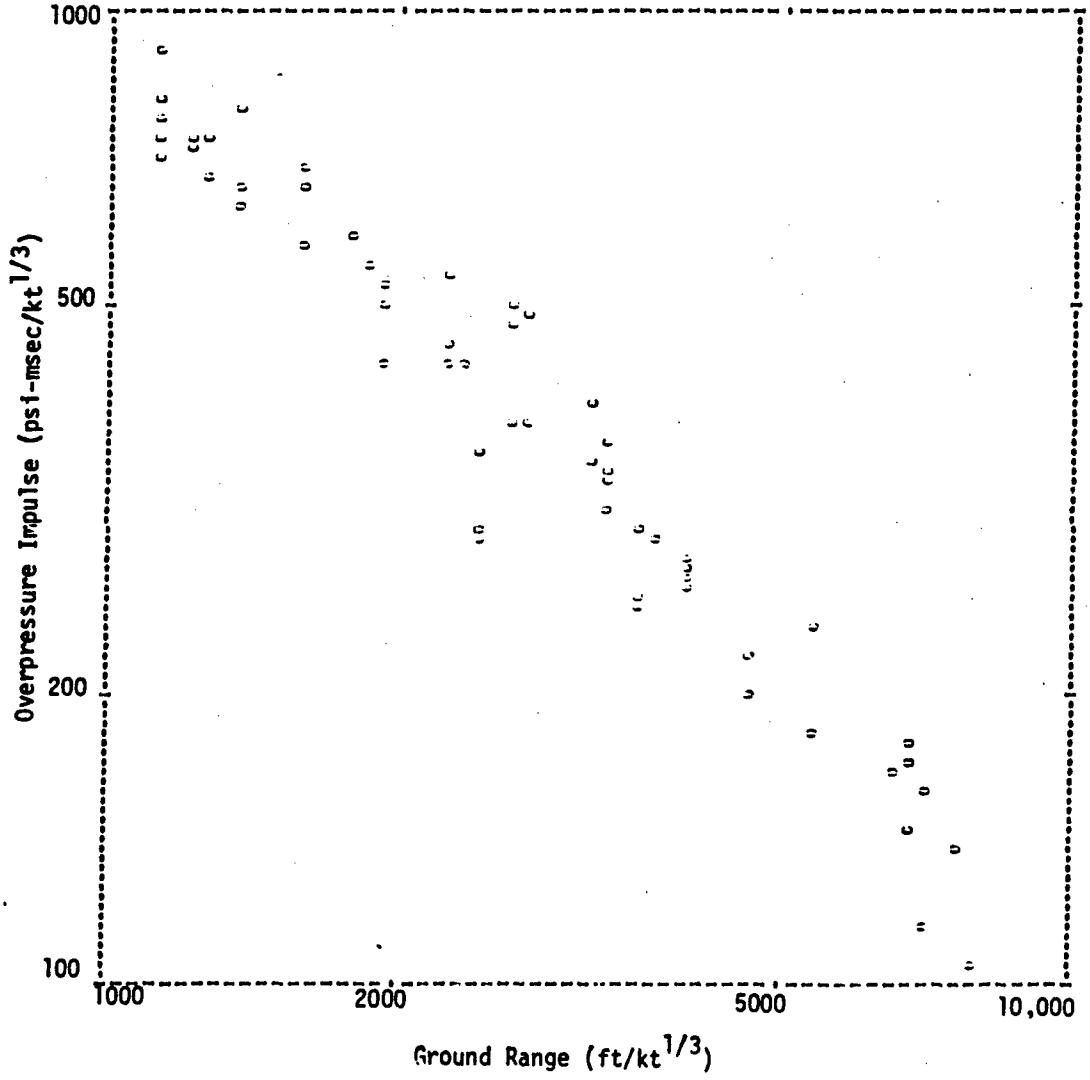

Figure 4.1-20. Overpressure Impulses for 1003 to 1249 ft/kt$^{1/3}$ HOB

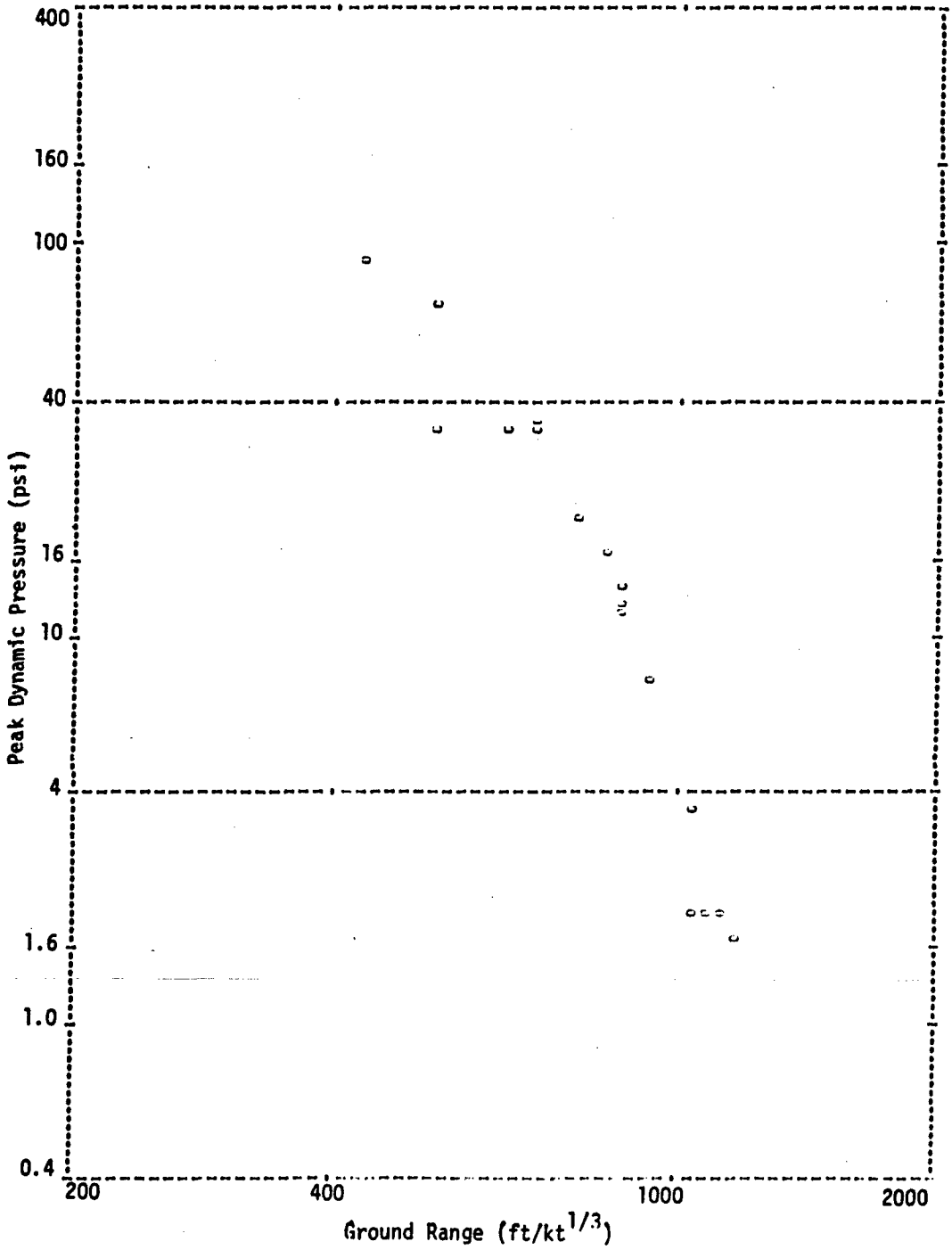

Figure 4.1-21. Peak Dynamic Pressure for 137 and 156 ft/kt$^{1/3}$ HOB (Heavy Dust)

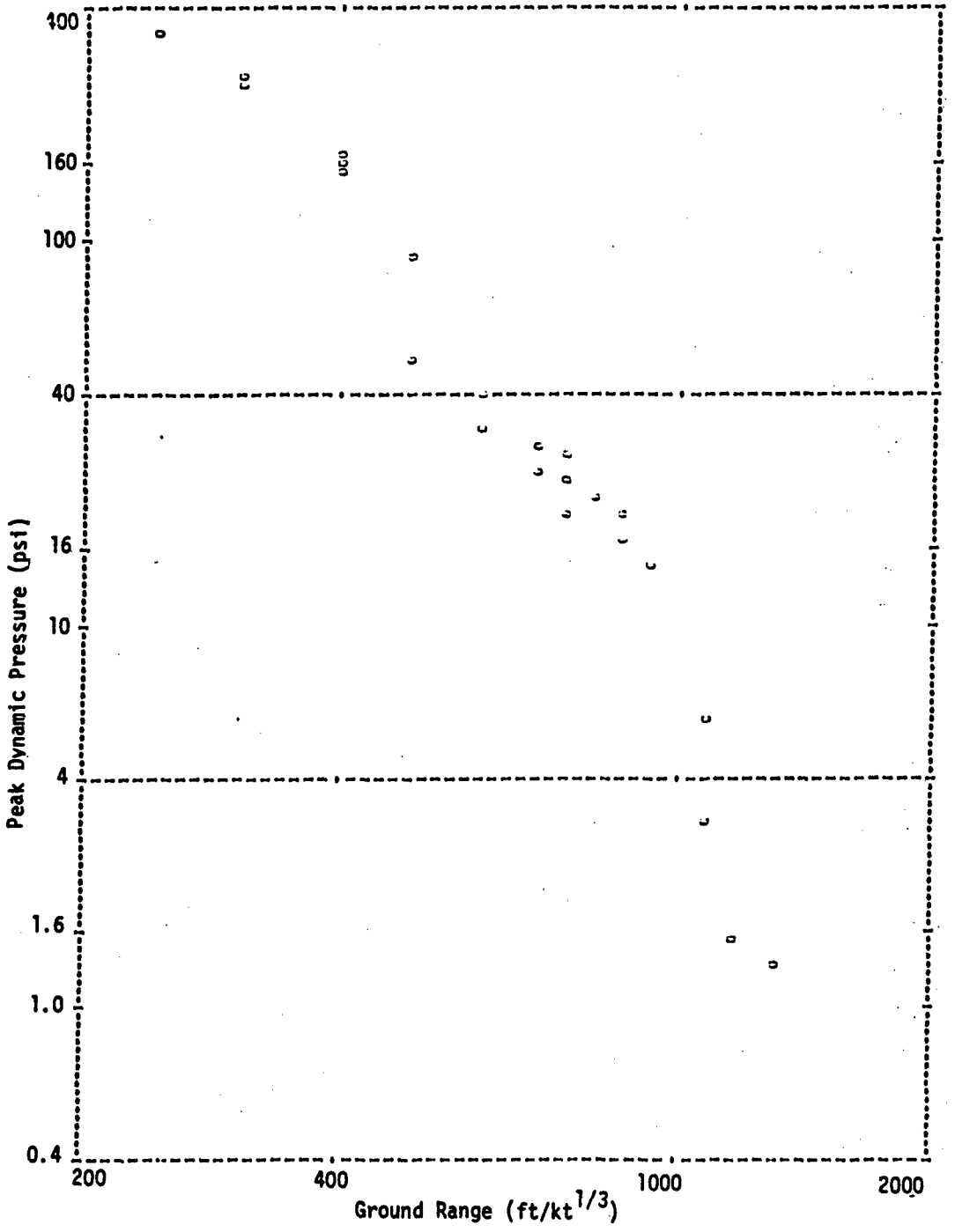

Figure 4.1-22. Peak Dynamic Pressure for 188 and 204 ft/kt$^{1/3}$ HOB (Heavy Dust)

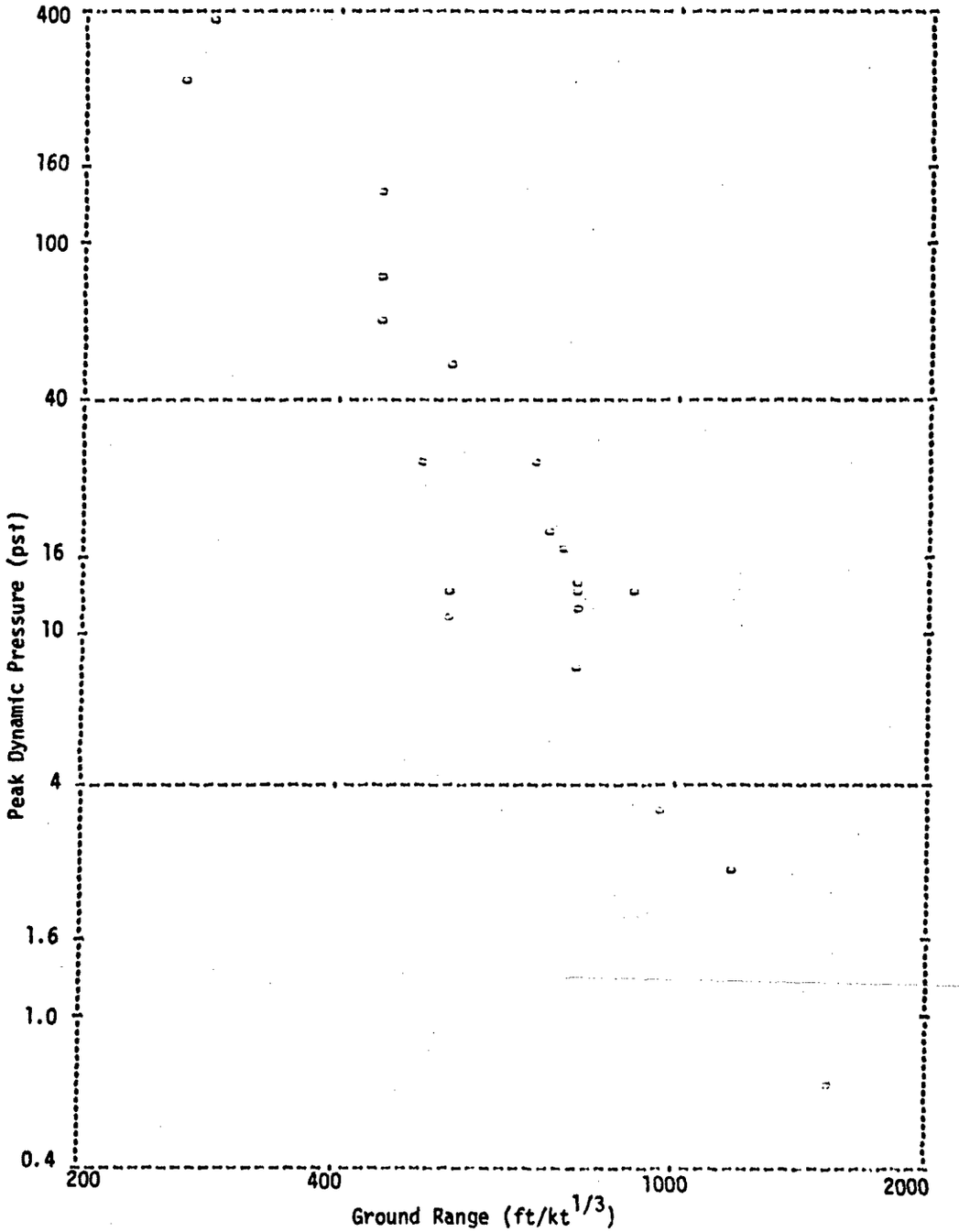

Figure 4.1-23. Peak Dynamic Pressure for 205 to 224 ft/kt$^{1/3}$ HOB (Heavy Dust)

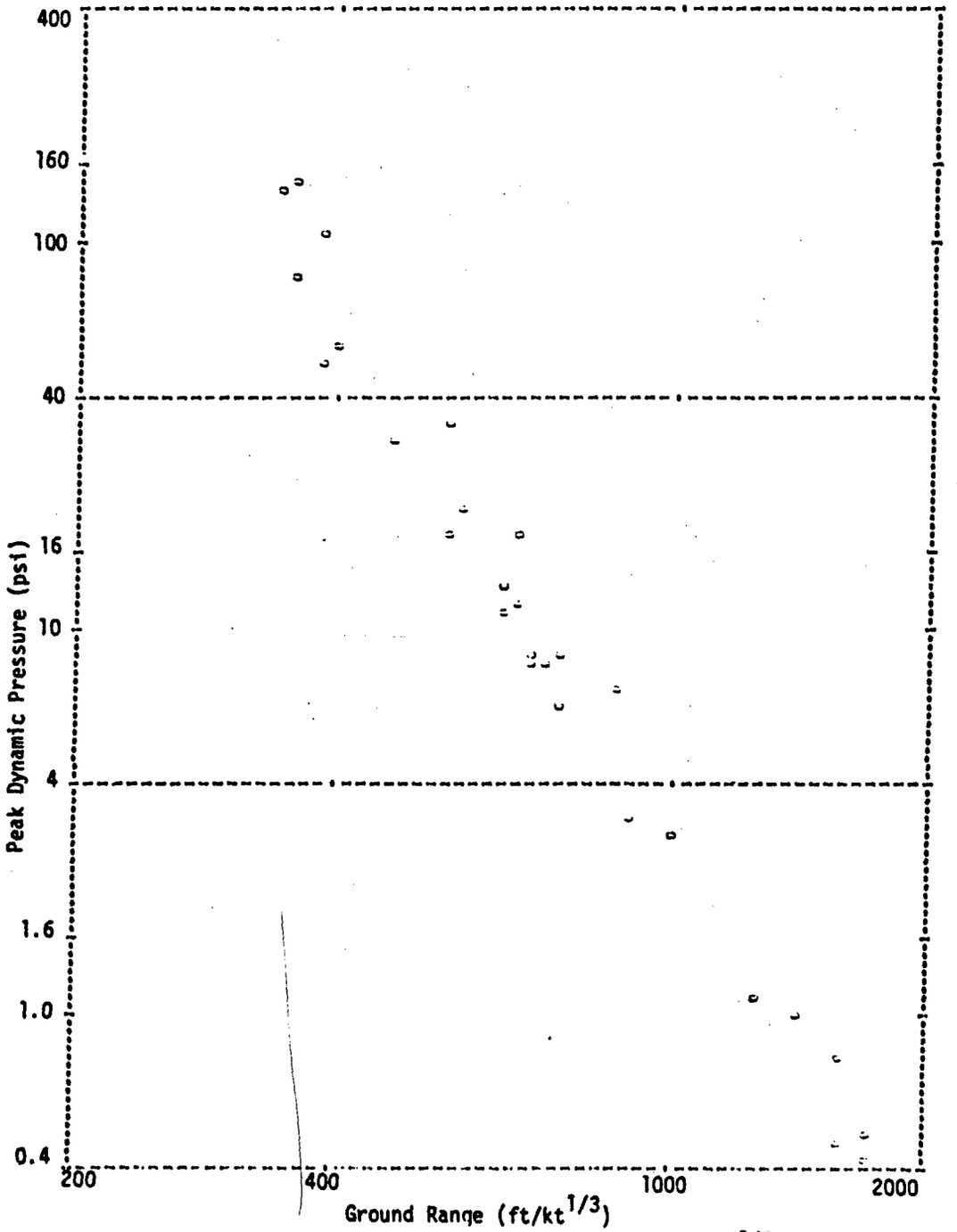

Figure 4.1-24. Peak Dynamic Pressure for 0 to 2.7 ft/kt$^{1/3}$ HOB (Light Dust)

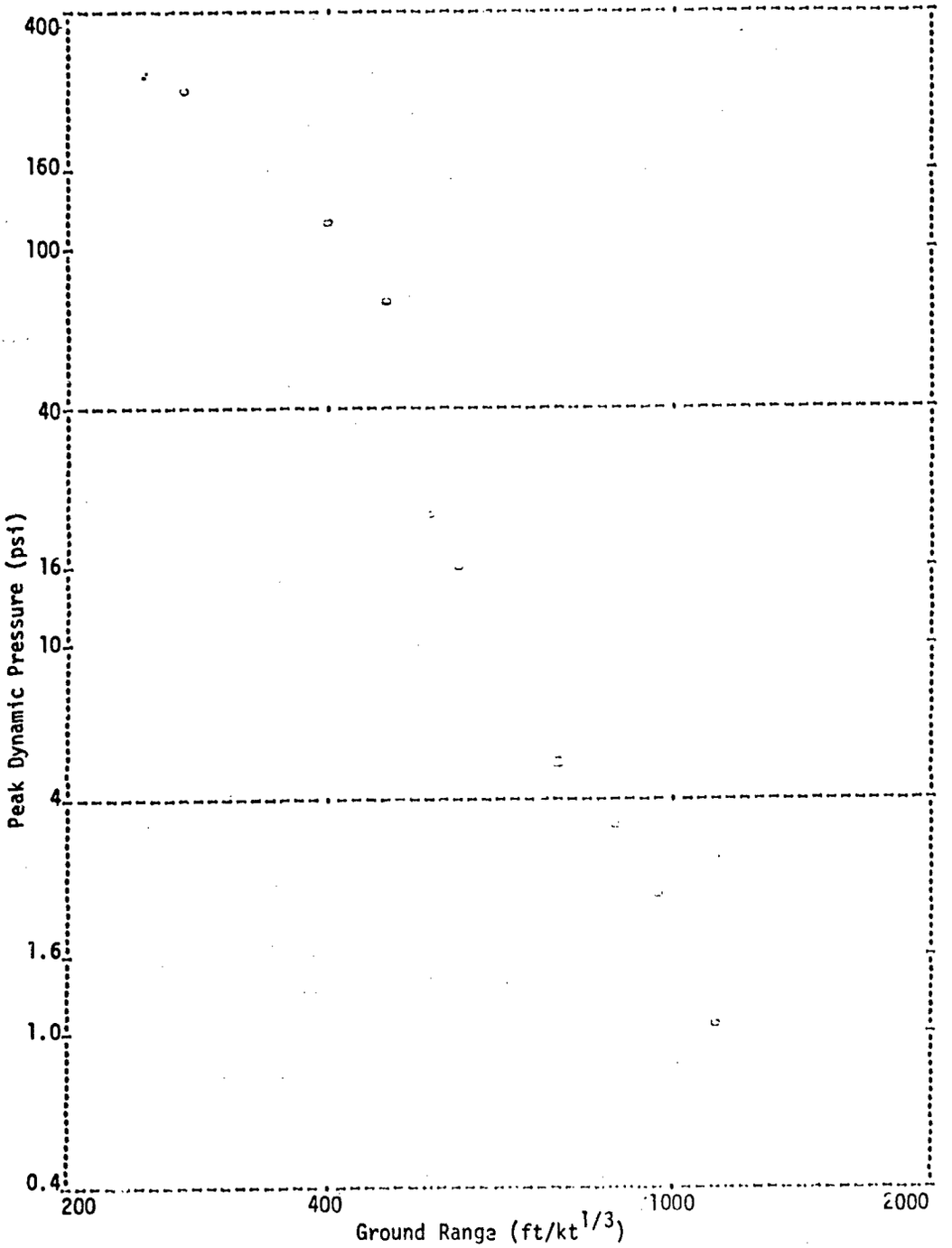

Figure 4.1-25. Peak Dynamic Pressure for 5 ft/kt$^{1/3}$ HOB (Light Dust)

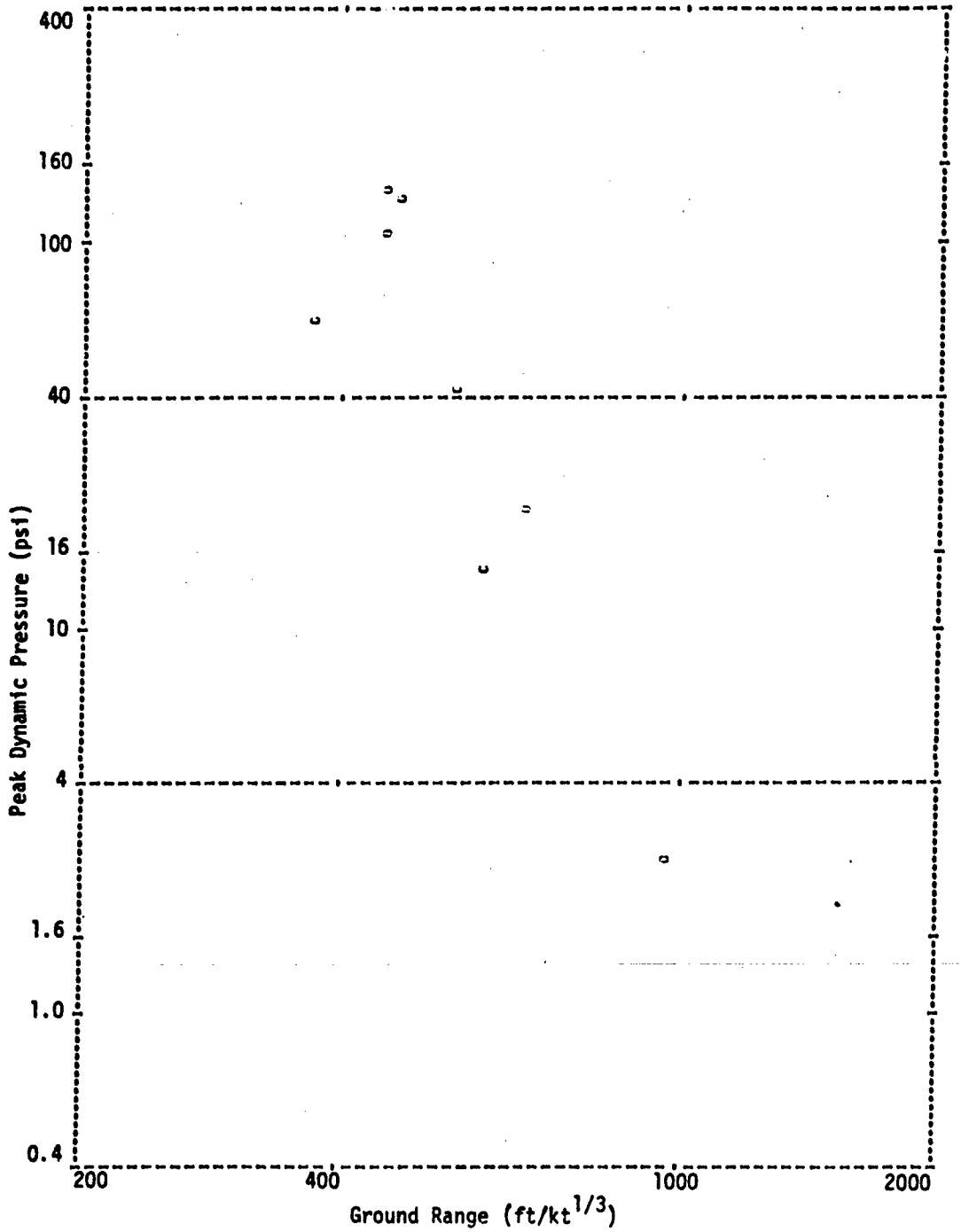

Figure 4.1-26. Peak Dynamic Pressure for 81 and 113 ft/kt$^{1/3}$ HOB (Light Dust)

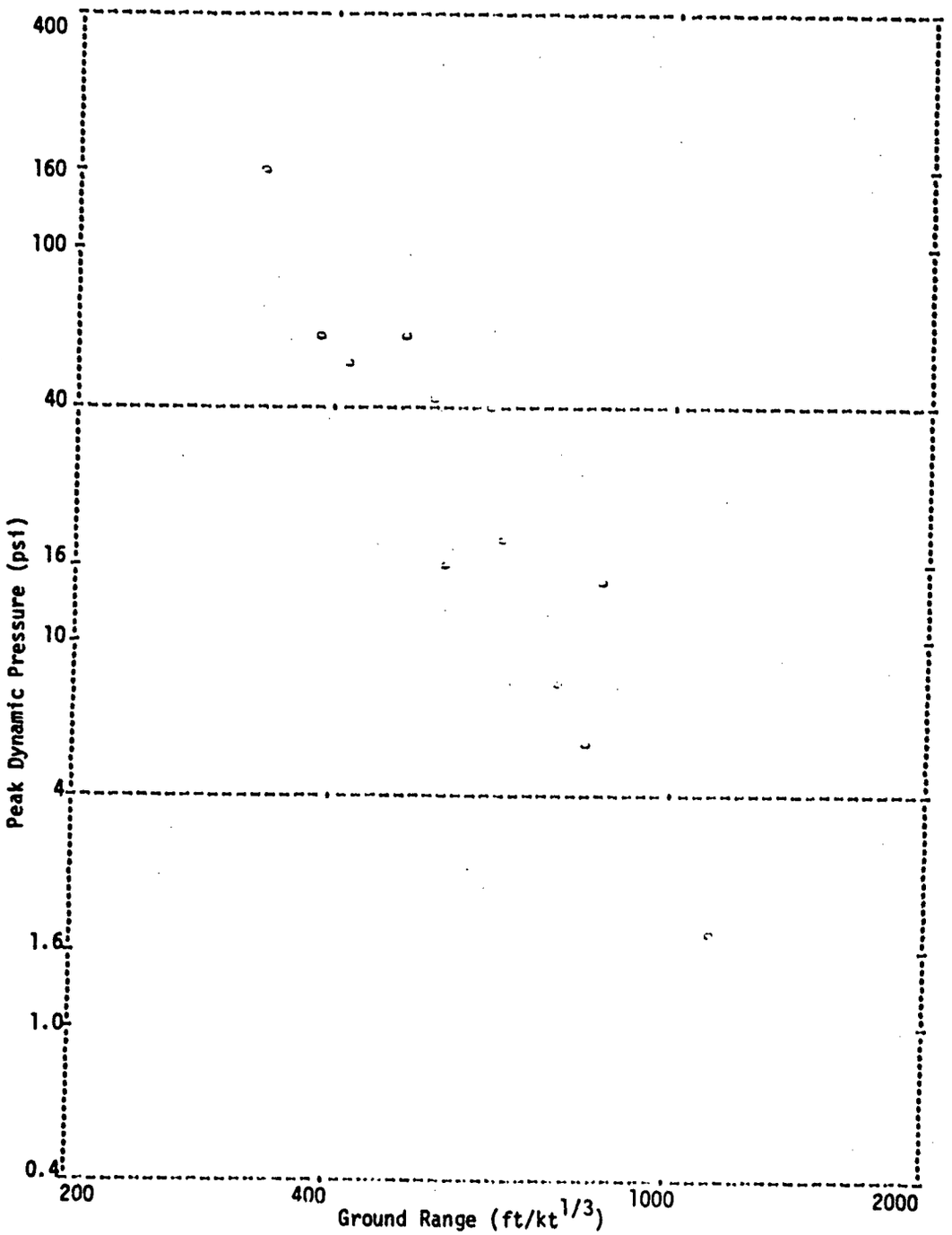

Figure 4.1-27. Peak Dynamic Pressure for 136 to 151 ft/kt$^{1/3}$ HOB (Light Dust)

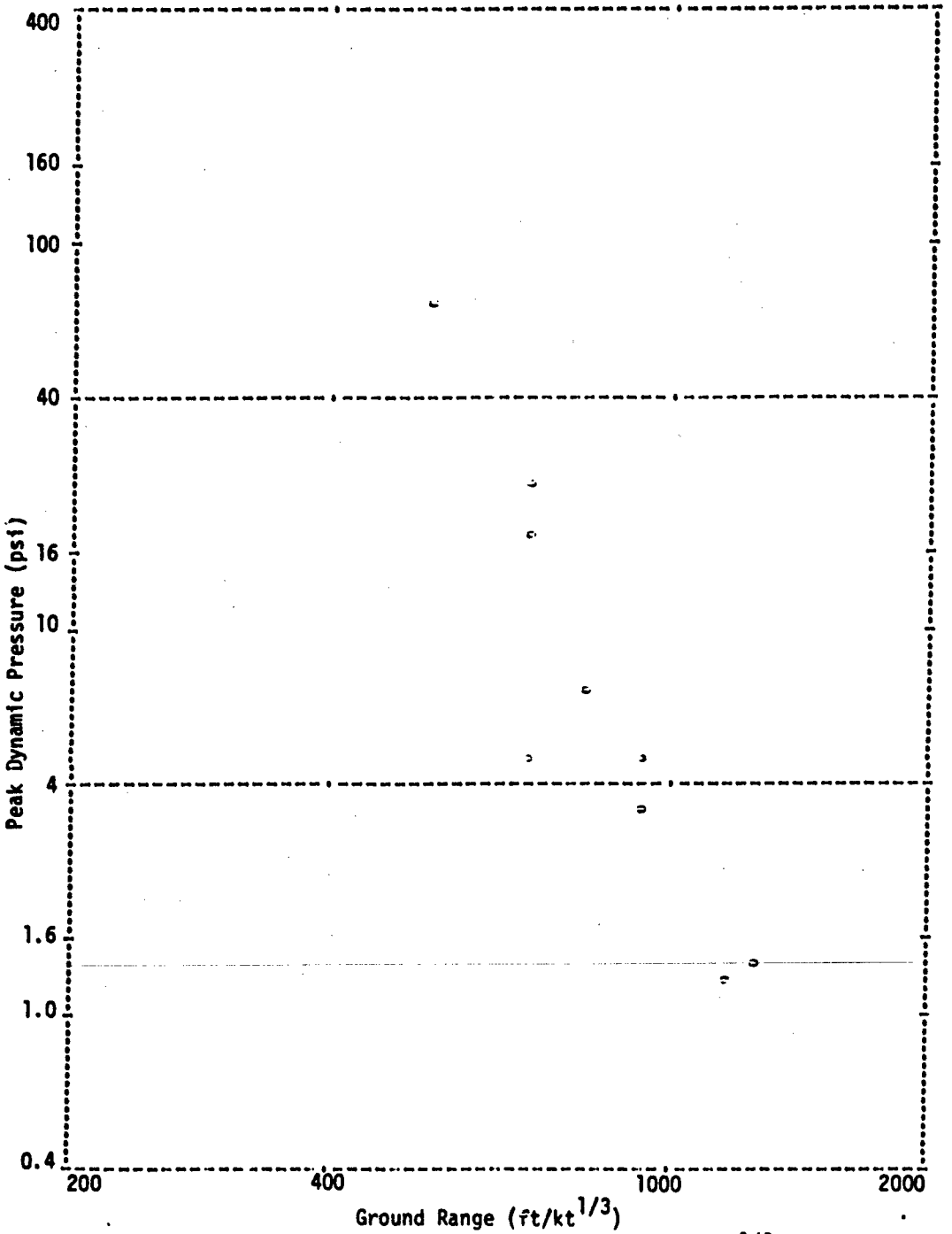

Figure 4.1-28. Peak Dynamic Pressure for 180 to 196 ft/kt$^{1/3}$ HOB (Light Dust)

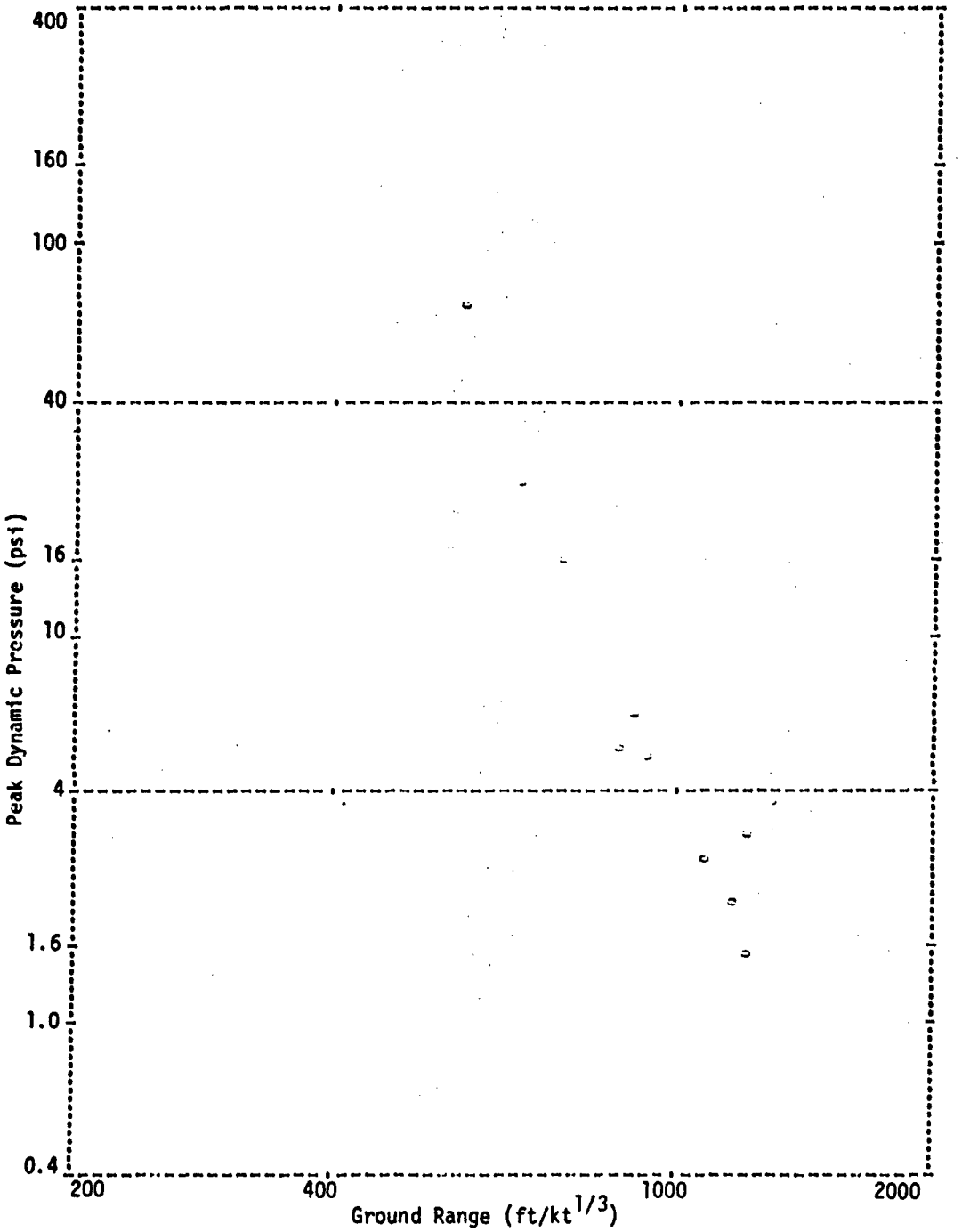

Figure 4.1-29. Peak Dynamic Pressure for 214 to 252 ft/kt$^{1/3}$ HOB (Light Dust)

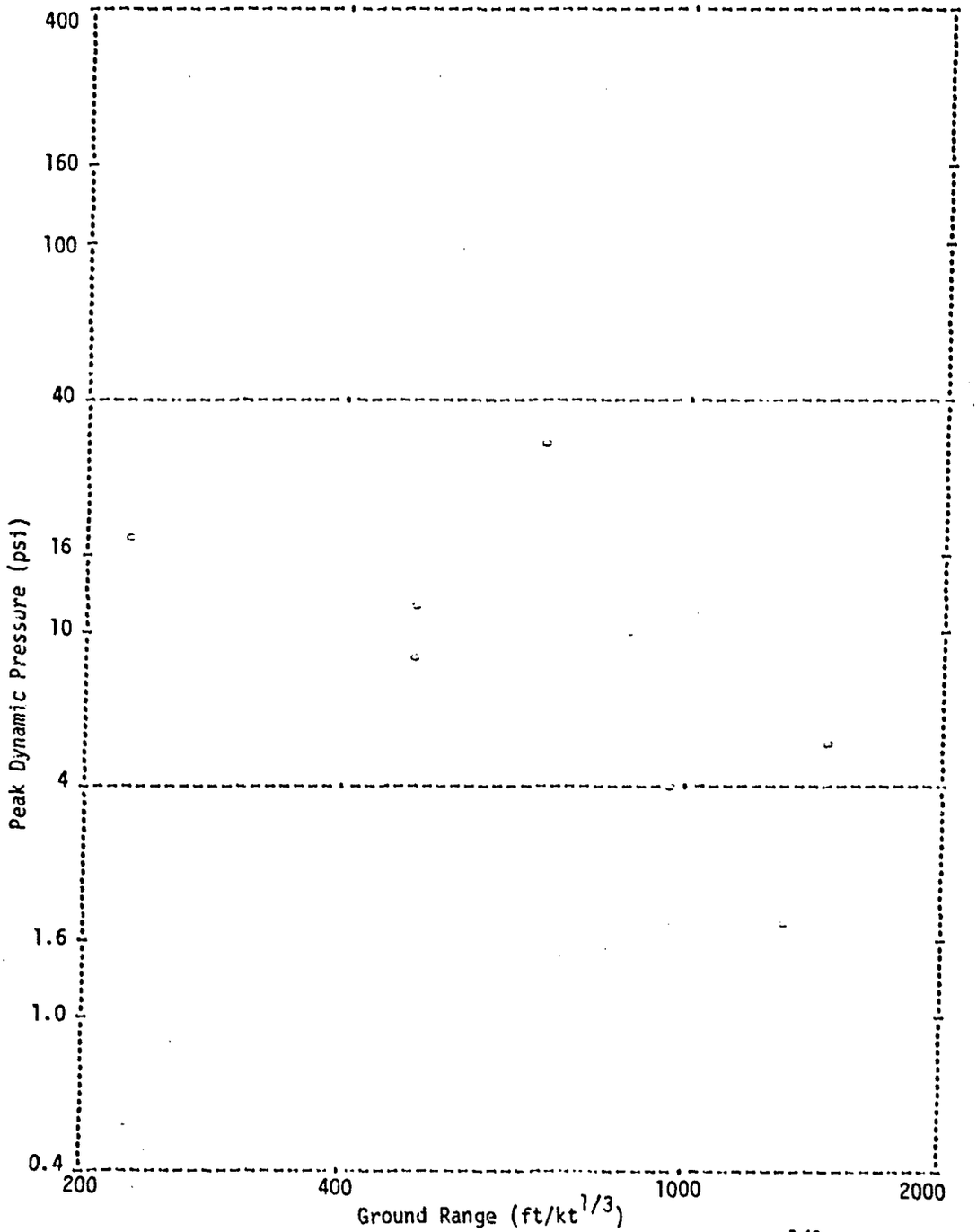

Figure 4.1-30. Peak Dynamic Pressure for 479 and 485 ft/kt$^{1/3}$ HOB (Light Dust)

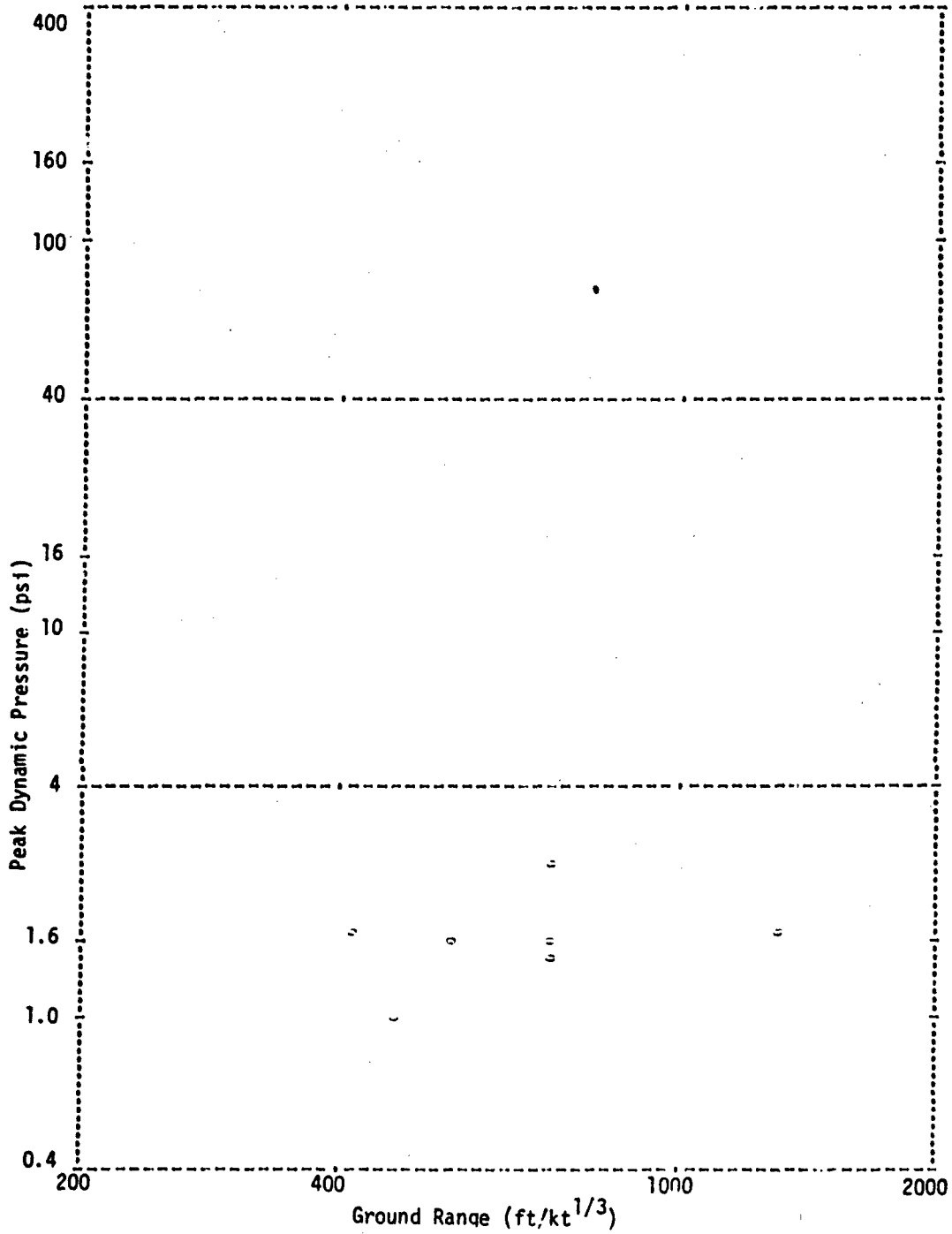

Figure 4.1-31. Peak Dynamic Pressure for 786 ft/kt$^{1/3}$ HOB (Light Dust)

range bins. Both coarse and fine range bins were chosen for this analysis so that any effects that could result from a particular grouping of these data would be illustrated (none were found; see Section 4.2). Bin sizes corresponding to 12 bins per decade and 3 bins per decade were chosen to group these data. To eliminate trends within bins, due to the power law relationship between range and the nuclearly produced environment within the bin, the data within each bin were adjusted by the approximate power law relationship.

Tables 4.1-1 through 4.1-3 present the range error factors computed for each bin for both peak pressures and overpressure impulse and for the scaled HOB ranges shown on the tables. Tables 4.1-1 and 4.1-2 show the range error factors computed by grouping these data into 12 bins per decade for peak overpressure and overpressure impulse, respectively, and Table 4.1-3 presents error factors for both of the above nuclear produced environments and peak dynamic pressure computed by grouping these data into 3 bins per decade. In addition, the tables show the range error factor averaged across SHOB's for each range bin (row averages) and across range bins for each SHOB bin (column averages). These error factors represent the variation in these data upon which the yield ratio measure developed in Section 3 was applied.

To compare the results for the different size bins, range error factors for each bin size were plotted versus range, for each of the scaled HOB's in the tables. Figures 4.1-32 through 4.1-41 show, for each scaled HOB bin, the superimposed plots of range error factor versus range for the peak overpressure data for both bin sizes. Figure 4.1-42 through 4.1-51 are similar plots for overpressure impulses, and Figures 4.1-52 and 53 show range error factors versus range for peak dynamic pressure (combining these light and heavy dust data would be possible since there appears to be no difference in range error factors). These data are summarized in Figure 4.1-54, which shows the average peak overpressure and overpressure impulse range error factors versus range for both types of binning. Figures 4.1-32 through 4.1-54 indicate the following:

- The grouping of these data into bins of various widths does not appear to appreciably affect the estimates of range error factors, since, in practically all cases the 3-bin per decade and 12-bin per decade curves are coincident.

- For peak overpressure and dynamic pressure, the plots of range error factor versus range appear to be constant. For overpressure impulse, there appears to be a slight decrease in range error factor with increasing range.

- The variation in range error factor from bin to bin, and across scaled HOB is not large; there appear to be few anomalous cases.

All of the above observations would suggest that there appear to be few "special cases" where the yield ratio measure would indicate a substantially different conclusion from that based on the measure applied to the average data.

The minimum and maximum range error factor values corresponding to the following combinations of characteristics in Tables 4.1-1 through 4.1-3 were chosen to compute the yield ratio measure:

- The cell minimum and maxiumum for peak overpressure, overpressure impulse, and peak dynamic pressure for 3 and 12 bins per decade.

- The minimum and maximum averaged for each column (corresponding to a particular SHOB) for peak overpressure, overpressure impulse, and peak dynamic pressure, for both types of binning.

- The minimum and maximum averaged for each row (corresponding to a particular range bin) for peak overpressure, overpressure impulse, and peak dynamic pressure, for both types of binning.

Table 4.1-4 presents both the range error factor and the yield ratio measure for these characteristic data. The yield ratio measures larger than 10 percent (i.e., that would suggest a possible maximum 10 percent or larger reduction in yield through additional underground environments testing) are displayed in Table 4.1-5 along with a brief discussion of the possible tactical significance of effecting a yield reduction.

Table 4.1-1 RANGE ERROR FACTORS PEAK OVERPRESSURE (12 BINS/DECADE)

R_o \ SHOB	0-3.1	(5-11)*	(55-83)*	(113-157)*	182-205	212-252	323-375	751-831	1003-1249	ROW AVE
237 (261)	1.11	1.05	-	-	1.10					1.09
287 (316)	1.14	1.28	-	-	1.05					1.16
348 (383)	1.10	1.17	-	-	1.10					1.12
422 (464)	1.11	-	1.27	-	1.14	1.12				1.17
511 (562)	1.13	1.14	1.17	1.29	1.16	1.22	1.06			1.17
620 (681)	1.07	1.12	1.21	1.33	1.22	1.22	-			1.20
750 (826)	1.11	1.06	1.23	1.14	1.28	1.25	1.25			1.21
909 (1000)	1.09	1.14	1.19	1.24	1.23	1.14	1.14			1.18
1101 (1212)	1.17	-	1.18	1.12	1.17	1.15	1.18			1.17
1334 (1468)	1.09	1.11	1.13	1.15	1.14	1.13	1.13	1.08		1.12
1616 (1778)	1.07	-	-	-	1.07	-	1.12	1.09		1.09
1957 (2154)	1.11	-	-	-	1.15	-	1.13	-		1.13
2371 (2610)	1.15	-	-	-	-	-	1.04	1.09	1.17	1.14
2873 (3162)	1.04	-	-	-	-	-	1.16		1.11	1.12
COLUMN AVERAGES	1.11	1.15	1.20	1.24	1.17	1.18	1.14	1.09	1.14	1.17

* Use ranges in parentheses

Table 4.1-2 RANGE ERROR FACTORS OVERPRESSURE IMPULSE (12 BINS/DECADE)

R_o \ SHOB	0-3.1	(5-11)*	(55-83)*	(113-157)*	182-205	212-252	323-375	751-831	1003=1249	ROW AVE
237 (261)	1.65	1.42	-	-	1.52					1.54
287 (316)	1.57	1.59	-	-	1.35					1.49
348 (383)	1.49	1.41	-	-	1.20					1.43
422 (464)	1.15	-	1.53	-	1.32	1.23				1.33
511 (562)	1.71	1.52	1.34	1.52	1.43	1.14	1.18			1.44
620 (681)	1.17	1.36	1.48	1.32	1.20	1.30	-			1.32
750 (826)	1.69	1.11	1.40	1.08	1.23	1.25	1.42			1.37
909 (1000)	1.26	1.21	1.18	1.14	1.21	1.12	1.58			1.22
1101 (1212)	1.41	-	1.28	1.14	1.38	1.15	1.15			1.28
1334 (1468)	1.17	1.16	1.20	1.06	1.16	1.11	1.15	1.08		1.15
1616 (1778)	1.16	-	-	-	1.02	-	1.24	1.24		1.19
1957 (2154)	2.18	-	-	-	1.27	-	1.11	-		1.64
2371 (2610)	1.30	-	-	-	-	-	1.21	1.07	1.42	1.29
2873 (3162)	1.22	-	-	-	-	-	1.28	-	1.22	1.25
COLUMN AVERAGES	1.47	1.39	1.36	1.26	1.31	1.20	1.25	1.18	1.33	1.35

* Use ranges in parentheses

Table 4.1-3 RANGE ERROR FACTORS - PEAK OVERPRESSURE, OVERPRESSURE IMPULSE, AND PEAK DYNAMIC PRESSURE (3 BINS/DECADE)

SHOB / R_o	0-3.1	5-11	55-83	113-157	182-204	(212-252) *	323-375	(478-500) *	751-831	1003-1249	ROW AVG
316 (464)	1.13 1.51 L1.14	1.21 1.44	1.21 1.61	1.30 1.41	1.11 1.38	1.19 1.24 H1.32					1.17 1.43 L1.14 H1.32
681 (1000)	1.10 1.49 L1.11	1.13 1.36 L1.14	1.22 1.41 L1.21	1.30 1.37 L1.22 H1.14	1.23 1.27 L1.27 H1.22	1.34 1.21 L1.11 H1.14	1.26 1.40	1.17 1.51 L1.34			1.23 1.36 L1.19 H1.16
1467 (2154)	1.19 1.57 L1.14	1.13 1.18	1.20 1.21	1.19 1.12 H1.10	1.20 1.27 H1.19	1.17 1.08	1.20 1.15	1.16 1.58	1.28 1.19 L1.15		1.20 1.28 L1.15 H1.17
3162 (4642)	1.18 1.25	1.22 1.67	- -	- -	1.19 1.22	- -	1.25 1.22	- -	1.15 1.15	1.14 1.30	1.18 1.28
6182 (10000)	1.51 1.22	- -	- -	- -	- -	- -	- -	1.59 1.12	- -	1.45 1.24	1.51 1.21
COLUMN AVERAGES	1.18 1.46 L1.12	1.17 1.39 L1.14	1.22 1.37 L1.21	1.27 1.33 L1.22 H1.13	1.19 1.30 L1.27 H1.20	1.28 1.21 L1.11 H1.23	1.23 1.24	1.37 1.41 L1.34	1.25 1.18 L1.15	1.26 1.28	1.22 1.35 L1.18 H1.19

* Use ranges in parentheses

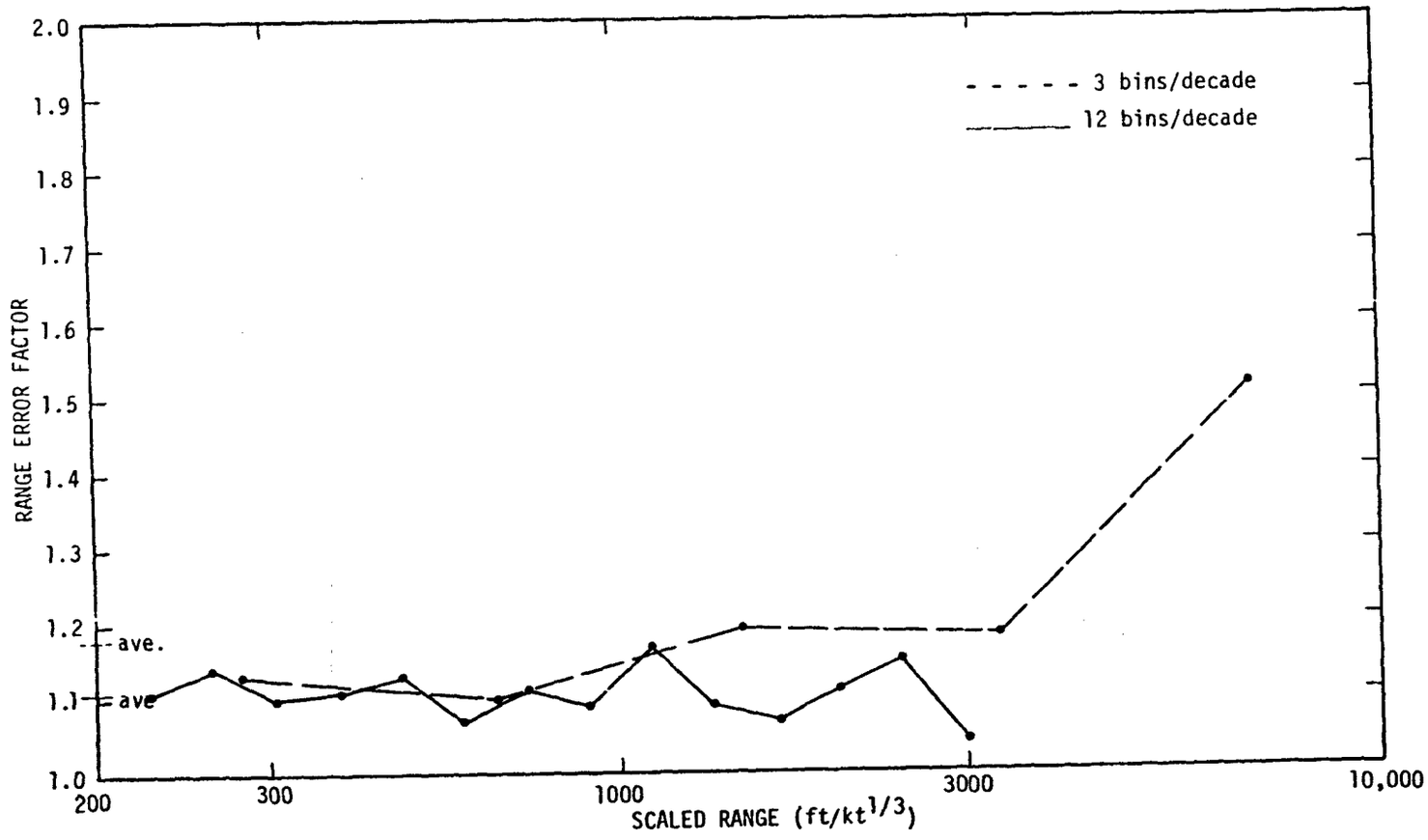

Figure 4.1-32. Range Error Factor vs. Scaled Range
SHOB: 0-3.1 ft (Peak Overpressure)

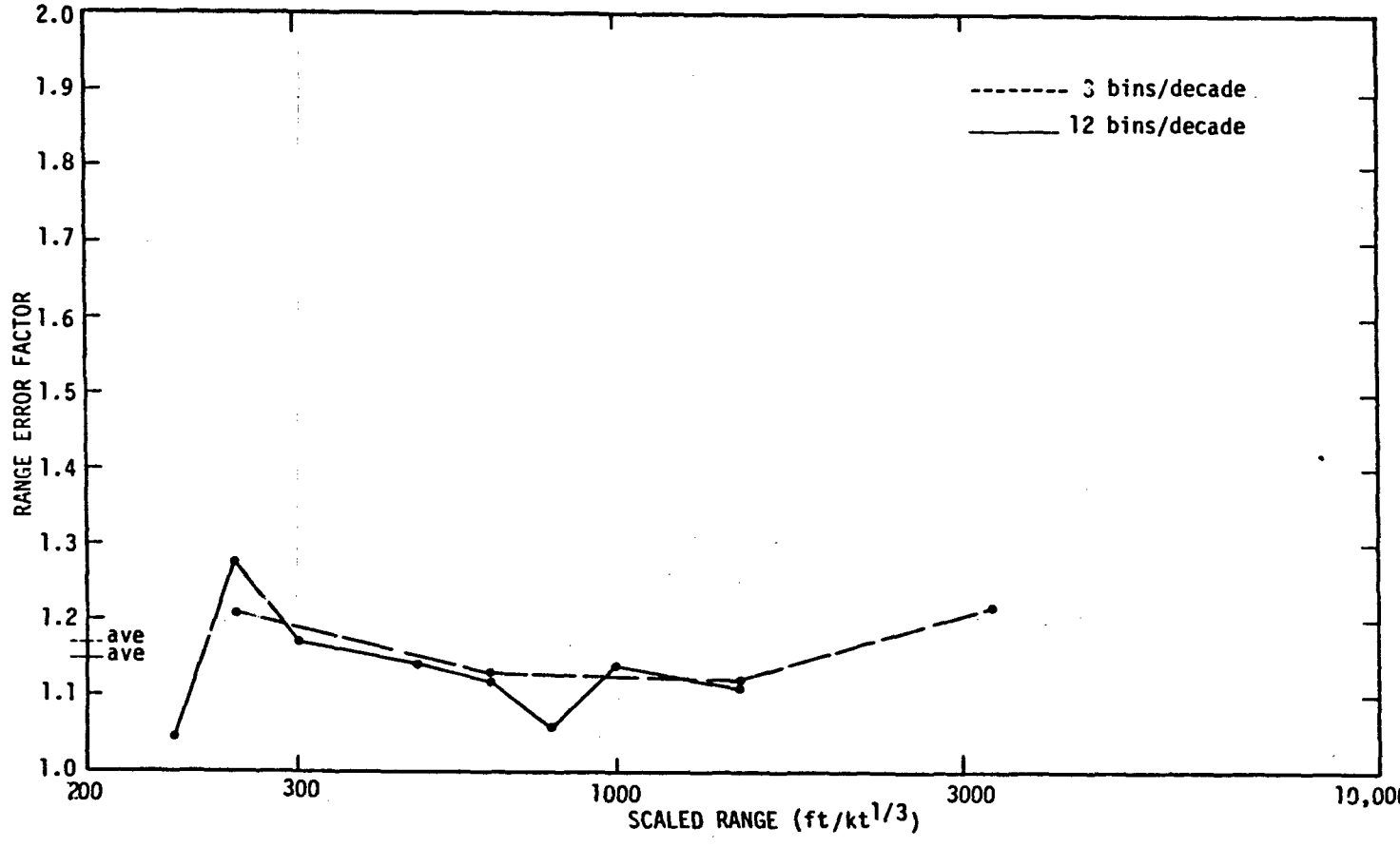

Figure 4.1-33. Range Error Factor vs. Scaled Range
SHOB: 5-11 ft (Peak Overpressure)

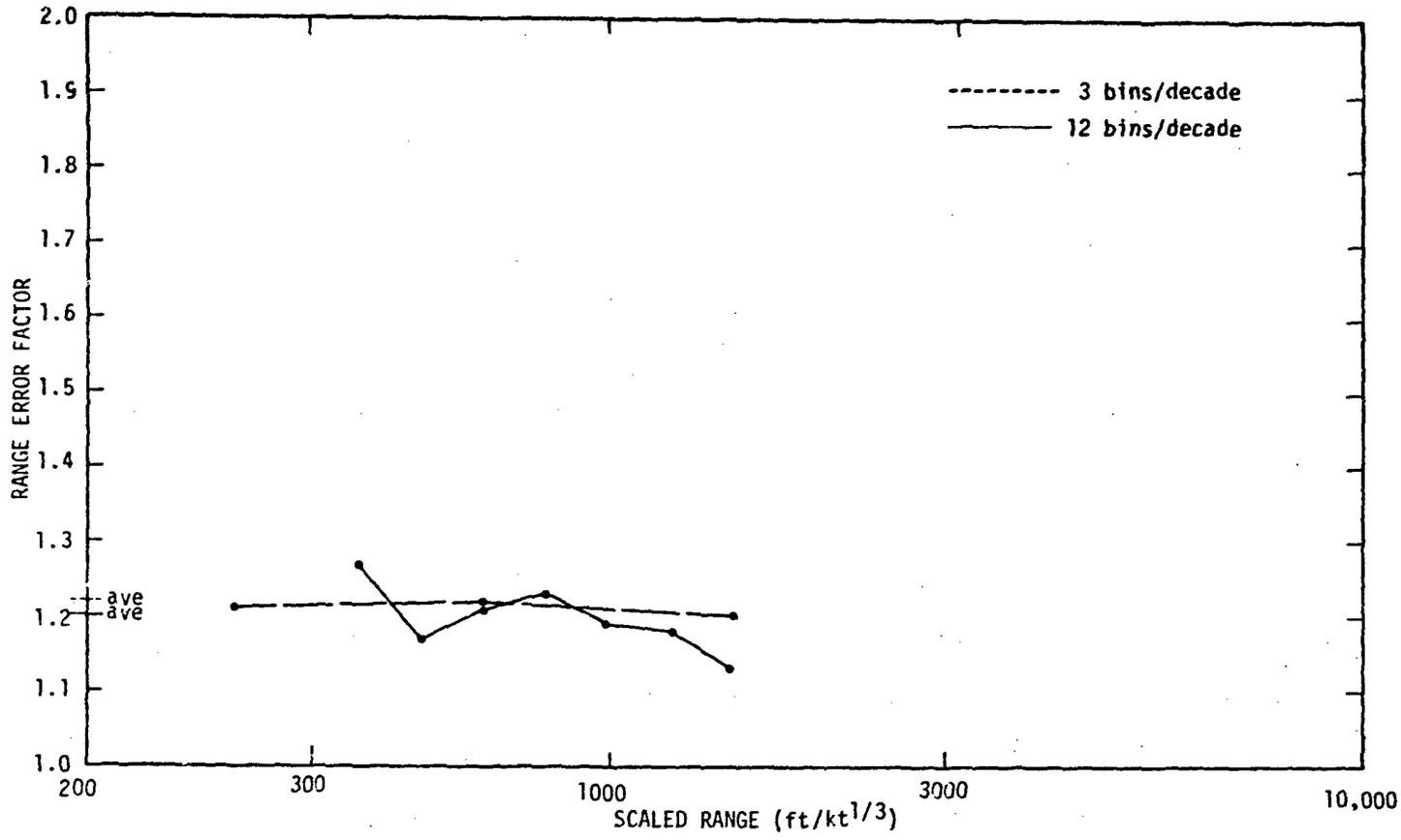

Figure 4.1-34. Range Error Factor vs. Scaled Range
SHOB: 55-83 ft (Peak Overpressure)

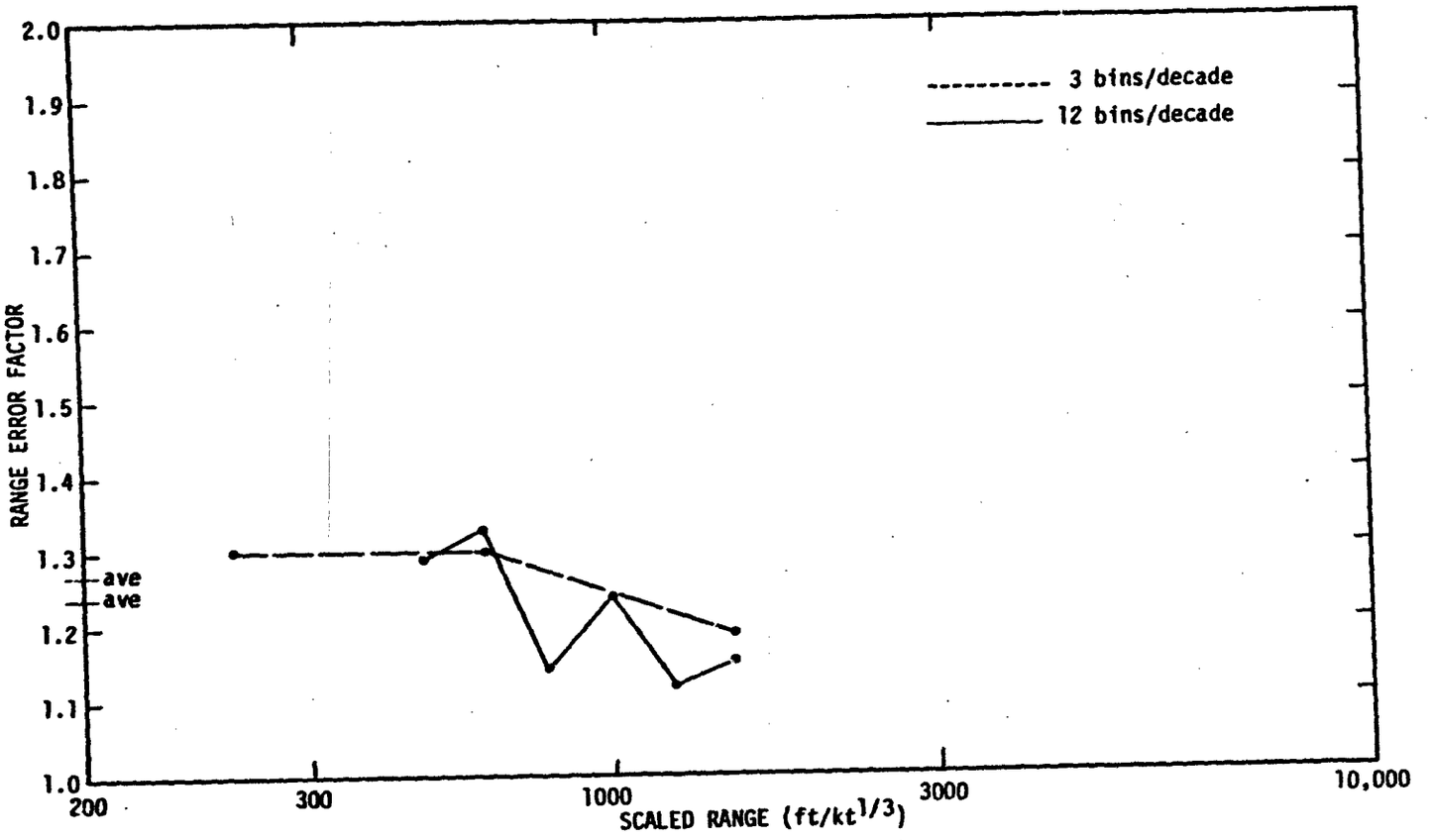

Figure 4.1-35. Range Error Factor vs. Scaled Range
SHOB: 113-157 ft (Peak Overpressure)

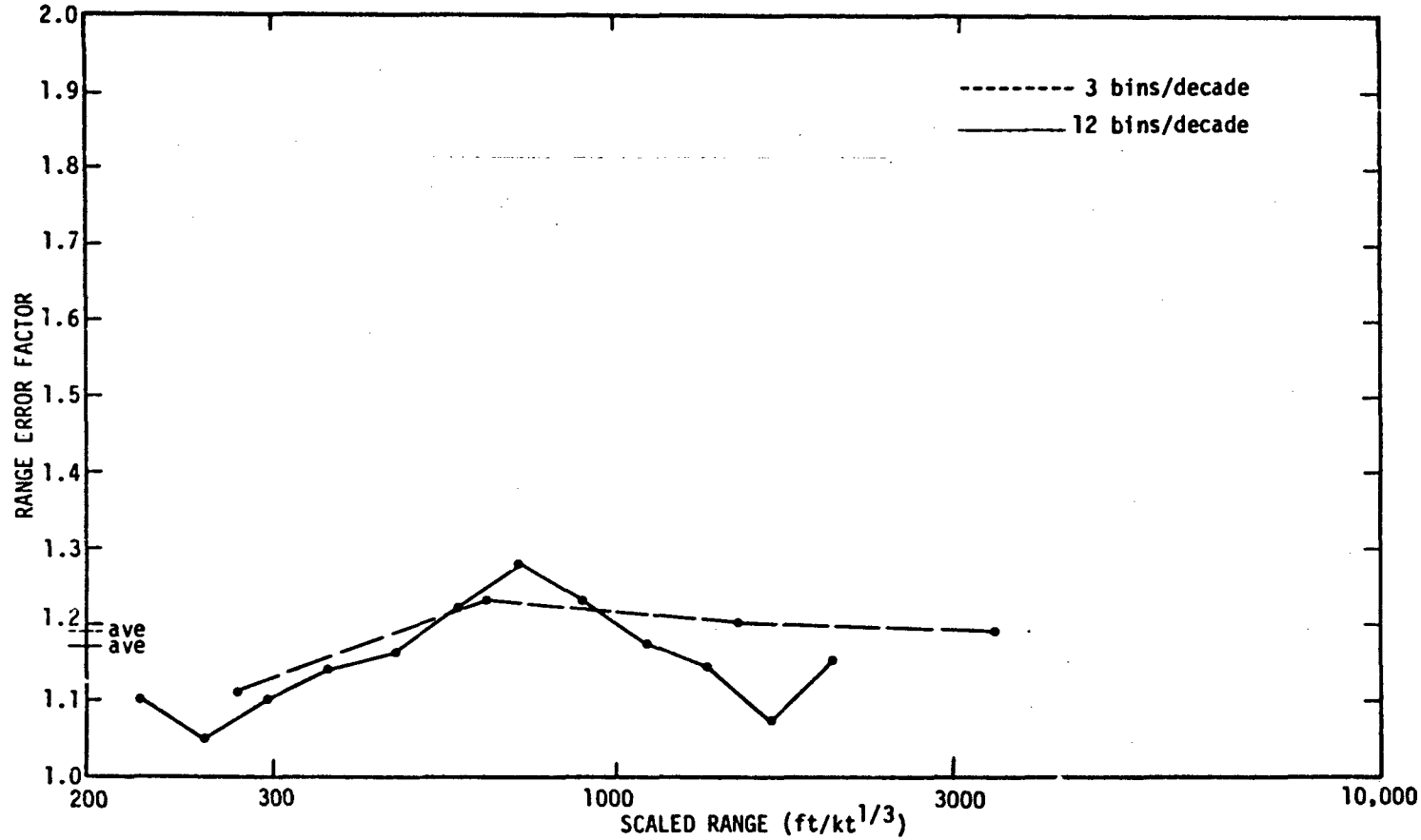

Figure 4.1-36. Range Error Factor vs. Scaled Range
SHOB: 182-205 ft (Peak Overpressure)

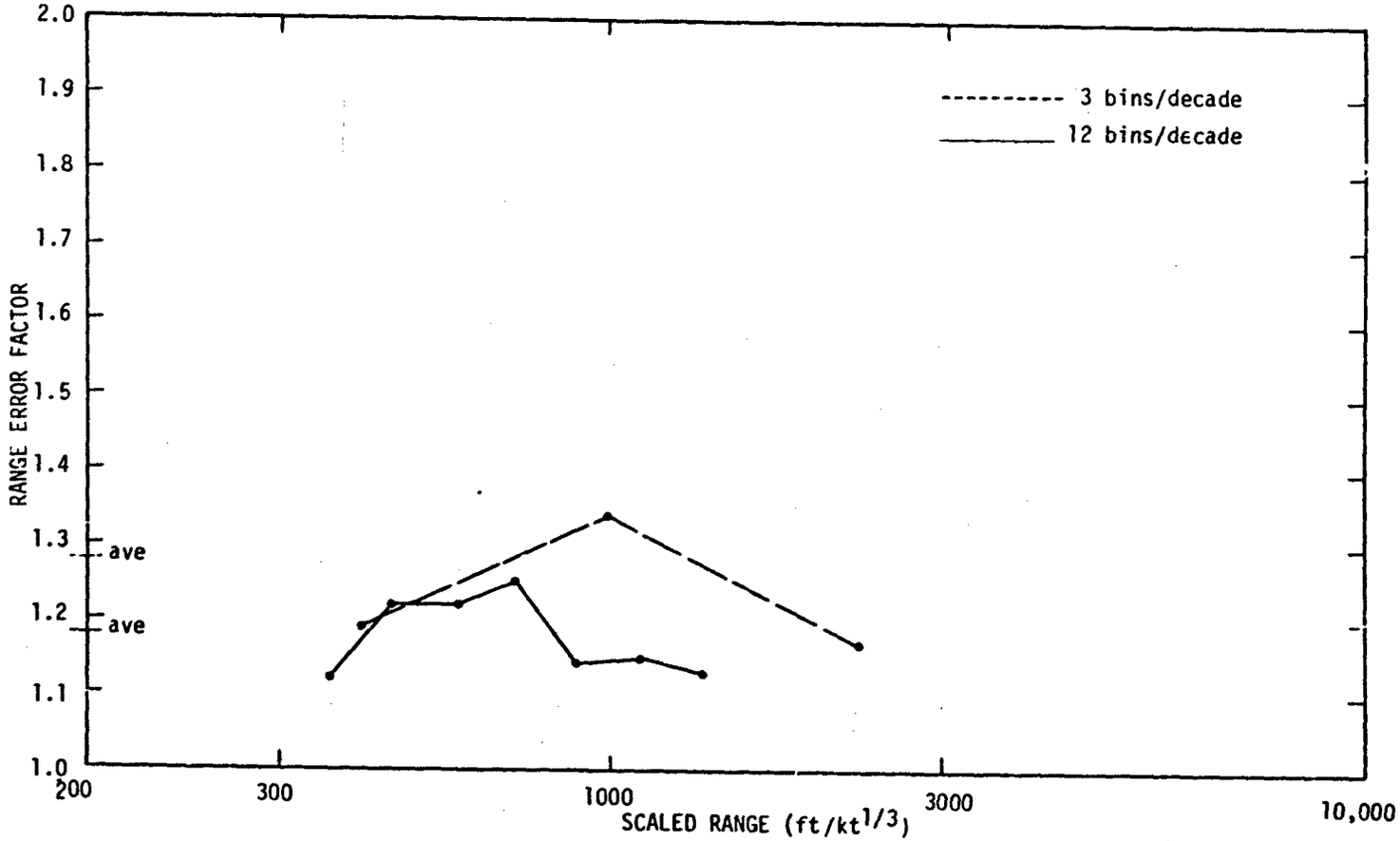

Figure 4.1-37. Range Error Factor vs. Scaled Range
SHOB: 212-252 ft (Peak Overpressure)

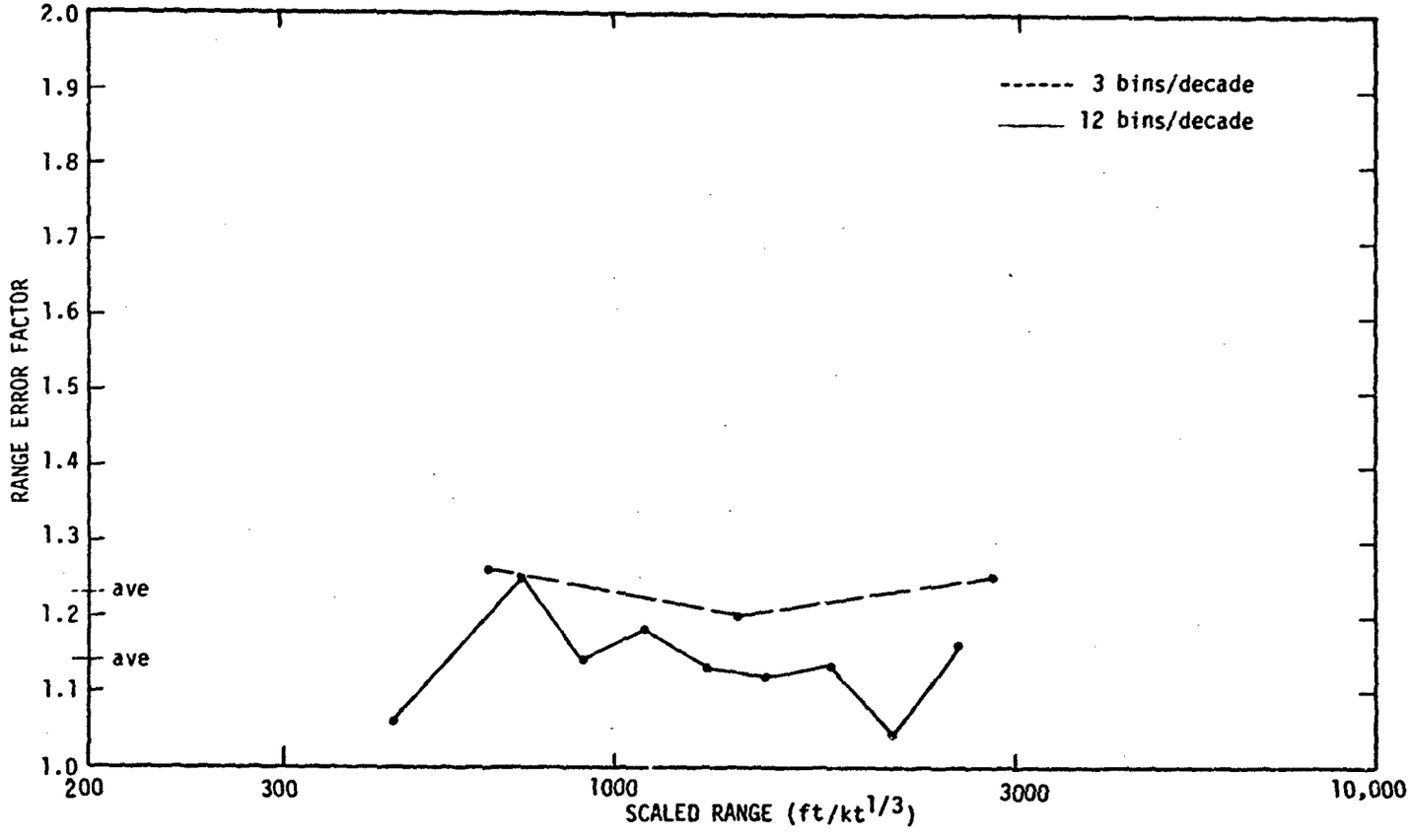

Figure 4.1-38 Range Error Factor vs. Scaled Range
SHOB: 323-375 ft (Peak Overpressure)

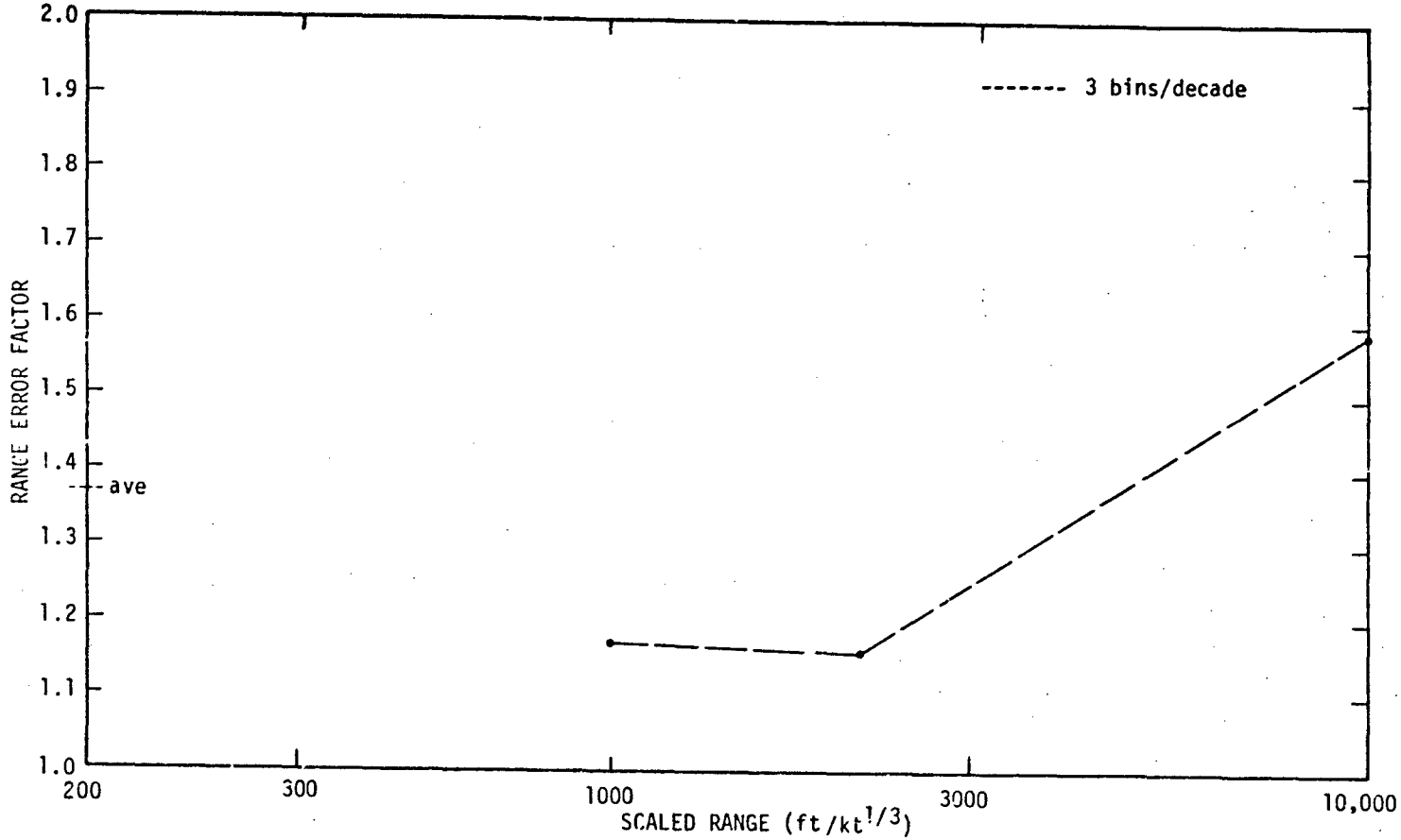

Figure 4.1-39. Range Error Factor vs. Scaled Range
SHOB: 478-500 ft (Peak Overpressure)

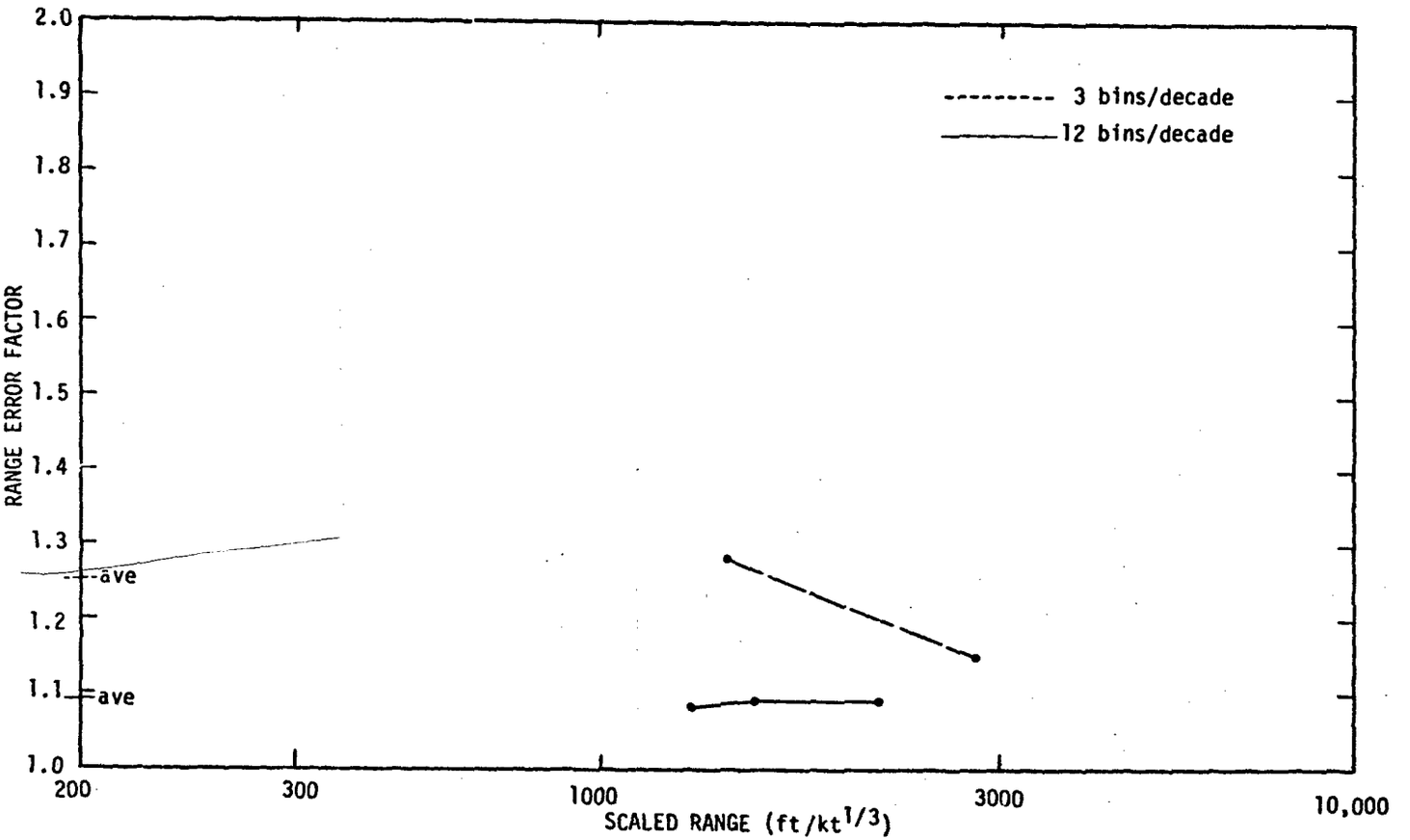

Figure 4.1-40. Range Error Factor vs. Scaled Range
SHOB: 751-831 ft (Peak Overpressure)

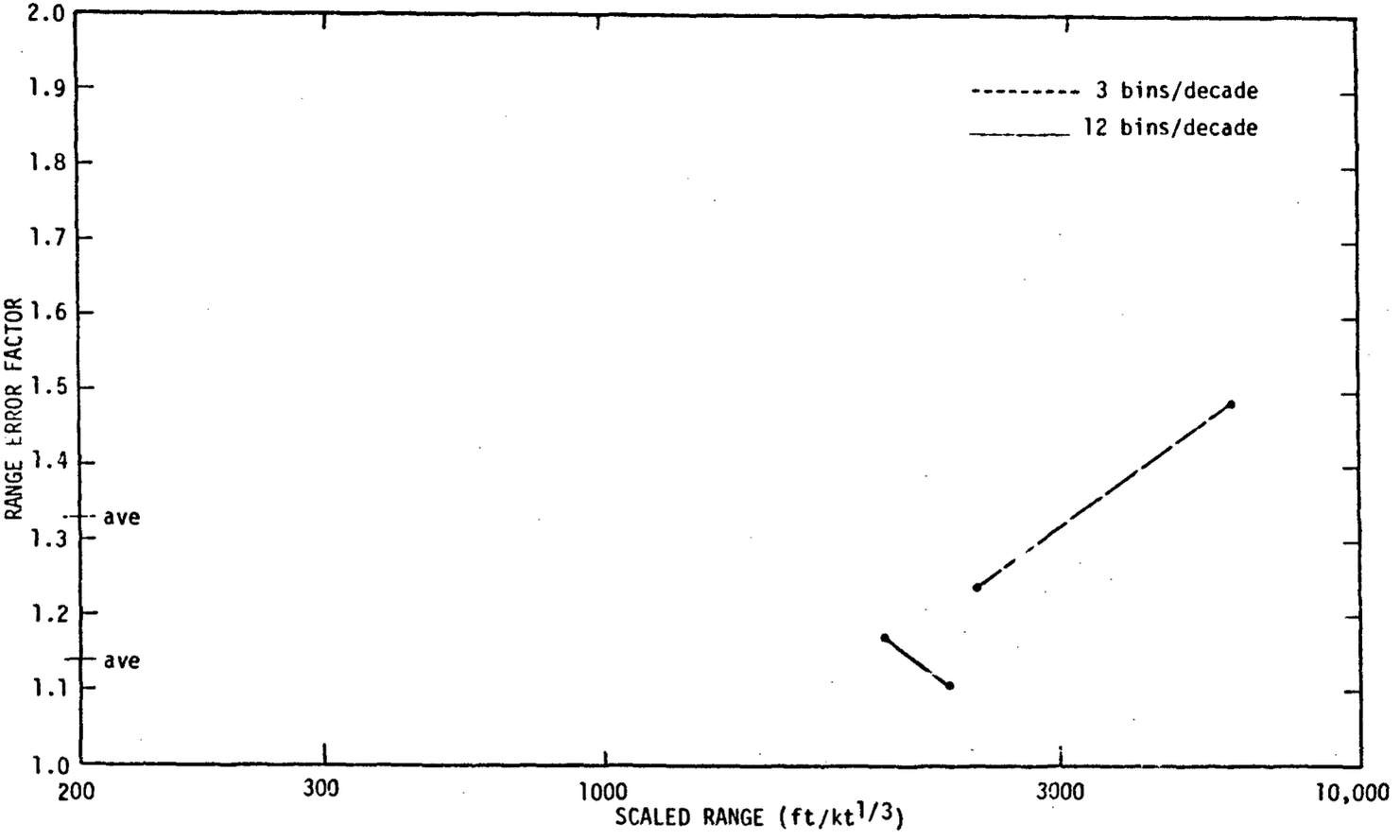

Figure 4.1-41. Range Error Factor vs. Scaled Range
SHOB: 1003-1249 ft (Peak Overpressure)

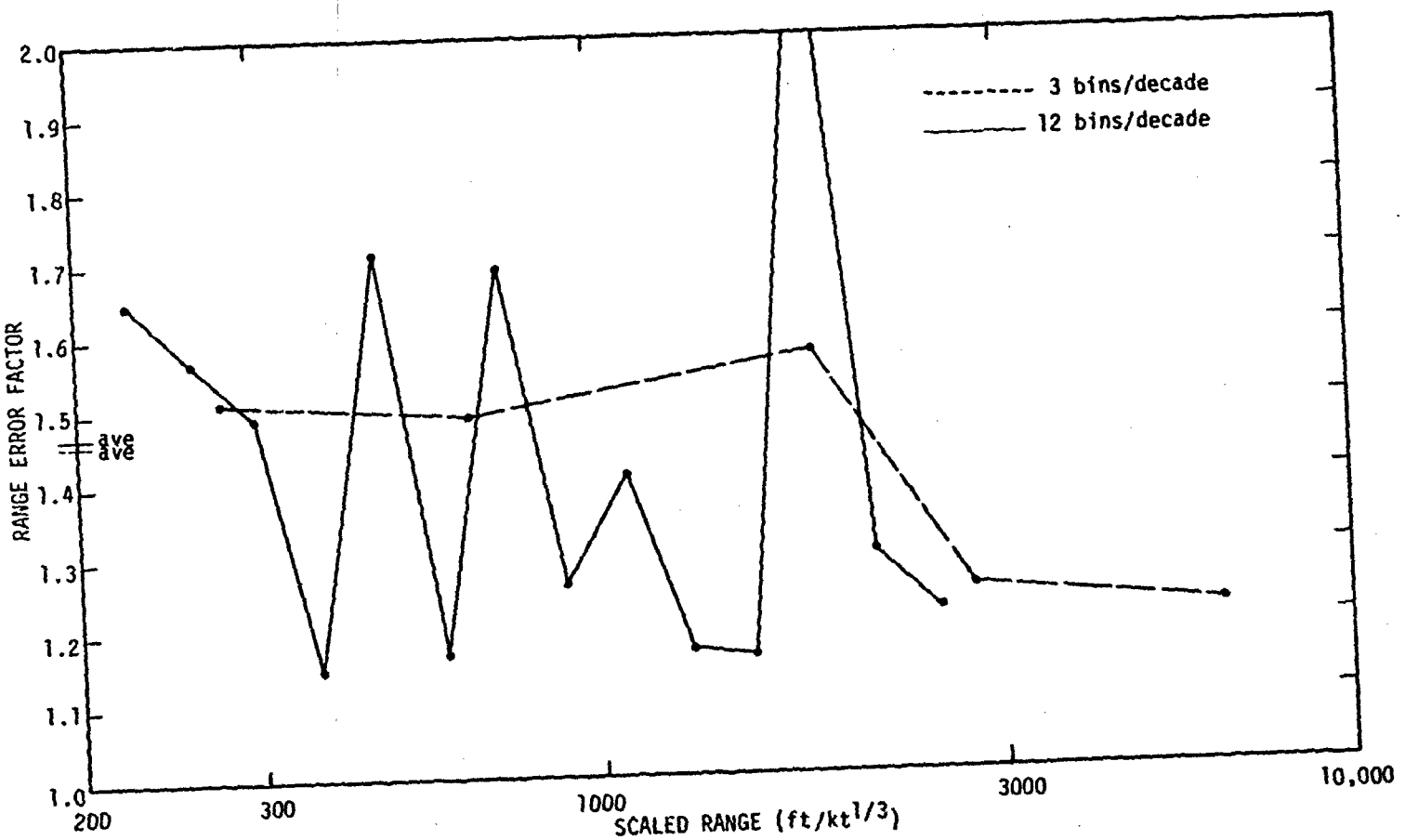

Figure 4.1-42. Range Error Factor vs. Scaled Range
SHOB: 0-3.1 ft (Overpressure Impulse)

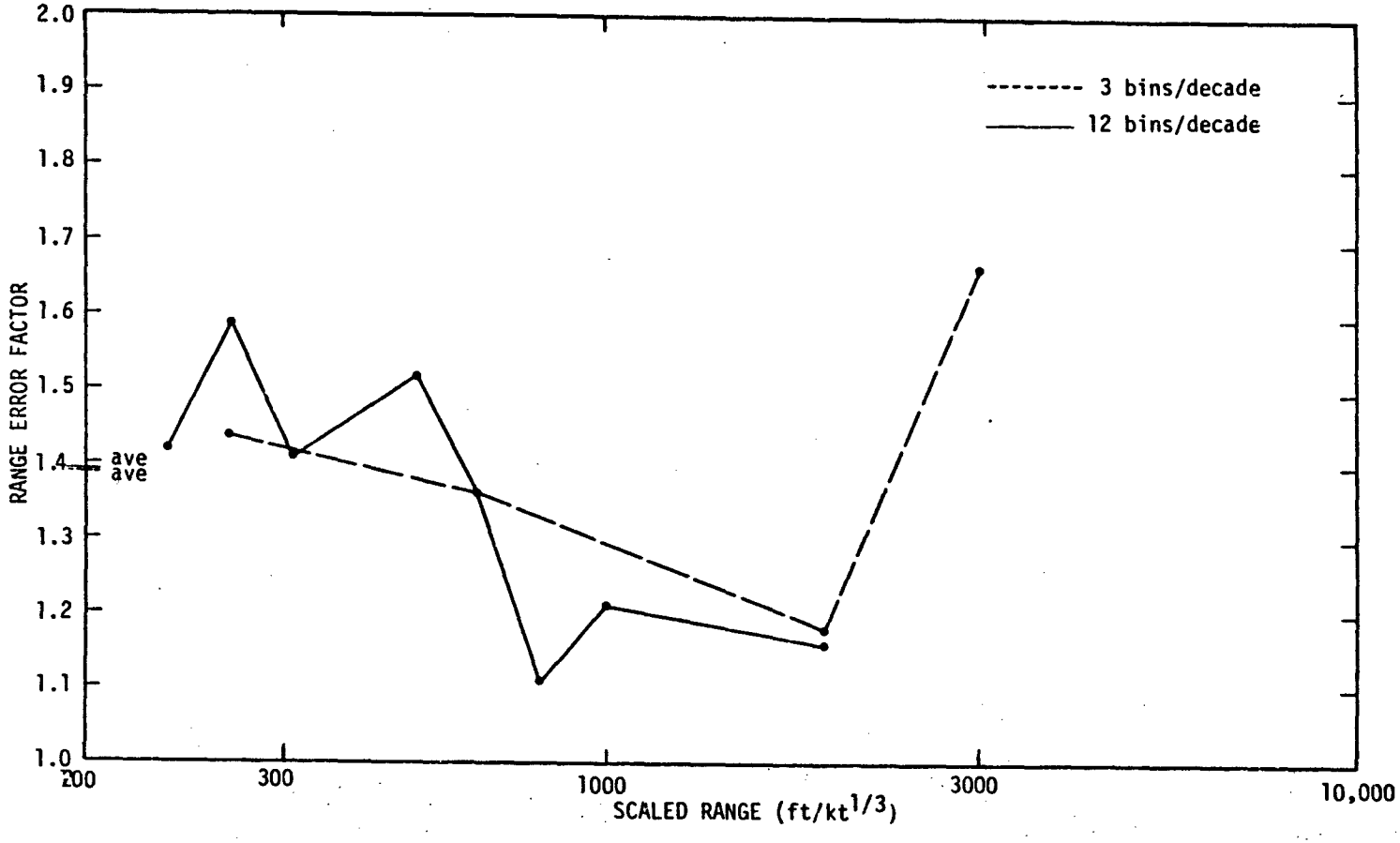

Figure 4.1-43. Range Error Factor vs. Scaled Range
SHOB: 5-11 ft (Overpressure Impulse)

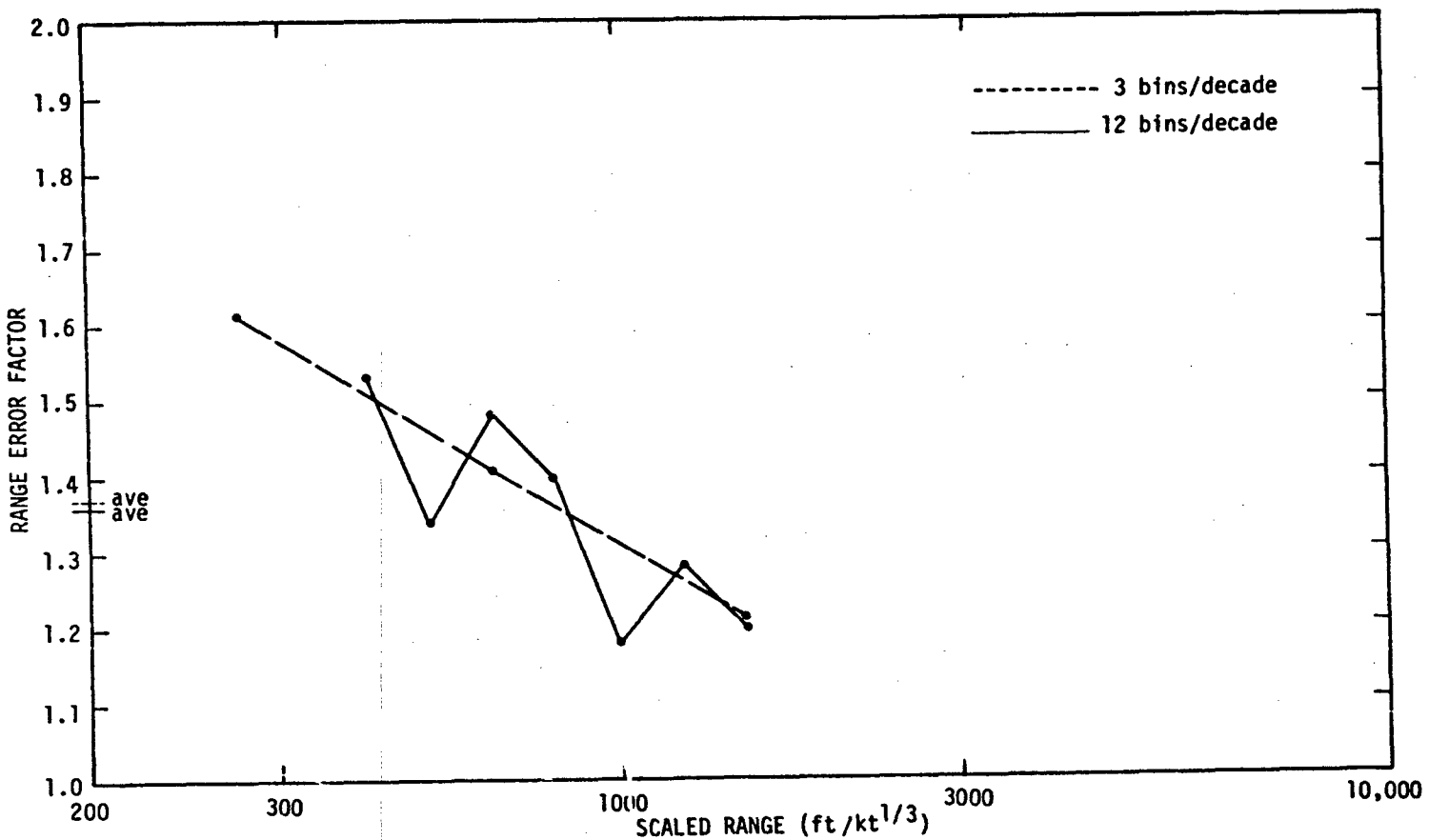

Figure 4.1-44. Range Error Factor vs. Scaled Range
SHOB: 55-83 ft (Overpressure Impulse)

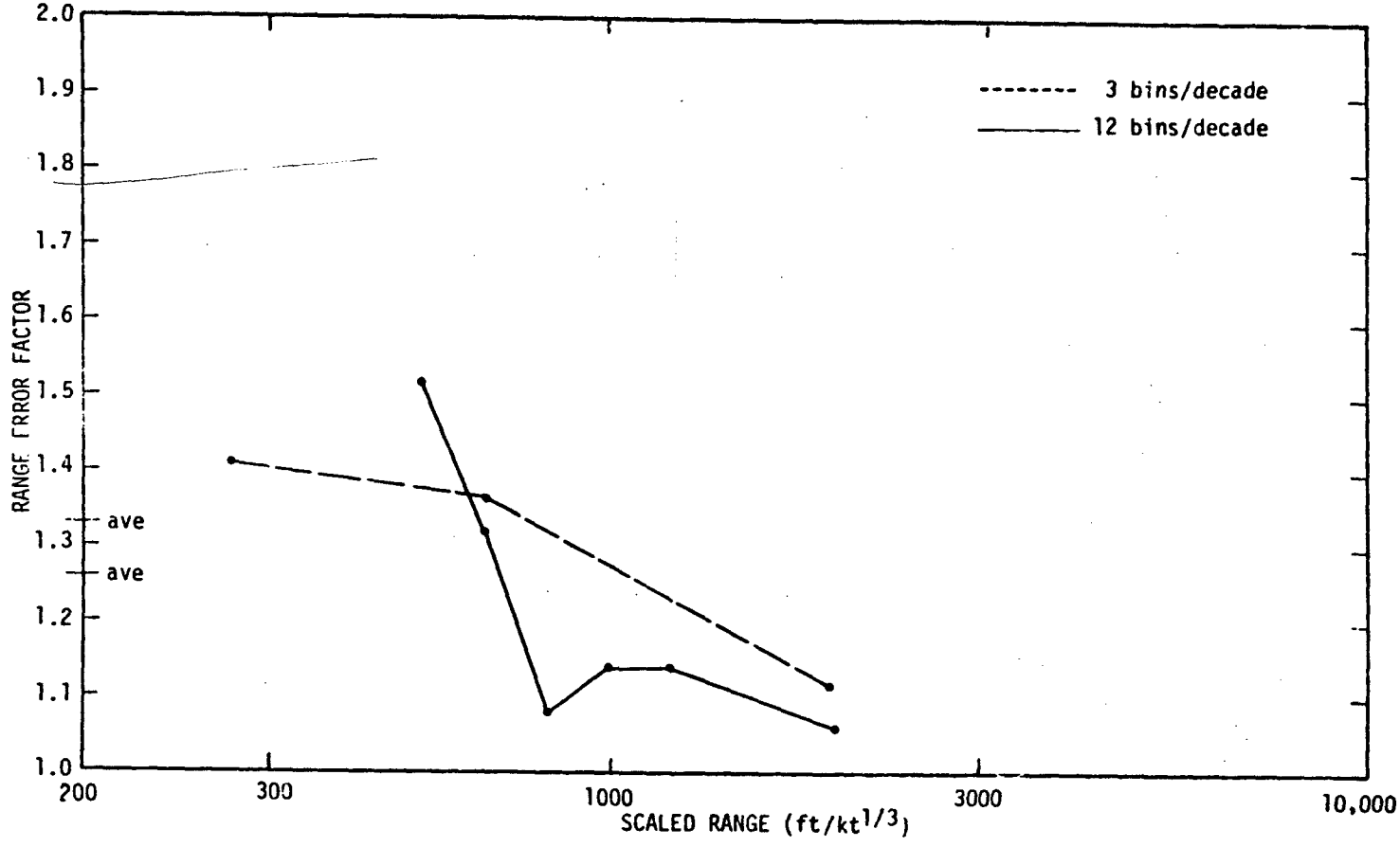

Figure 4.1-45. Range Error Factor vs. Scaled Range
SHOB: 113-157 ft (Overpressure Impulse)

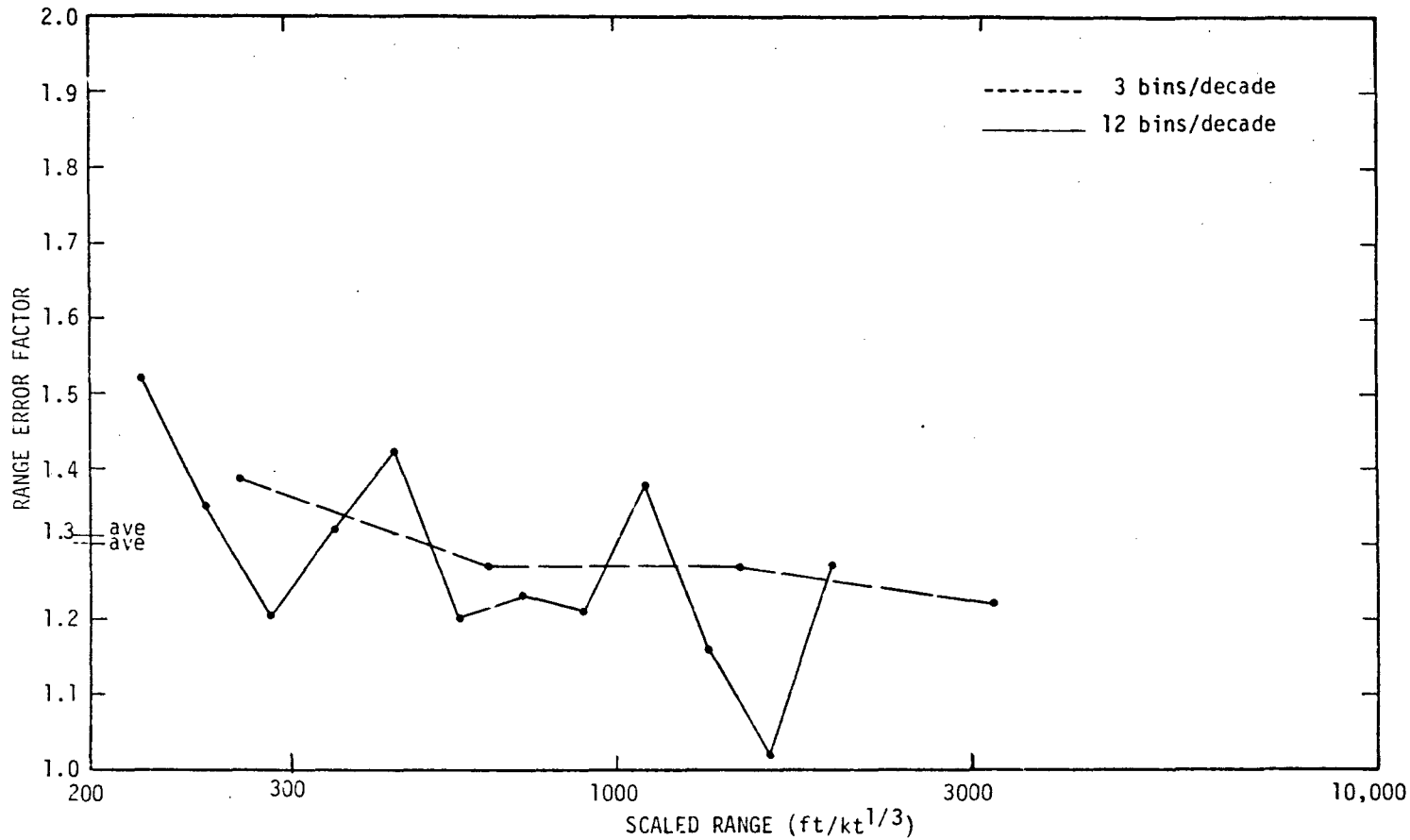

Figure 4.1-46. Range Error Factor vs. Scaled Range
SHOB: 182-205 ft (Overpressure Impulse)

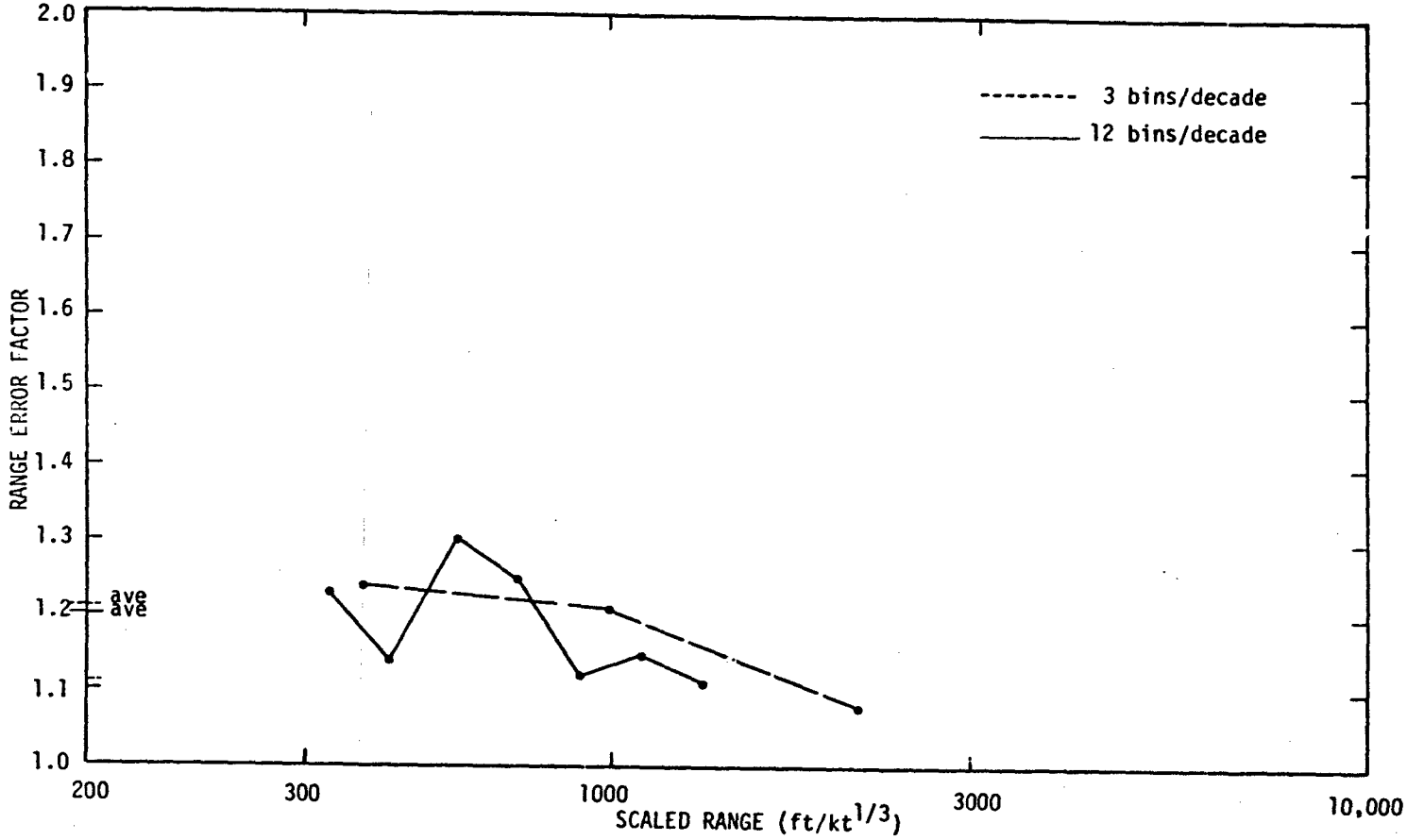

Figure 4.1-47. Range Error Factor vs. Scaled Range
SHOB: 212-252 ft Overpressure Impulse)

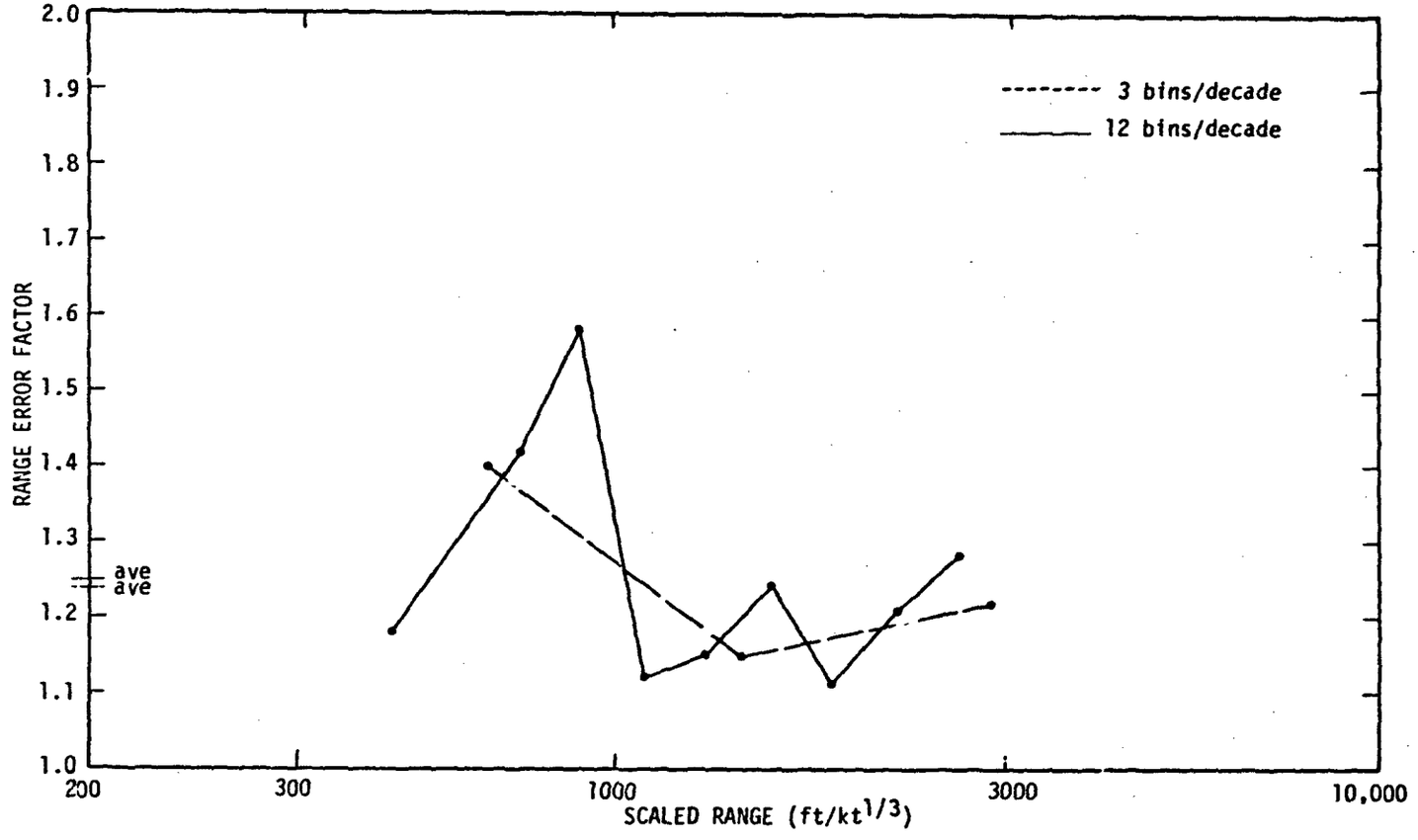

Figure 4.1-48. Range Error Factor vs. Scaled Range
SHOB: 323-375 ft (Overpressure Impulse)

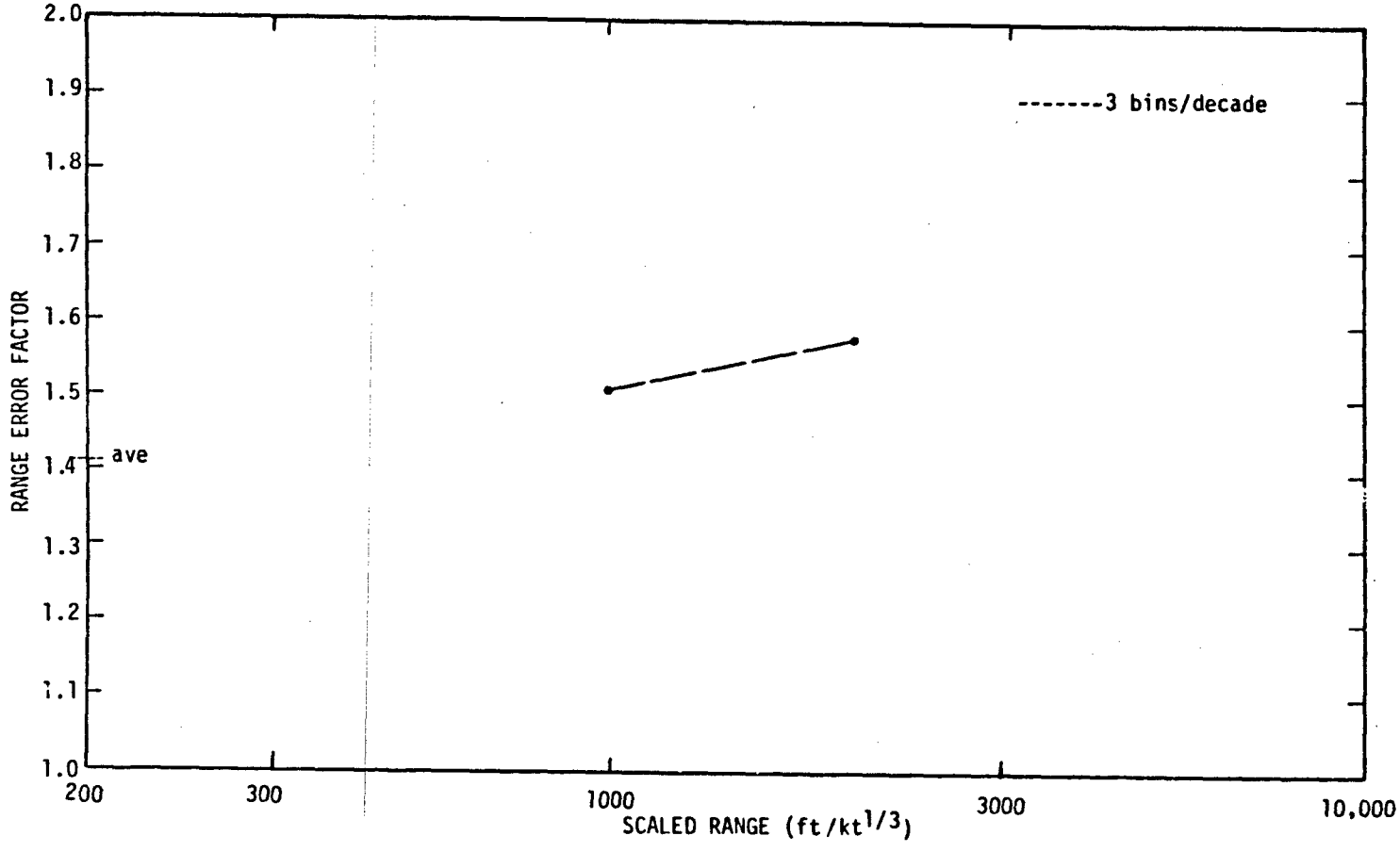

Figure 4.1-49. Range Error Factor vs. Scaled Range
SHOB: 475-500 ft (Overpressure Impulse)

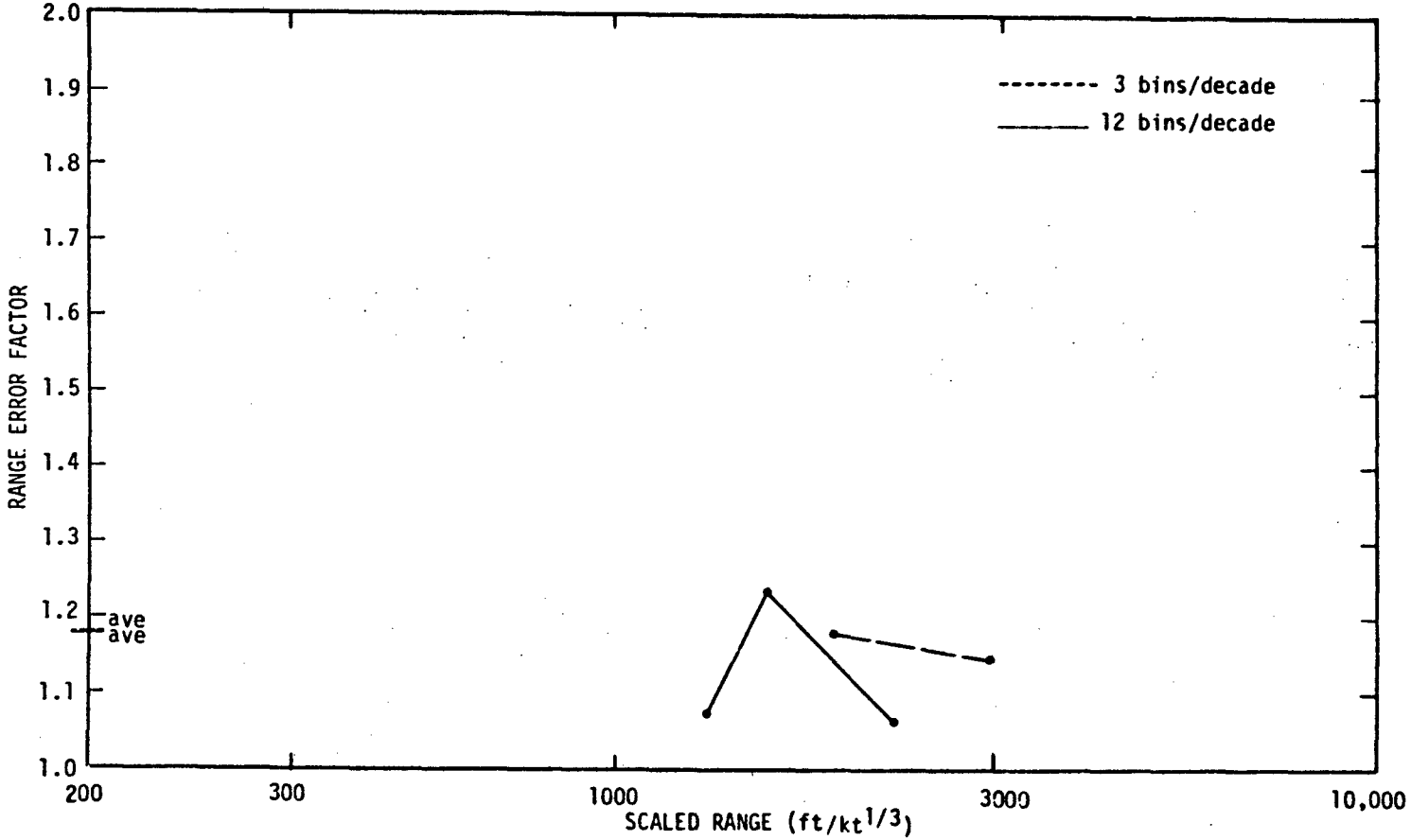

Figure 4.1-50. Range Error Factor vs. Scaled Range
SHOB: 751-831 ft (Overpressure Impulse)

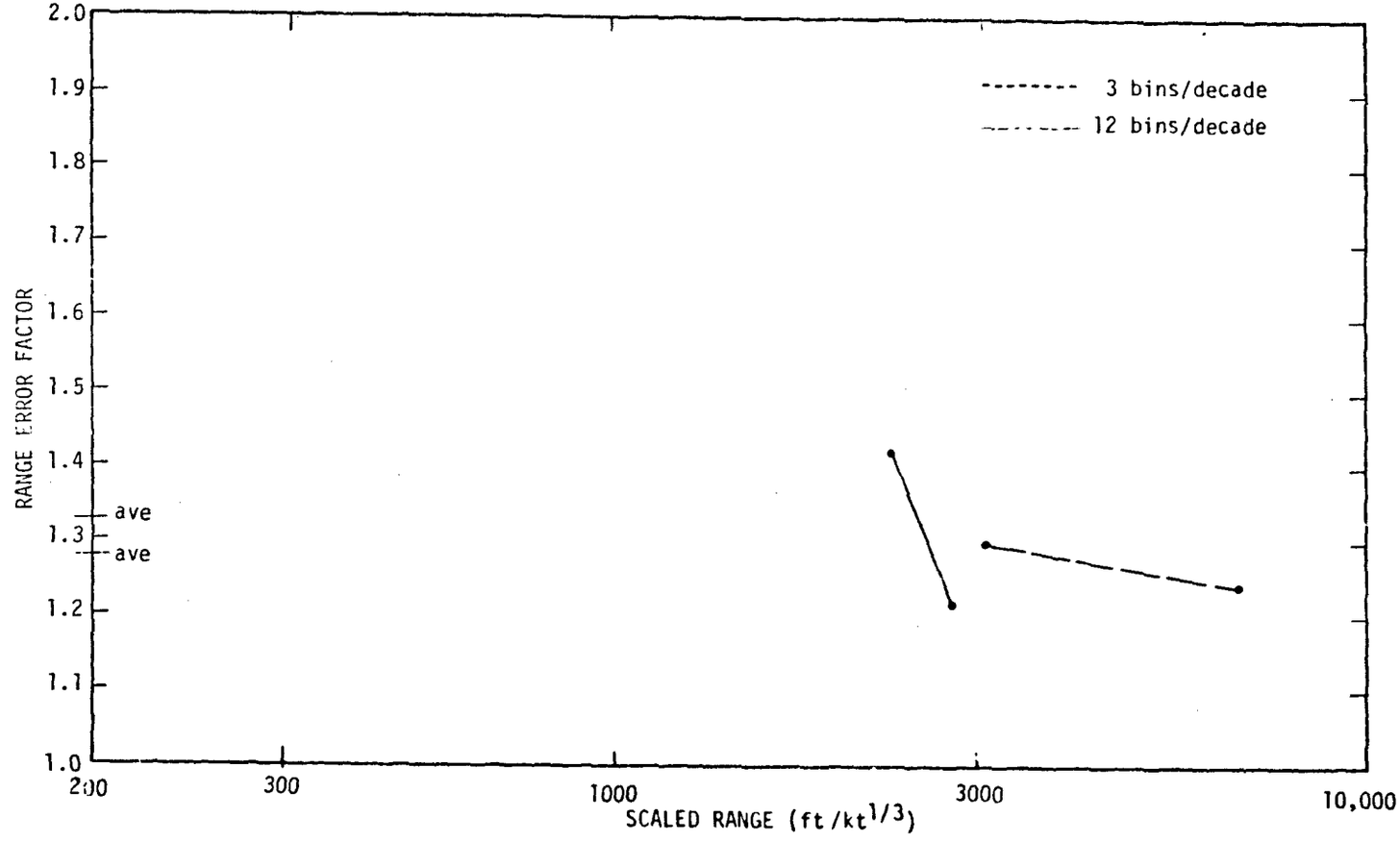

Figure 4.1-51. Range Error Factor vs. Scaled Range
SHOB: 1003-1249 ft (Overpressure Impulse)

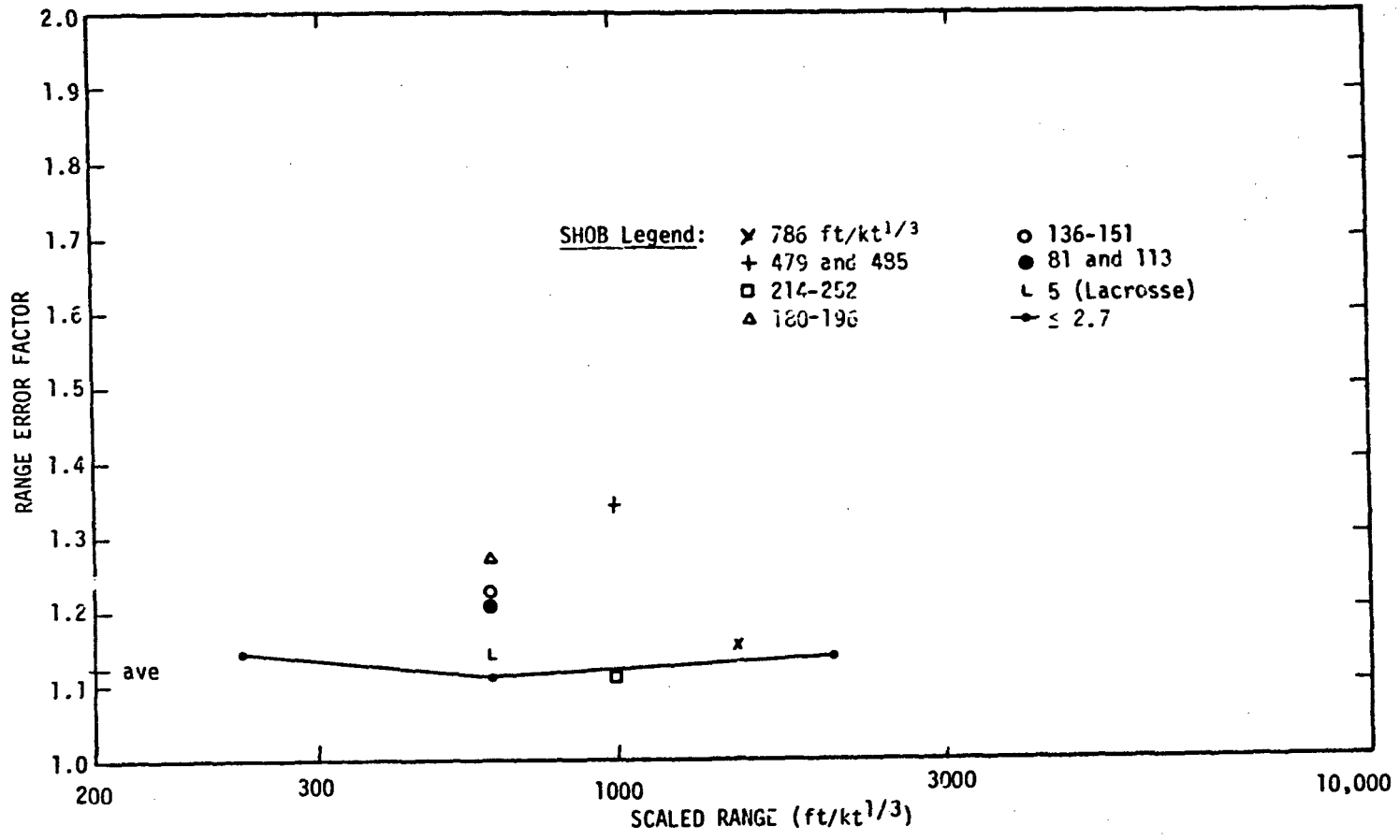

Figure 4.1-52. Range Error Factor vs. Scaled Range All SHOBs where Data Exist (Dynamic Pressure) Light Dust Conditions

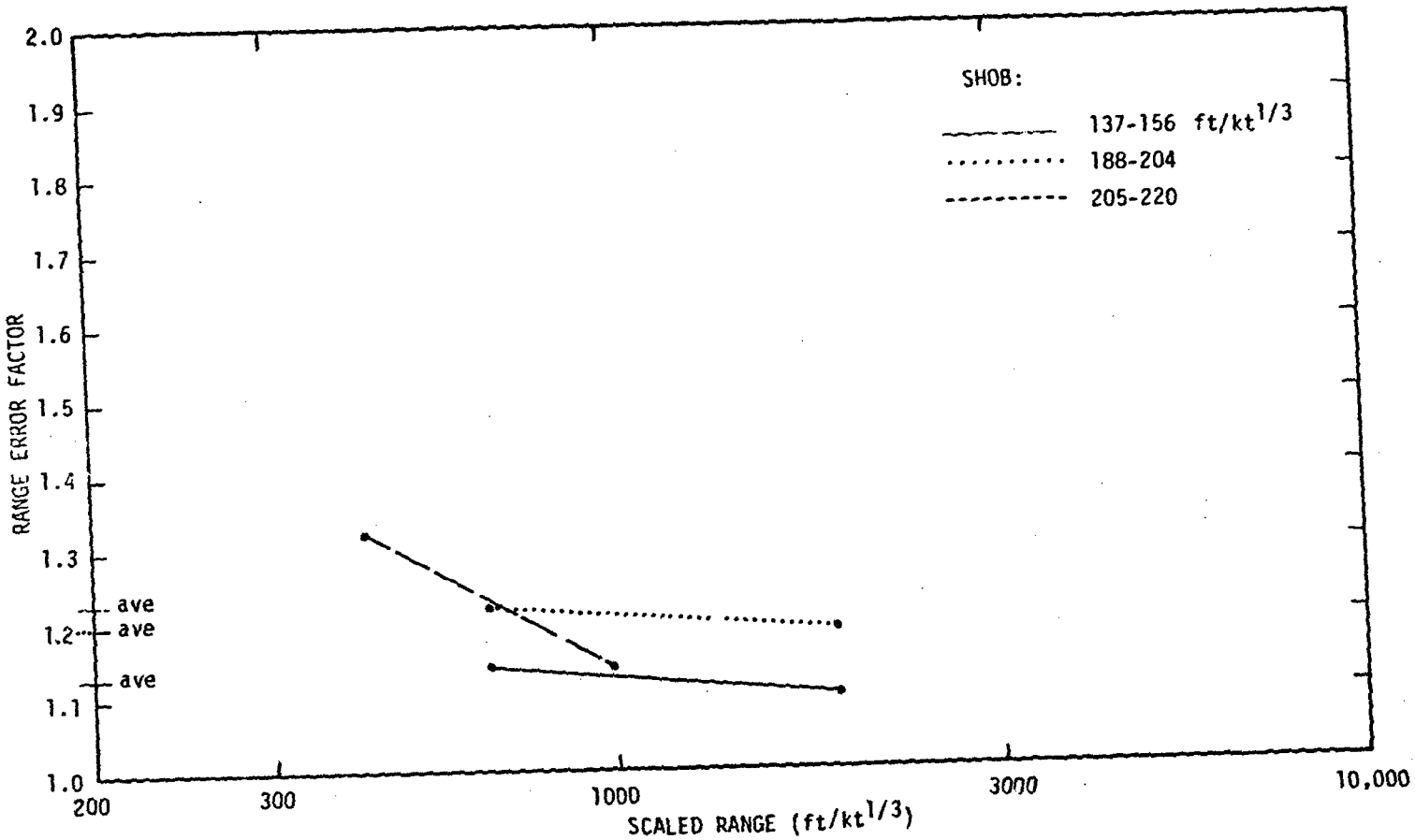

Figure 4.1-53. Range Error Factor vs. Scaled Range All SHOBs where Data Exist (Dynamic Pressure) Heavy Dust Conditions

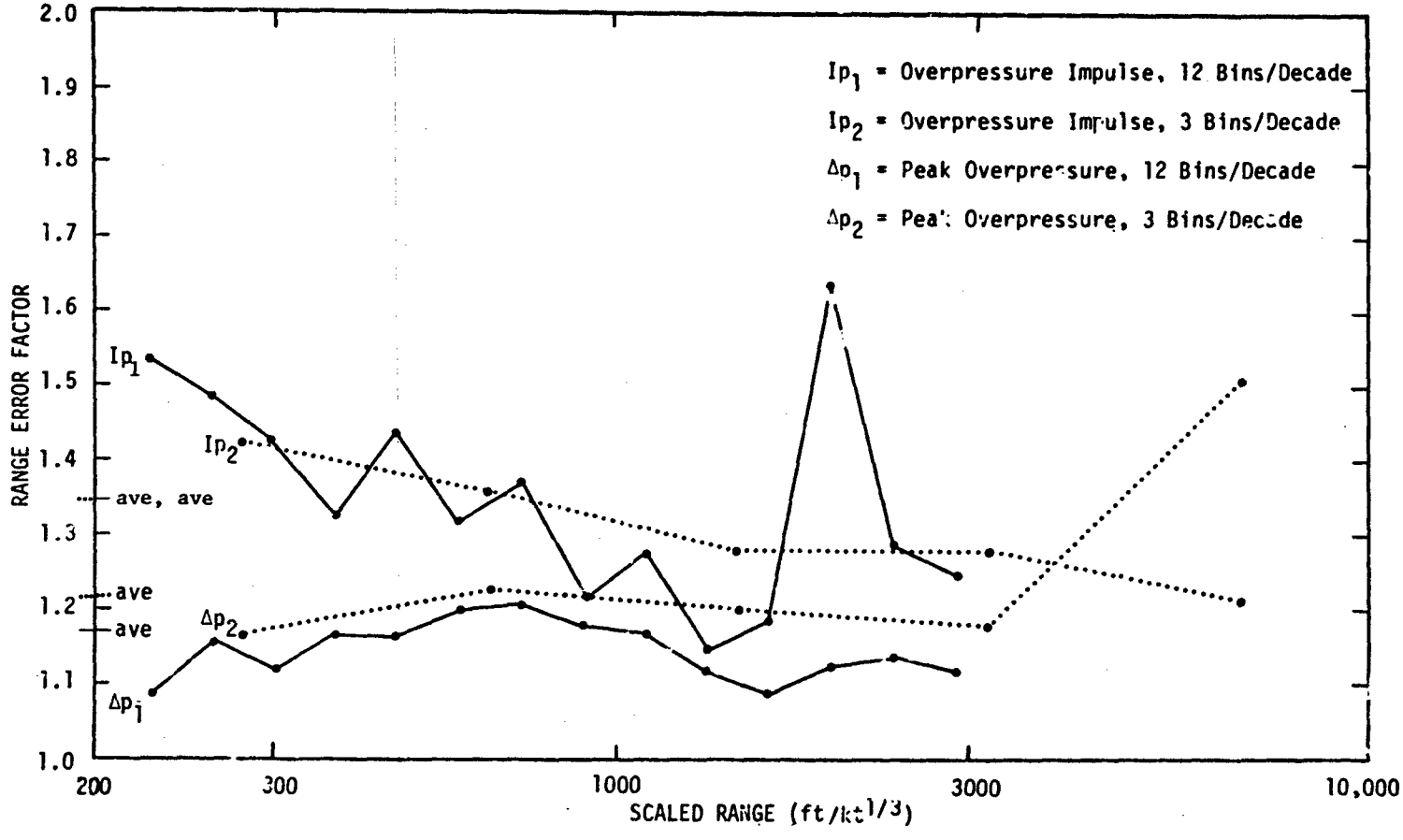

Figure 4.1-54. Range Error Factor vs. Scaled Range Average Across All SHOBs (Peak Overpressure and Overpressure Impulse)

Table 4.1-4 SUMMARY OF YIELD RATIO MEASURE FOR BLAST ENVIRONMENTS
(by cell, SHOB, and range bin)

		Error Factor Yield Ratio	Minimum			Average	Maximum		
			Cell	Scaled HOB* Column	Range Bin* Row		Cell	Scaled HOB* Column	Range Bin* Row
3 bins/decade	Peak Overpressure	f_R W/W_{EPC}	1.10 1.01	1.17 1.028	1.17 1.028	1.22 1.045	1.59 1.267	1.37 1.115	1.51 1.206
	Overpressure Impulse	f_R W/W_{EPC}	1.08 1.003	1.18 1.015	1.21 1.020	1.35 1.051	1.67 1.156	1.48 1.082	1.43 1.073
	Peak Dynamic Pressure	f_R W/W_{EPC}	1.10 1.01	1.12 1.014	1.14 1.019	1.19 1.034	1.34 1.099	1.34 1.099	1.32 1.089
12 bins/decade	Peak Overpressure	f_R W/W_{EPC}	1.04 1.002	1.09 1.008	1.09 1.008	1.17 1.028	1.33 1.094	1.24 1.052	1.21 1.041
	Overpressure Impulse	f_R W/W_{EPC}	1.02 1.000	1.18 1.015	1.15 1.011	1.35 1.051	1.71+ 1.172	1.39+ 1.062	1.54+ 1.108

* 10 columns denote varying SHOB; 5 rows for 3 bins/decade and 14 rows for 12 bins/decade denote varying scaled (horizontal) range

+ A "bad" SUGAR datum having large impact on the error factor was ignored

Table 4.1-5 IMPACT OF ANALYSIS ON TACTICAL UTILITY

PHENOMENON	RANGE BIN	NOMINAL NUCLEAR PRODUCED ENVIRONMENT	SHOB BIN	YIELD RATIO (W/Wepc)	POTENTIAL TACTICAL UTILITY
PEAK OVERPRESSURE	6812	< 2 psi	478-500	1.267	NONE, SINCE NOMINAL NUCLEARLY PRODUCED ENVIRONMENT BELOW COLLATERAL INTEREST
PEAK OVERPRESSURE	(1)	(1)	478-500	1.115	POSSIBLE SMALL (< 11.5%) ACROSS-THE-BOARD DECREASE IN YIELD FOR ∿500 ft/kt$^{1/3}$
PEAK OVERPRESSURE	6812	< 2 psi	(2)	1.206	NONE, ENVIRONMENT BELOW COLLATERAL INTEREST
OVERPRESSURE IMPULSE	3162	<400 psi-msec	5-11	1.156	PROBABLY BELOW COLLATERAL INTEREST
OVERPRESSURE IMPULSE	511	1600 psi-msec	0-3.1	1.172	POSSIBLE SMALL (< 17%) DECREASE IN YIELD FOR SURFACE DETONATIONS
OVERPRESSURE IMPULSE	∿250	High psi-msec	(2)	1.108	POTENTIAL SMALL (< 10%) DECREASE IN YIELD FOR HIGH OVERPRESSURE IMPULSE DETONATIONS

1 AVERAGE OVER RANGE BINS
2 AVERAGE OVER HOB BINS

4.2 DISTRIBUTION TYPE FOR BLAST DATA

4.2.1 Introduction

The measurements of scaled range to a selected pressure value have a distribution which can be statistically described. The distribution must be characterized in order to calculate the scaled range, to the selected pressure value, with high and low probabilities for target and collateral damage analyses respectively. Since the total population is required to specify the exact distribution, the existing sample can only be used to specify a best distribution.

The following analysis was performed to find the dependence of range uncertainty on range. The hypothesis is that a linear or higher order dependence completely negates the applicability of a normal distribution. Specifically a lognormal distribution applies for a linear dependence. For higher order dependence, a linear dependence approximation is usually dominant and thus assumed to apply, but not to the total exclusion of another continuous non-normal distribution such as beta and gamma which have non-zero skewness. The lognormal is more convenient than beta or gamma because the data are frequently plotted on a logarithmic scale and the data uncertainty is then a symmetric factor in linear space.

The measurements used in this analysis are the scaled range to static (over) pressure peak and scaled impulse values. A data quality control was attempted by selecting only the ranges where both peak and impulse values were simultaneously measured. The data base is that previously culled set which is reported in DASA 1200, Volume V (Reference 4). In addition, the biased data (Reference 5) of the Franklin event was not used The similar data base for dynamic pressure is unpublished but has been partially compiled by Mr. J. Keefer, et al., of the U. S. Army Ballistics Research Laboratory. This dynamic set is much smaller than the static set so estimating the standard deviation would not be as accurate and thus the hypothesis proof is more complex.

The approach for calculating the standard deviation of scaled range as a function of scaled range is the following. The measurements are systematically grouped or binned in scaled range. The data within a range bin are normalized to the range at the mid-point of the bin using a power law approximation. Then these range-square-normalized peak overpressures and range-normalized overpressure impulses are analyzed for a mean and variance. This overpressure variance is then propagated to a range variance using the law of covariance propagation:

$$\sigma_R^2 = \left(\frac{\partial R}{\partial z}\right)^2 \sigma_z^2 + \frac{\partial R}{\partial z} \frac{\partial^2 R}{\partial z^2} \mu_{3z}$$

where z is either overpressure peak or impulse.

The second term involving the third central moment (skewness indicator) can be ignored. The few cases having an adequate number of values (i.e., ≥ 15) in a bin to estimate skewness have both positive and negative contributions. The standard deviation change attributable to the correction for skewness was less than 15 percent which can later be inferred as insignificant.

The final steps consist of plotting the standard deviations of range versus the mid-points of the range bins and fitting a linear equation through the values. The uncertainty of the slope coefficient allows testing for significance of the linear fit. The following material discusses the details of this procedure and the results.

4.2.2 Procedure

The lack of a large amount of data for a single scaled HOB other than Priscilla requires SHOB grouping or binning to accumulate a large number of data within each range bin. Since a simple SHOB normalization for all types of blast data is unavailable, the SHOB bins are kept small. The data base was compartmented into 10 SHOB bins using the bar graph of Figures 4.2-1 through 4.2-4 as guides.

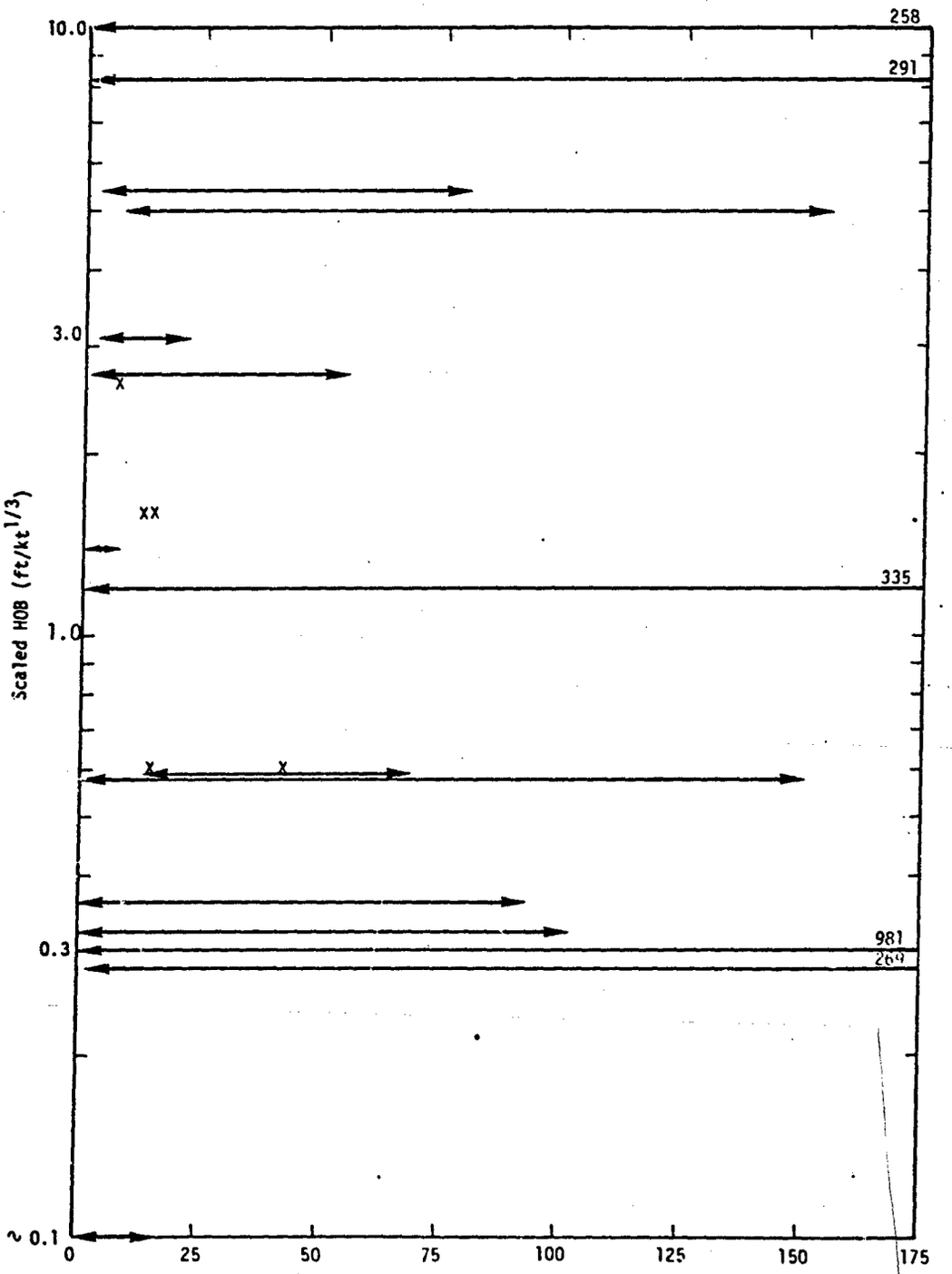

Figure 4.2-1. Ranges of Peak Overpressure for 0 to 10 ft/kt$^{1/3}$ HOB

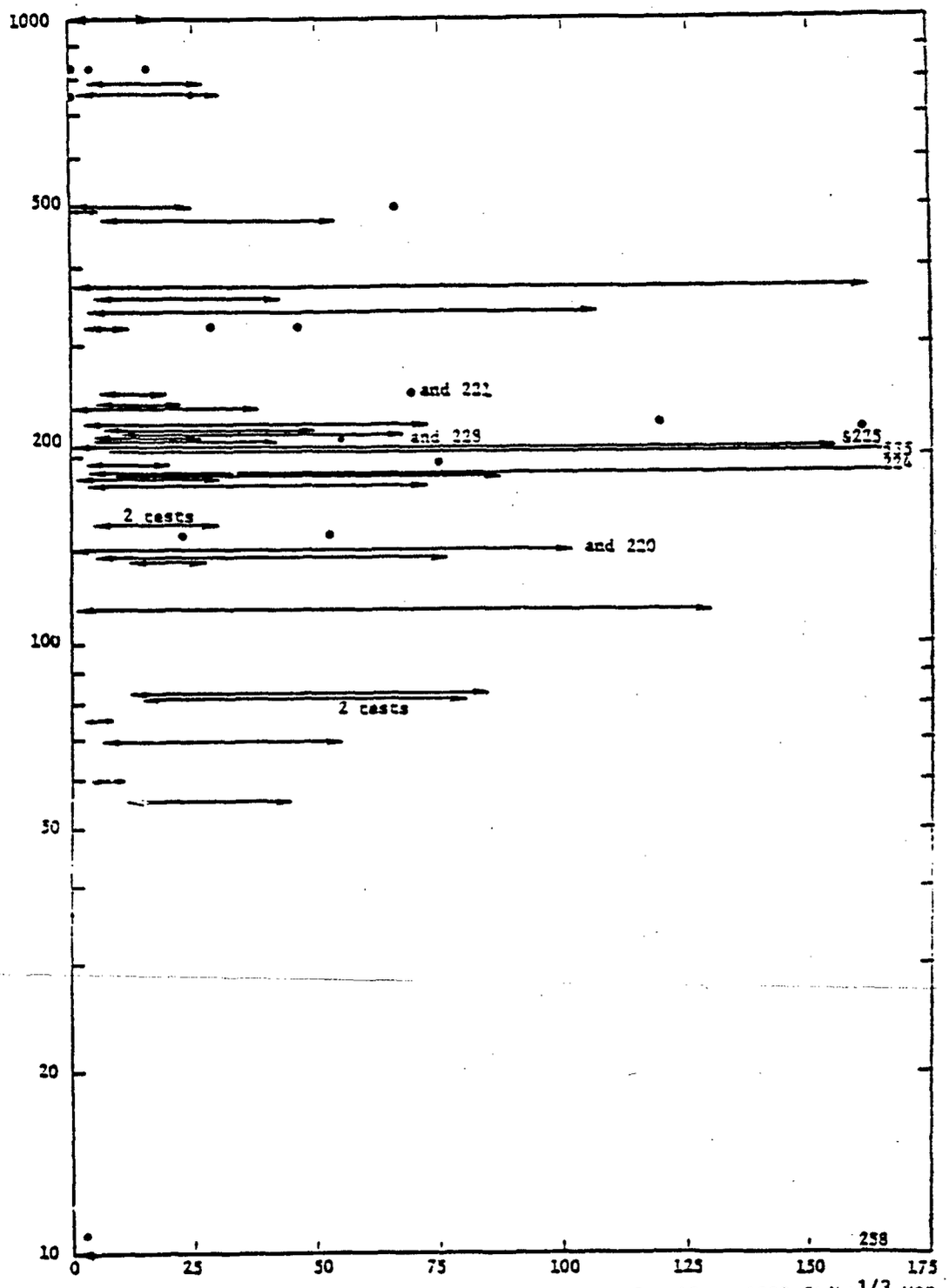

Figure 4.2-2. Ranges of Peak Overpressures for 10 to 1000 ft/kt$^{1/3}$ HOB

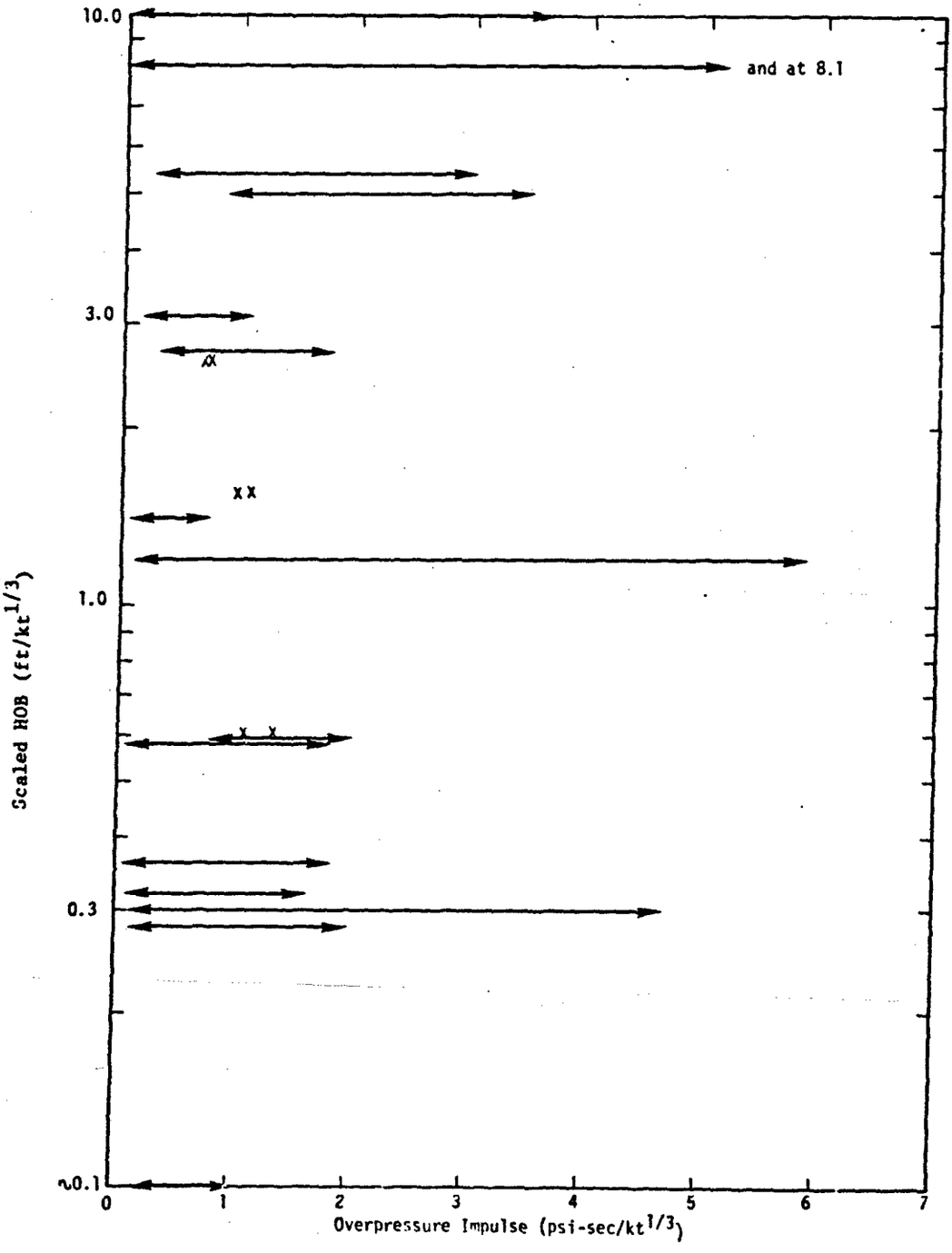

Figure 4.2-3. Ranges of Overpressure Impulse for 0 to 10 ft/kt$^{1/3}$ HOB

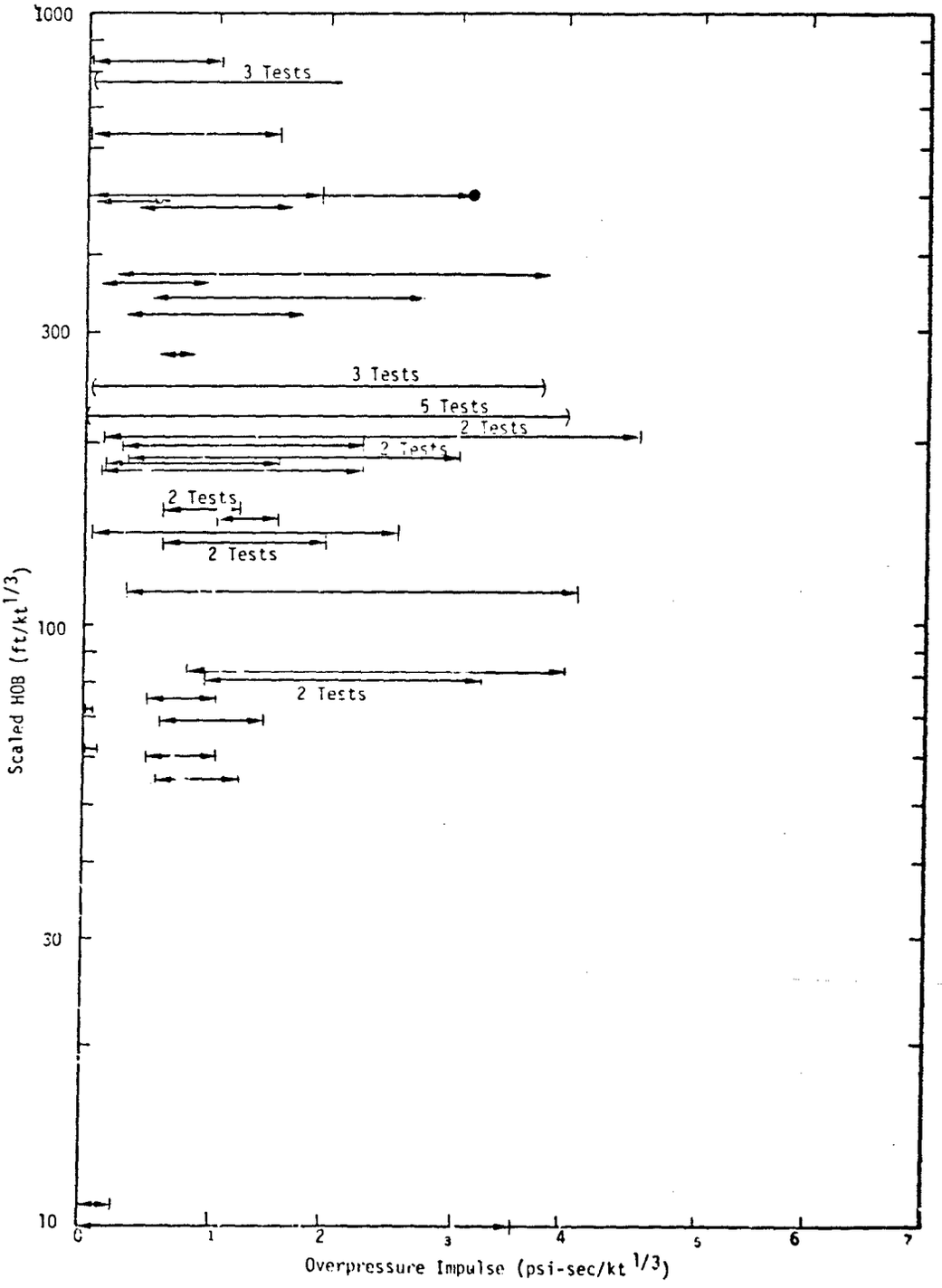

Figure 4.2-4. Ranges of Overpressure Impulse for 10 to 1000 ft/kt$^{1/3}$

The SHOB range, number of simultaneous peaks and impulses, and names of tests in the 10 bins are as follows:

HOB - ft/kt$^{1/3}$(ID)	No. of Data	Events
0 - 3.1 (03)	177	Mike, Walnut, Yankee, Union, Romeo, Zuni, Koa, Bravo, Nectar Cactus, Yellowwood, Aspen, Sycamore, Koon, Sugar
5.0 - 10.8 (511)	87	Lacrosse, Fig, Small Boy, Little Feller I & II
55 - 83 (5583)	104	Dog, Zebra, Simon, Inca, Easy, Yoke, X-Ray
113-157 (113157)	62	Annie, Turk, Met, Humboldt, Zucchini, Tesla, Apple 2
182 - 205 (182205)	143	King, Shasta, Hornet, Smoky, Apple 1, Priscilla, Grable
212 - 252 (212252)	96	Galileo, Moth, Kepler, Wilson, Owens, Morgan, Bee, Post
323 - 375 (323375)	81	Climax, Hood, Yuma, Dog
478 - 500 (478500)	41	Wasp Prime, Ruth, Hamilton
751 - 831 (751831)	65	Soccorro, Able, Encore, Rushmore
1003 - 1249 (10031249)	97	Baker, Charlie, Eddy, Mora, Lea

Specific events with numerous data in the 1 to 100 psi interval are the following:

1.2	28	Cactus
8.2	36	Small Boy
83	37	Easy
204	57	Priscilla
375	40	Dog

The data measured near the surface are for both regular and Mach stem reflections of the initially spherical air blast wave. The knee at the transition between the reflection regions on a plot with HOB and ground range coordinates is very nonlinear and not directly combatible with a statistical treatment. Most targeting analyses use the Mach stem overpressure enhancement so only the data below the knee are used, in this tactical analysis, for air burst events. The bottom of the knee used to isolate these data was described by the approximate empirical equation for units of $ft/kt^{1/3}$:

$$R = \frac{2000 \times HOB}{2000 - HOB}$$

where R is 222 for a 200 HOB and R is 500 for a 400 HOB.

The variance has both a true and an error component unless all points have the same mean. This same mean is achieved by removing the analytical dependence on range in addition to HOB. The error variance is very small by using a power law approximation for normalization within the range bin. Peak overpressures were normalized by inverse range squared and overpressure impulses were normalized by inverse range. This approximate power of two for peak overpressure could be refined by using the Brode Direct Fit (Reference 2) to estimate the power. But the Brode pressure time equations are not adequately suitable for impulse calculations where the scaled measurements were made so range normalization of impulses would not benefit by using Brode's Direct Fit.

Another more direct approach to minimizing the error variance is to use very narrow range bins so the range normalization is negligible. This also has the effect of emphasizing duplicate measurements at the same point which provide a true variance. Both linear and logarithmic range bins were used to force different groupings of the data as the range bin size was varied. The sizes for both types of bins were varied by a factor of ten between largest and smallest with minor differences in the calculated variances and no apparent biases or trends.

The square roots of some variances for group 5533 are plotted in Figure 4.2-5 and listed in Table 4.2-1. This result consistency is verification of the adequacy of the simple power law range normalizations for peak and impulse values within each bin.

The possible error variance from mixing data from precursor and non-precursor measurements is also of interest. For this immediate analysis, the interest is only in the possible systematic bias of the variance with range. Since neither the respective means nor their difference are precisely defined, the issue was indirectly treated by assessing the representativeness of the true variance from a given event by the variance from the SHOB group including that event. Specifically, event Easy from group 5533 and event Priscilla from group 182205 were used for this intra-comparison. The standard deviations of peak overpressures are plotted in Figures 4.2-6 and 4.2-7 to show the representativeness. Note that some event variances are larger than the respective group variances and no bias or trends are noticeable. Too few values exist for a linear fit of the event's variances to allow reliable quantitative comparison with a linear fit of the group's variances.

The sparsity of data causes concern for the reliability of variance estimates. Five points were chosen (approximately one in the middle and two on both sides) to help maximize the number of variance estimates. Using the variance as the accepted measure of data dispersion, not as the estimator of the standard deviation (which implies normality), reduces the concern for mixing variances from five and, for example, twenty-seven points. Four points are expected to all be within one standard deviation and twenty-seven points are expected to all be within two standard deviations for points normally distributed around an average. This guidance provides analytical justification for dropping points which differ drastically from the average, that is, outliers. Empirical justification for dropping outliers was also necessary in the form of severe departure from the trend line of the other points for the same event.

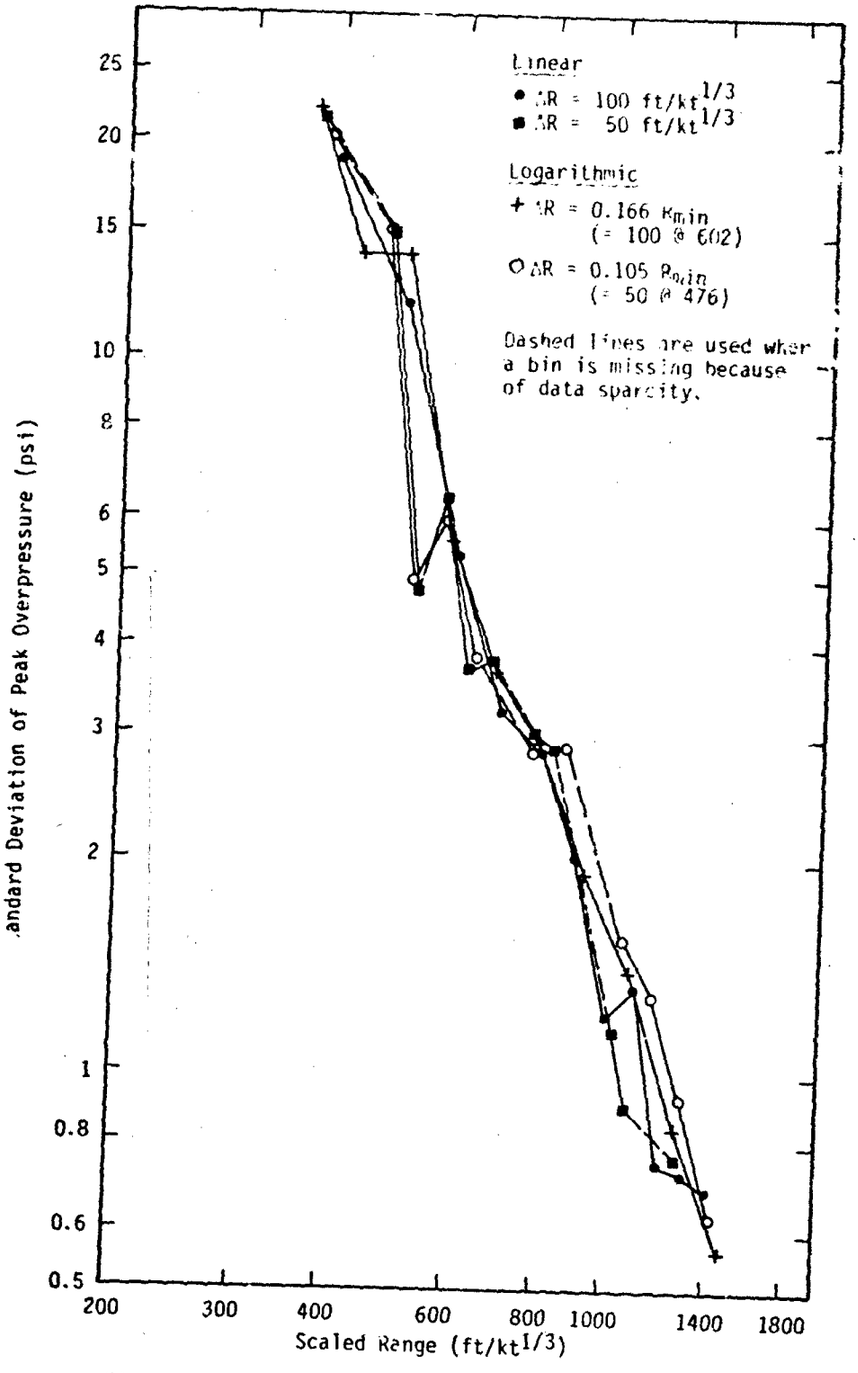

Figure 4.2-5. Standard Deviation of Peak Overpressure for 5583

Table 4.2-1. Standard Deviations of Peak Overpressures and Overpressure Impulses for Linear and Logarithmic Range Bins

• ΔR=100 ft/kt$^{1/3}$				■ ΔR=50 ft/kt$^{1/3}$				+ ΔR=0.166 R^{*}_{min}				o ΔR=0.105 R^{**}_{min}			
R	N	$S_{\Delta p}$	S_{IP}	R	N	$S_{\Delta p}$	S_{IP}	R	N	$S_{\Delta p}$	S_{IP}	R	N	$S_{\Delta p}$	S_{IP}
400	5	19	1065	375	5	22	1135	370	5	22	1150	385	5	20	1100
500	16	12	650	475	11	15	740	430	9	14	610	470	11	15	745
600	14	5.3	220	525	5	4.8	330	500	7	14	830	520	5	4.9	335
700	7	3.3	205	575	9	6.4	195	585	14	5.6	225	575	10	6.0	190
800	18	2.9	195	625	5	3.7	210	680	5	3.7	230	635	9	3.8	305
900	6	2.0	275	675	5	3.8	235	795	20	2.9	220	780	14	2.8	265
1000	9	1.2	50	775	10	3.0	255	925	6	1.9	270	860	11	2.9	215
1100	10	1.3	130	825	8	2.9	93	1080	20	1.4	110	1050	16	1.5	96
1200	6	0.76	120	1025	9	1.15	48	1260	11	0.84	87	1160	7	1.3	136
1300	5	0.73	76	1075	7	0.90	125	1470	7	0.56	84	1280	7	0.93	95
1400	5	0.69	17	1275	5	0.76	78	-	-	-	-	1420	6	0.62	18

* 15 bins/decade

** 23 bins/decade

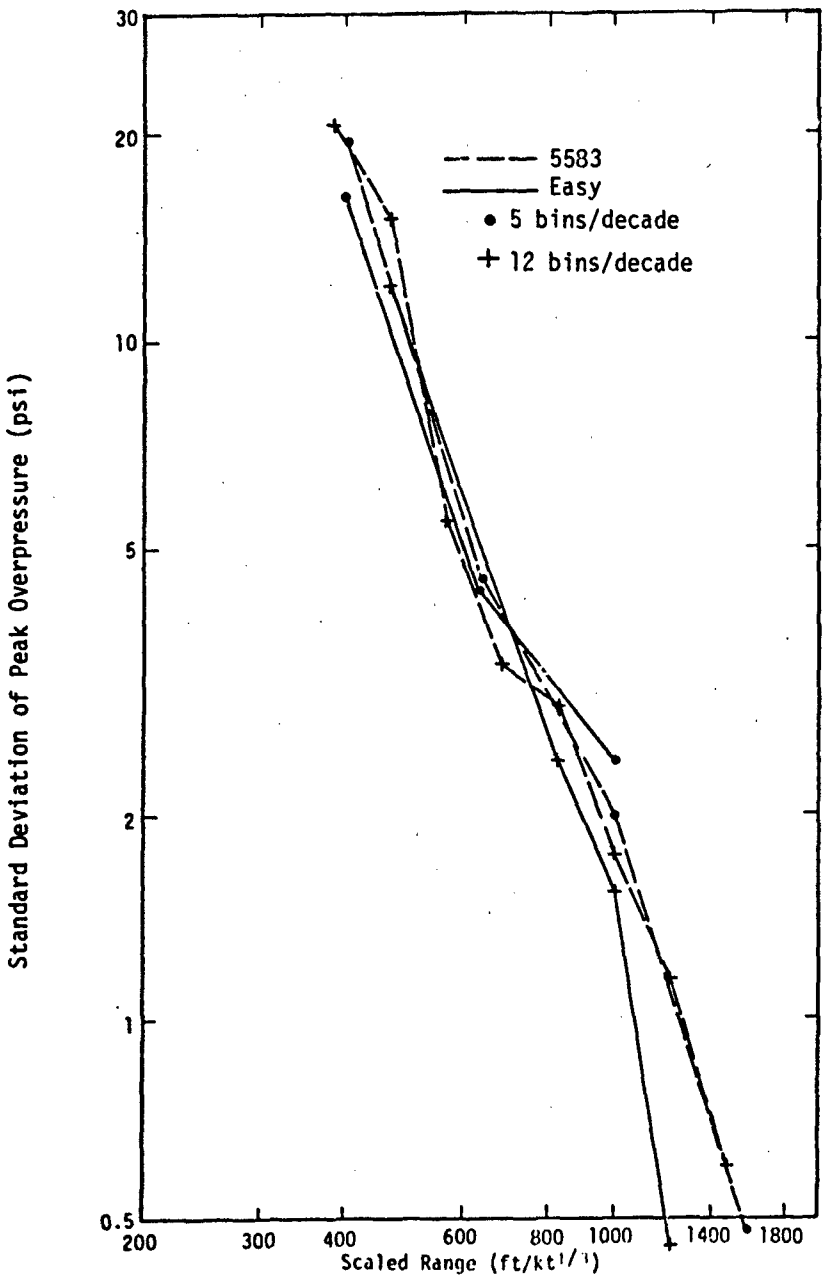

Figure 4.2-6. Standard Deviation of Peak Overpresure for Easy and 5583

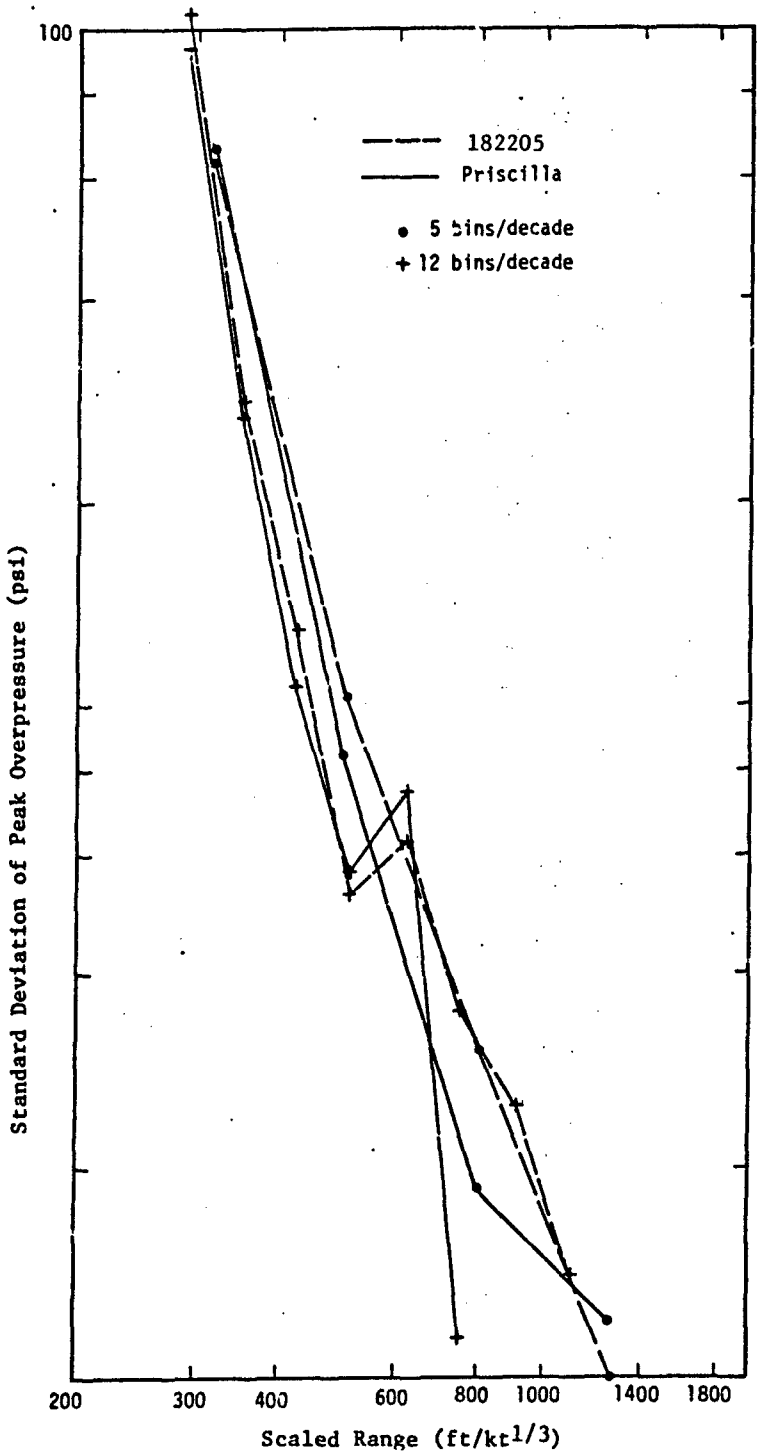

Figure 4.2-7. Standard Deviation of Peak Overpressure for Priscilla and 182205

The representativeness of as few as five points can also be discussed without reference to any assumption about the type of distribution (Reference 6). The result is expressed as the continuous probability, with number of points in the sample as parameter, for a fraction of the population being within the sample extremes. The expected value of the fraction, from many samples each of n points, is (n-1)/(n+1) but the probability of this value of the fraction slowly increases from 0.5 for n=3 to an asymptotic value below 0.6. Thus the 0.542 probability of including 67 percent of the population with a sample of 5 points is not too different than the 0.586 probability of including 93 percent of the population with a sample of 27 points. See the expected value curve in Figure 4.2-8. Also plotted on the graph is the more interesting dashed curve labelled most probable. The most probable value of the fraction, from one sample of n points, is (n-2)/(n-1), but the probability of this value of the fraction steadily decreases. Thus one is not automatically assured of having a fraction larger than that for the expected value. The net result is that 5 points was selected as a minimum which implies a minimum of 4 degrees of freedom for the variance estimate.

The bin centers were also staggered to maximize the number of variances. Two runs of an identical bin size were made with 50 percent offset of each bin with respect to the bins in the other run. This effort produced an algorithm which could successfully bin and calculate variances from more than 90 percent of the data. The results for group 5583 are tabulated as follows:

Bins/Decade	No. of S^2	Max No./Bin	No. of S^2	Max. No/Bin
46	8	10	11	10
23	11	16	12	12
15	10	20	9	16
12	7	23	8	23
8	6	30	5	27
5	4	38	4	41
3	3	52	2	62

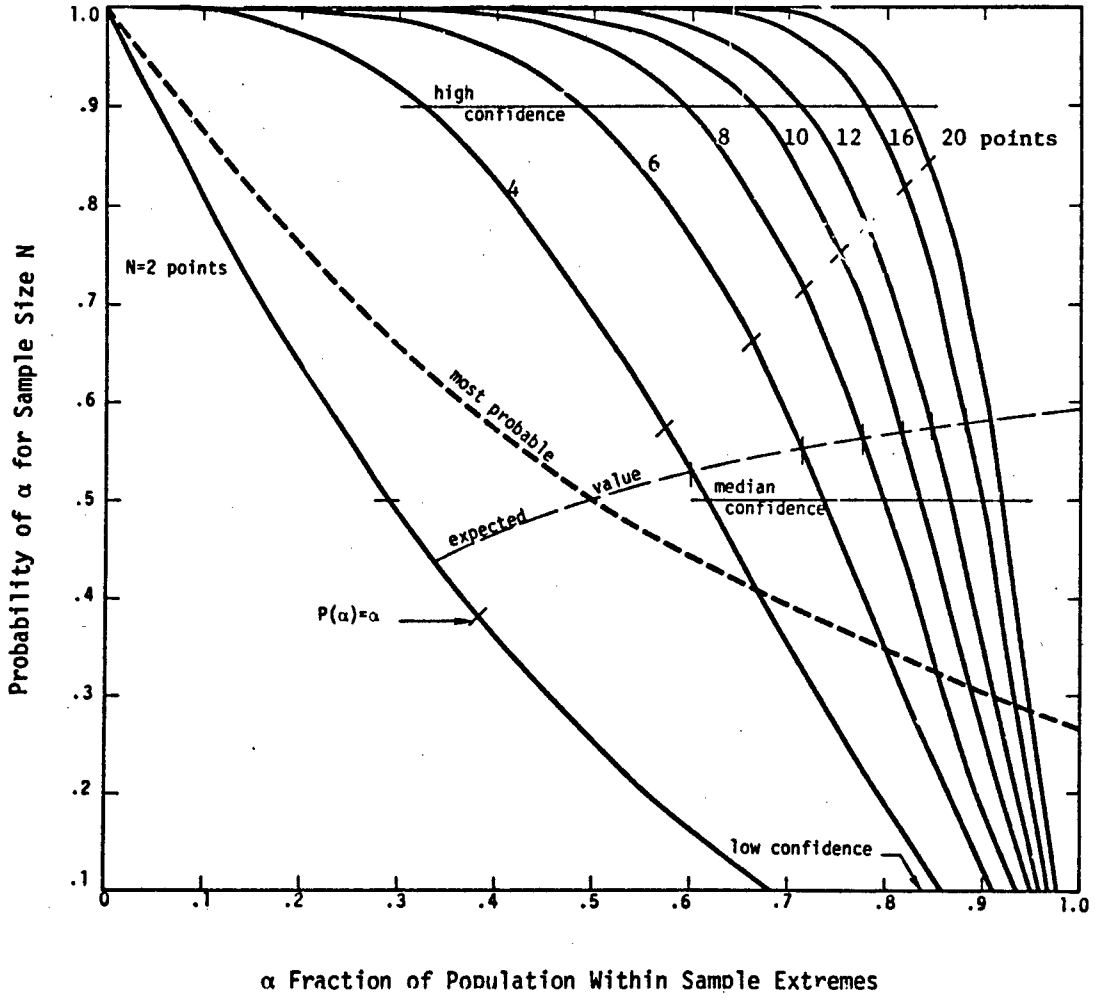

Figure 4.2-8. Probability of a Fraction of the Population Being Within Sample Extremes

Note that even the 4 variances are sufficient to least squares fit a linear curve and test for a statistically significant slope.

This group of 104 points has some range redundancy as evident by the large number of bins with 5 through 10 points for 46 bins per decade (that is, the ratio of maximum to minimum ranges for the bin is only 1.051). This much data prevents the offset feature from operating effectively. For event Easy (only 37 points) at the maximum SHOB of this group, the following tabulation results:

Bins/Decade	No. of S^2	Max. No./Bin	No. of S^2	Max. No./Bin
46	1	8	1	8
23	2	10	2	8
15	3	14	3	8
12	2	10	4	14
8	2	14	4	14
5	3	14	3	16
3	2	20	2	28

Thus the final algorithm is applicable to many individual events where independent blast instrumentation lines were used. An empirical estimate of the maximum number of variances from these two examples is one-ninth of the number of points.

The next step required obtaining an approximate analytical relationship for differentiating in order to convert pressure variance to range variance. The log p - log scaled R data was linearly regressed with attention on the coefficient of determination (squared regression coefficient) which measures the amount of variation from the mean explained by the fitted curve. (Alternatively, a "forecast efficiency" is calculated from $1 - (1-r^2)^{\frac{1}{2}}$ which is plotted in Figure 4.2-9; only 50 percent efficiency results from $r = 0.866$ or $r^2 = 0.75$.) Note also that the coefficient of determination is the product of the slopes from independently regressing y-on-x on x-on-y so it implies the inaccuracy

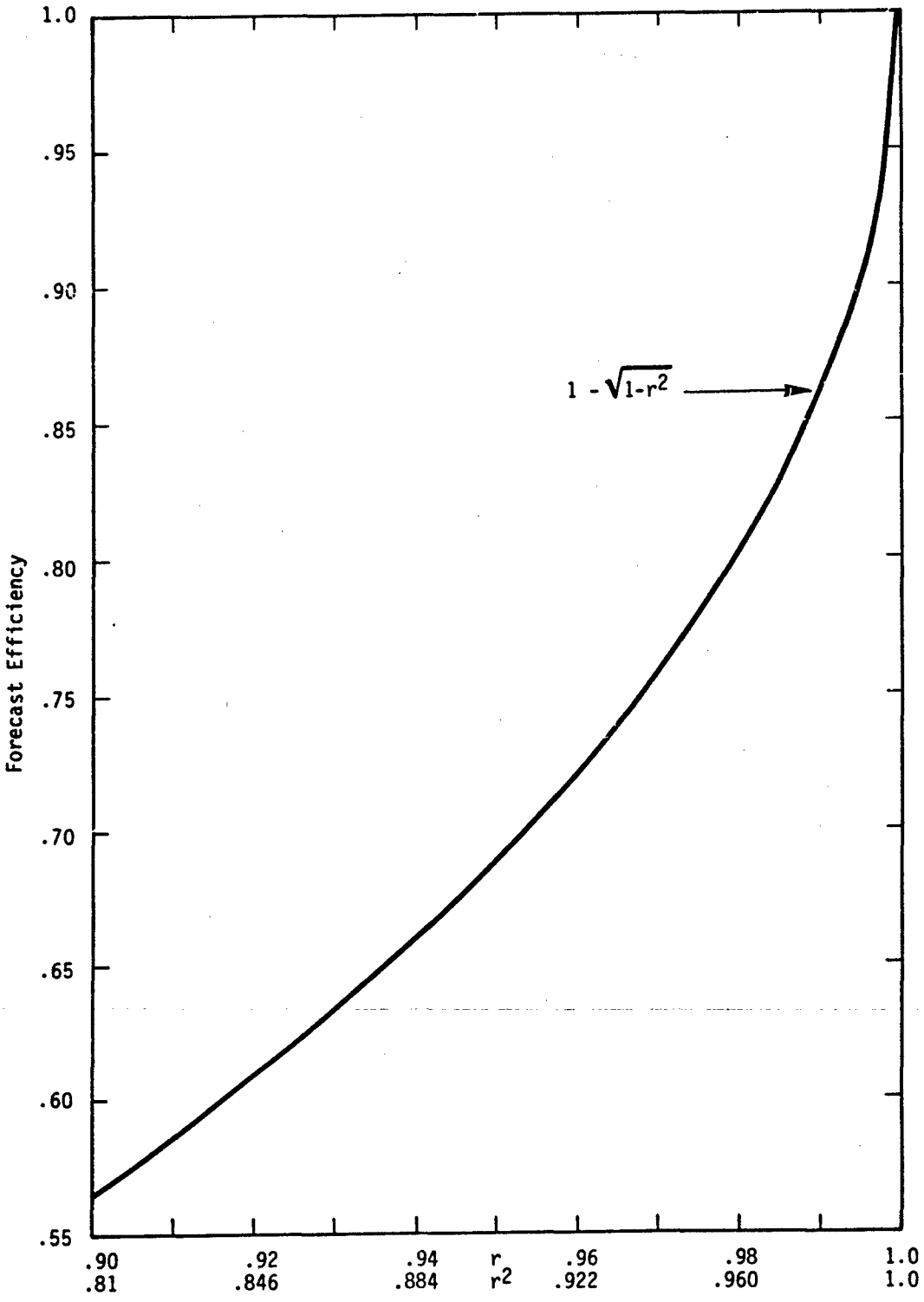

Figure 4.2-9. Forecast Efficiency for Regression Coefficient ≥ 0.9

of using the inverse of the p-on-R (i.e., Brode equation) for a R-on-p fit which is needed for differentiation and use in the variance propagation. Recognizing that one straight line across all the data is wrong, the linear regression was performed in independent intervals using very wide bins; a quadratic fit is more appropriate but causes a messy differentiation. The results for various data and bin widths follow in Table 4.2-2.

Table 4.2-2. Coefficient of Determination for Broad Range Bins

2 Bins/Decade				3 Bins/Decade				5 Bins/Decade			
R_{med}	N	$r^2_{\Delta p}$	r^2_{Ip}	R_{med}	N	$r^2_{\Delta p}$	r^2_{IP}	R_{med}	N	$r^2_{\Delta p}$	r^2_{IP}
				Group 5585							
562	66	.86	.51	316	14	.28	.01	398	17	.15	.01
1778	40	.74	.63	681	52	.79	.42	631	33	.66	.13
				1469	40	.74	.63	1000	41	.35	.30
								1585	15	.87	.61
				Priscilla							
278	6	.62	.42	316	29	.96	.59	316	22	.93	.50
562	46	.96	.64	681	23	.82	.43	501	21	.81	.10
1778	5	.39	.04	1469	5	.39	.04	794	9	.56	.31
								1259	5	.39	.04
				Group 212252							
562	63	.88	.82	464	29	.94	.81	316	6	.92	.86
1778	28	.92	.93	1000	54	.47	.67	501	18	.73	.59
				2153	8	.98	.96	794	39	.16	.24
								1259	21	.67	.58
								1995	6	.97	.89

These results have a clear message. The peak overpressure measurements are much better described by a power law than are the overpressure impulse measurements. The consequence is that the following quadratic form should be used for overpressure impulse without range binning for all the data:

$$I_p = e^a R^{b+c\ln R} \quad .$$

For peak overpressure, the self-consistency of the data is not adequate to prefer these fits to the Brode equation as far as calculating the derivative or slope for the variance propagation. Thus the two peak overpressures were calculated from the Brode equation for bin edges and the finite difference approximation calculated for the slope at the mid-point. The second derivative was likewise approximated so the ratio of the skewness term to the variance term could be calculated and used for propagation of peak overpressure scatter to scaled range variance.

The scaled overpressure impulse propagating in free air is inversely proportional to scaled range (Reference 7), and this simple power law approximation was adequate for range normalization within both linear and logarithmic bins (see Figure 4.2-10 for consistency of variance estimates from narrow range bins). Thus the inverse linear power is assumed so the derivative is as follows;

$$\frac{\partial R}{\partial I_p} = \frac{\partial\left(CI_p^{-1}\right)}{\partial I_p} = -CI_p^{-2} = -\frac{R^2}{C}$$

which leads to the propagation formula;

$$\sigma_{RI} = \frac{R^2}{C}\sigma_{I_p}, \text{or } C\sigma_{RI} = R^2\sigma_{I_p} \quad .$$

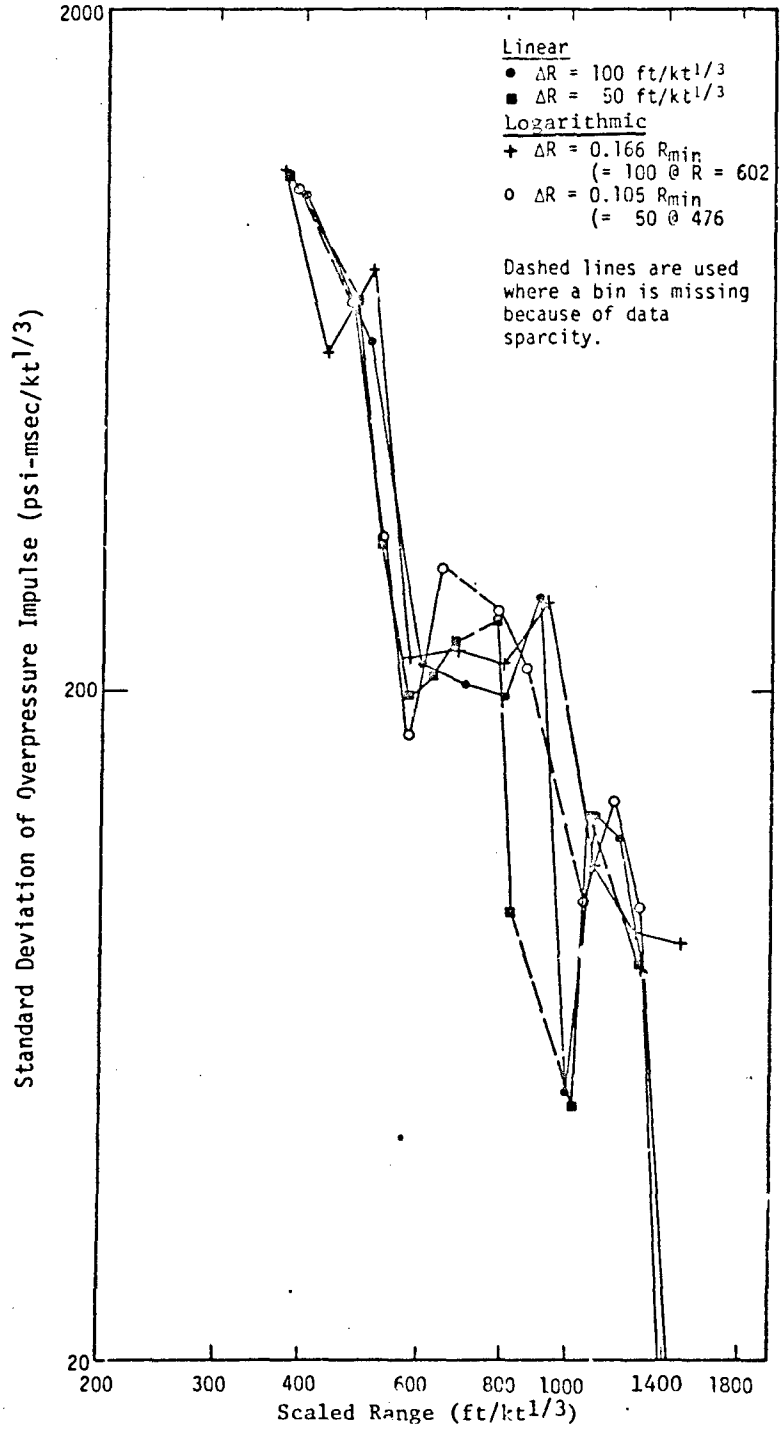

Figure 4.2-10. Standard Deviations of Overpressure Impulse for Linear and Logarithmic Range Binning

The proportionality constant C becomes a scale factor and can be ignored later.

The final step is the fitting of the range uncertainty to range. The highest correlation is expected by fitting in logarithmic space. But the lognormal hypothesis requires fitting specifically in linear space. That is, the polynomial

$$\sigma_{R_z} = a + bR$$

is used and b is tested for significance using its standard deviation calculated from the remaining average residual.

4.2.3 Results

Most of the data base of static pressures is presented graphically in the 20 plots of Section 4.1 for various scaled HOB bins. Only peaks with associated impulses were used so the results could be intercompared directly. The sparce amount of data beyond the edges of the plots were neglected only for plotting convenience. The minimum and maximum axes values cover the region of tactical interest, but the scientific interest extends another factor of ten or more.

This analysis has emphasized data in Reference 4 which was further culled so systematic processing could be used. The culled data were primarily impulses. The following tabulation presents one of the author's (JEC) subjective reasons for culling the value. A small I_p value of 145 at 2064 $ft/kt^{1/3}$ for Sugar was not culled so its effect can be followed through the computerized analysis.

Series	Event	$R(ft/kt^{1/3})$	Subjective Reason
Hardtack I	Koa	296	Both I_p too large
Redwing	Zuni	454	I_p too small
Castle	Bravo	521	I_p too small
Hardtack I	Fig	253, 326	I_p too large
Sunbeam	Small Boy	313	I_p too large
Greenhouse	Easy	383, 466	I_p too large
Tumbler	Dog	794	I_p too large
Hardtack II	Hamilton	1839	I_p too small

The standard deviations of range were normalized to the smallest one in the respective SHOB group and this ratio is plotted in the next set of nine graphs, Figures 4.2-11 through 4.2-19. (Too few data exist in this analysis of SHOB group 478500 for the 8 or 12 bins per decade so no graph is available.) The statistical significance of the slope is implied by the b/σ_b value also tabulated for each curve. The variances of range were also averaged over all SHOB groups pertinent to each range and the resulting standard deviation presented graphically in Figure 4.2-20. Note the very strong linear dependency in this composite data from 590 points. The linearity is also evident in the sub-intervals above and below 1 $kft/kt^{1/2}$, the approximate scaled range to 10 psi peak overpressure and 0.9 $psi\text{-}sec/kt^{1/3}$ overpressure impulse. Thus the lognormal distribution is implied as more appropriate than the normal distribution for both the peak and impulse.

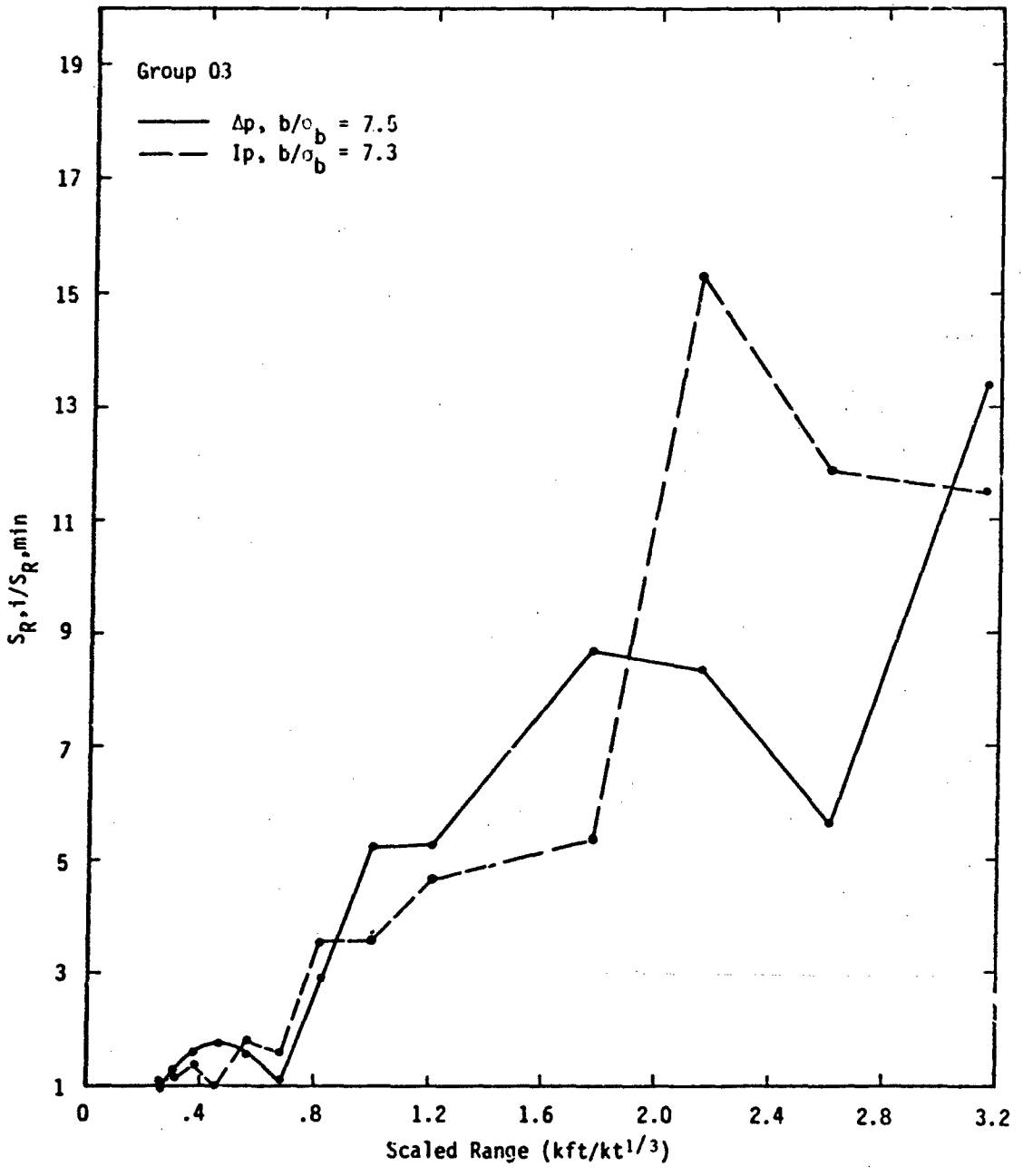

Figure 4.2-11. STANDARD DEVIATION OF RANGE VERSUS RANGE FOR 0 to 3 ft/kt$^{1/3}$ HOB

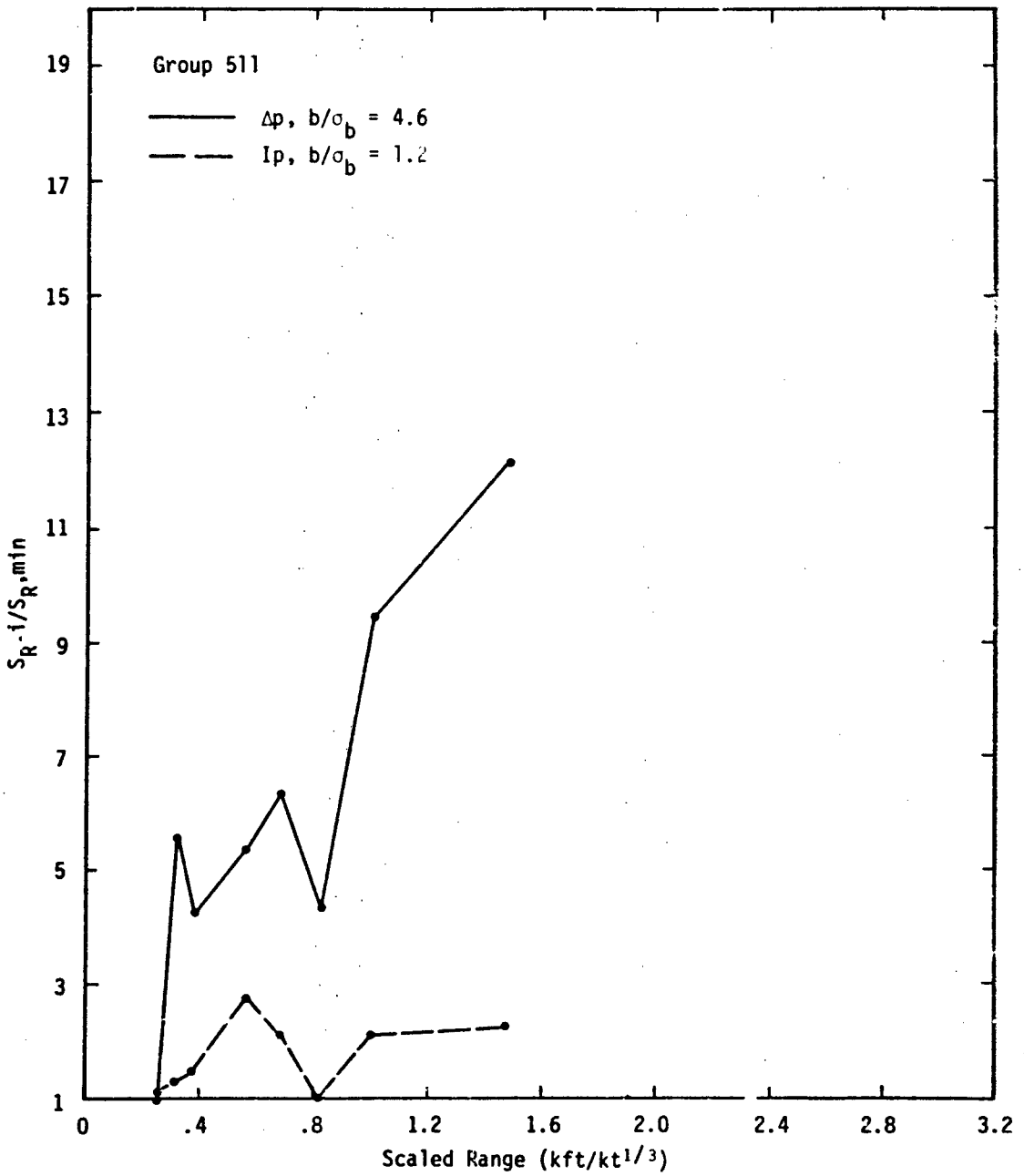

Figure 4.2-12. STANDARD DEVIATION OF RANGE VERSUS RANGE FOR 5 to 11 ft/$kt^{1/3}$ HOB

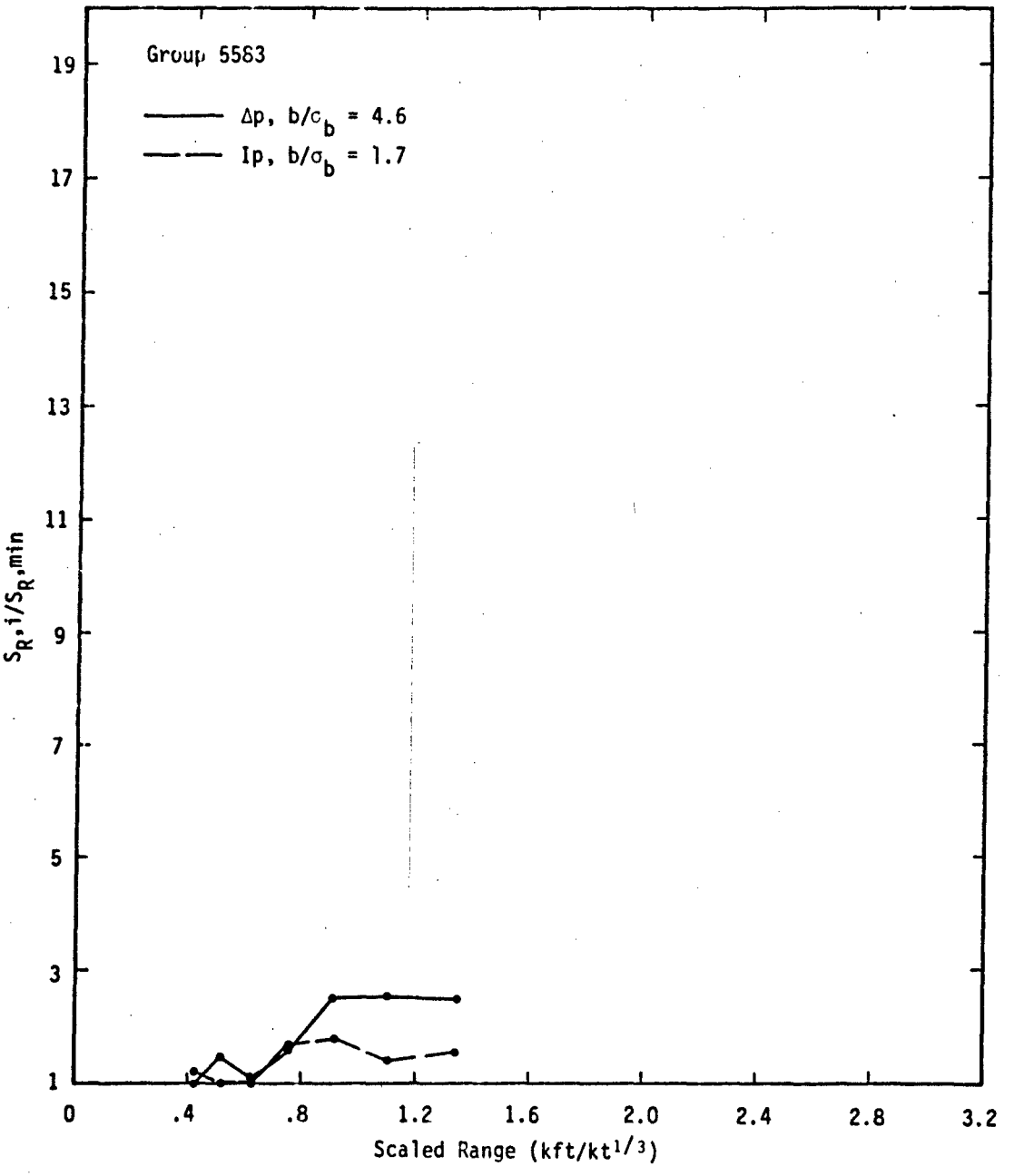

Figure 4.2-13. STANDARD DEVIATION OF RANGE VERSUS RANGE FOR 55 to 83 ft/kt$^{1/3}$ HOB

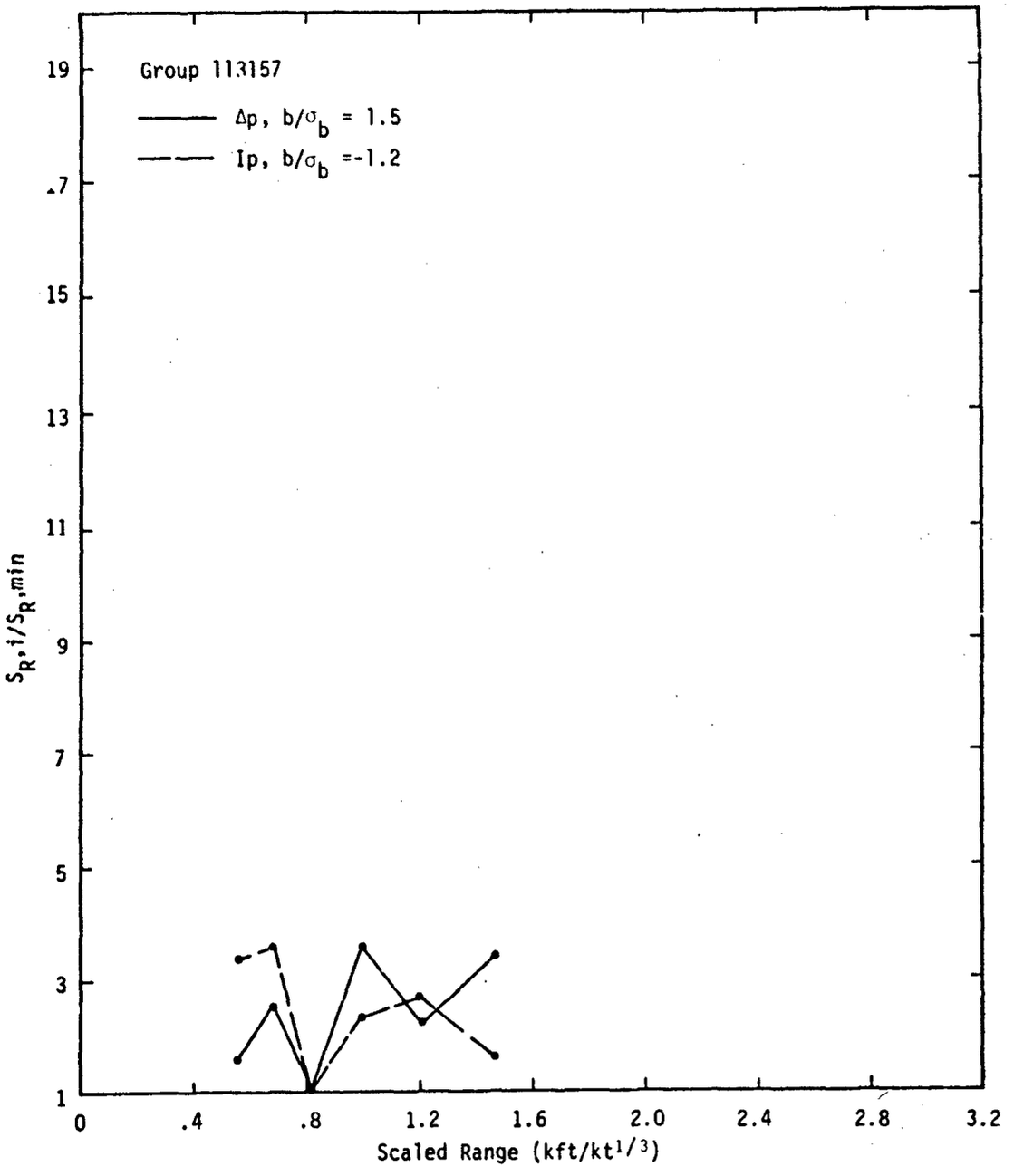

Figure 4.2-14. STANDARD DEVIATION OF RANGE VERSUS RANGE FOR 113 to 157 ft/kt$^{1/3}$ HOB

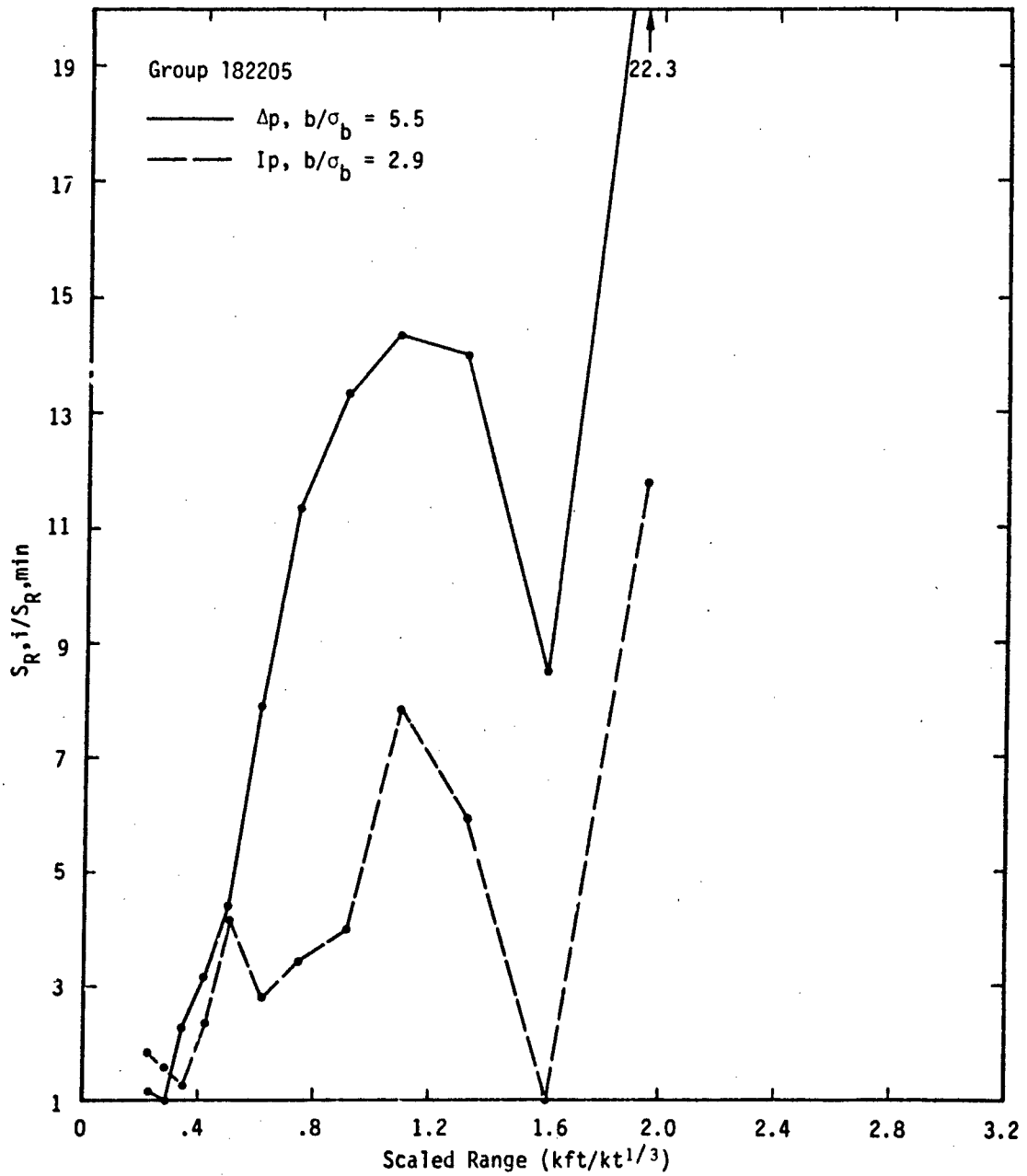

Figure 4.2-15. STANDARD DEVIATION OF RANGE VERSUS RANGE FOR 182 to 205 ft/kt$^{1/3}$ HOB

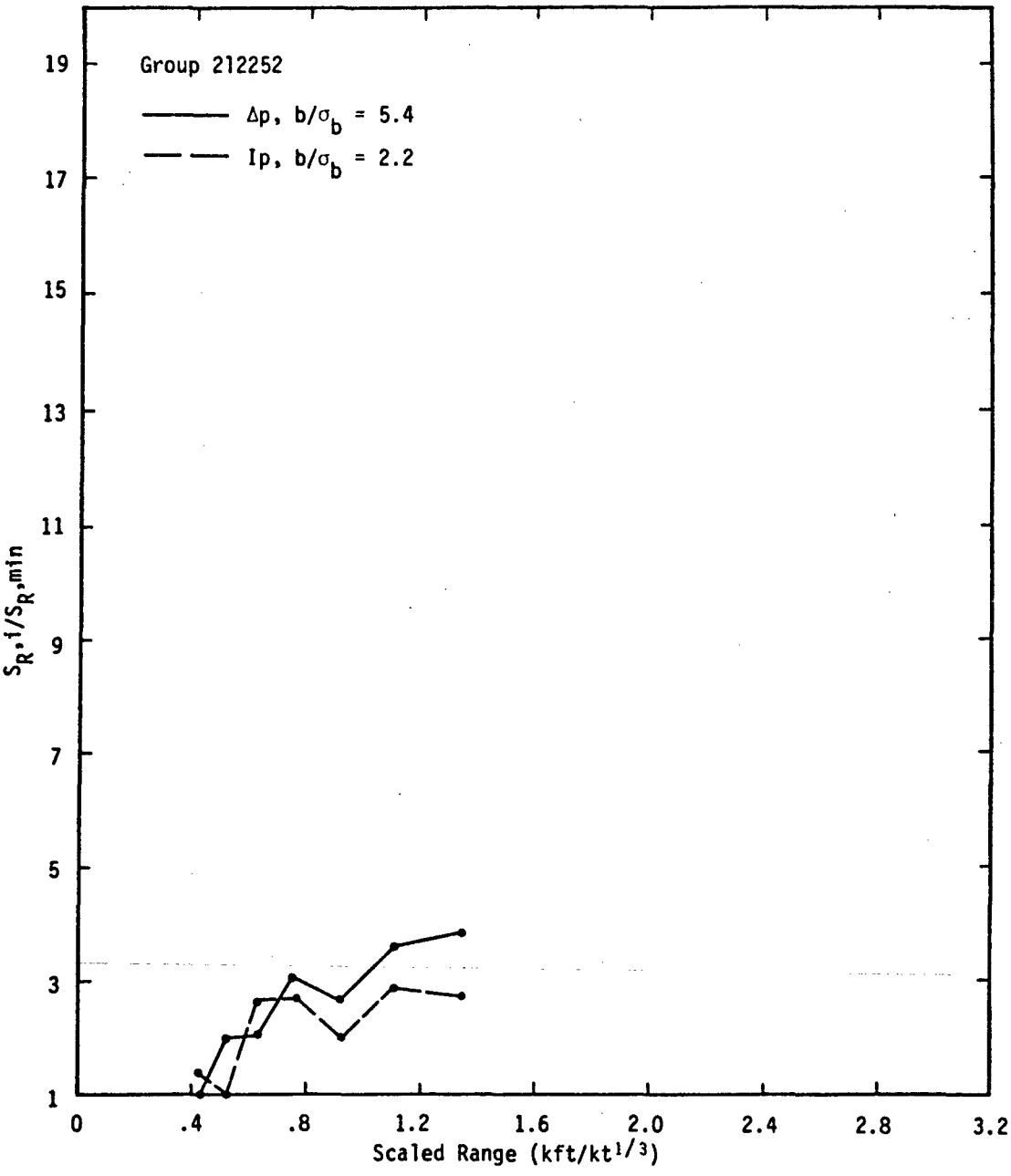

Figure 4.2-16. STANDARD DEVIATION OF RANGE VERSUS RANGE FOR 212 to 252 ft/kt$^{1/3}$ HOB

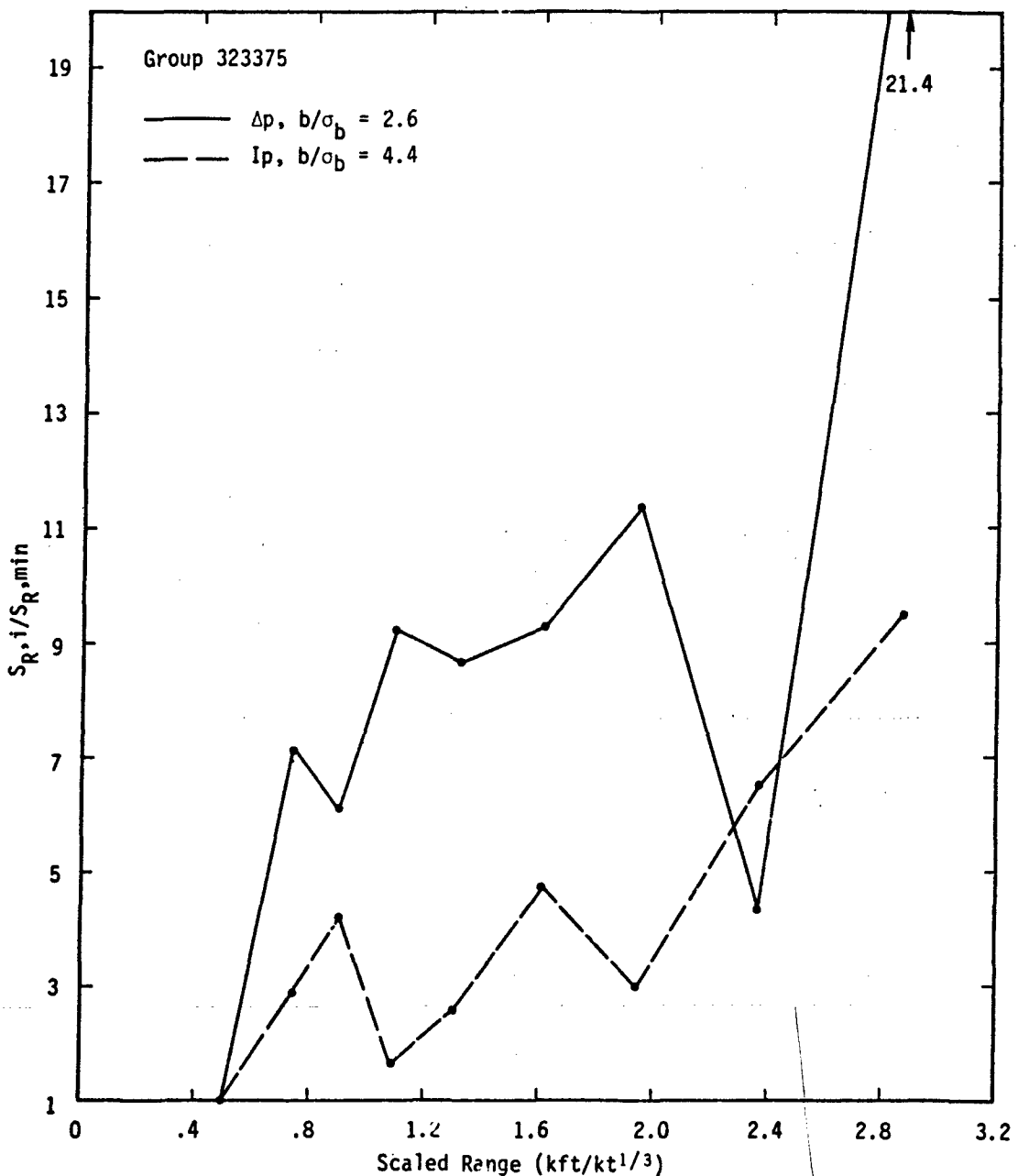

Figure 4.2-17. STANDARD DEVIATION OF RANGE VERSUS RANGE FOR 323 to 375 ft/kt$^{1/3}$ HOB

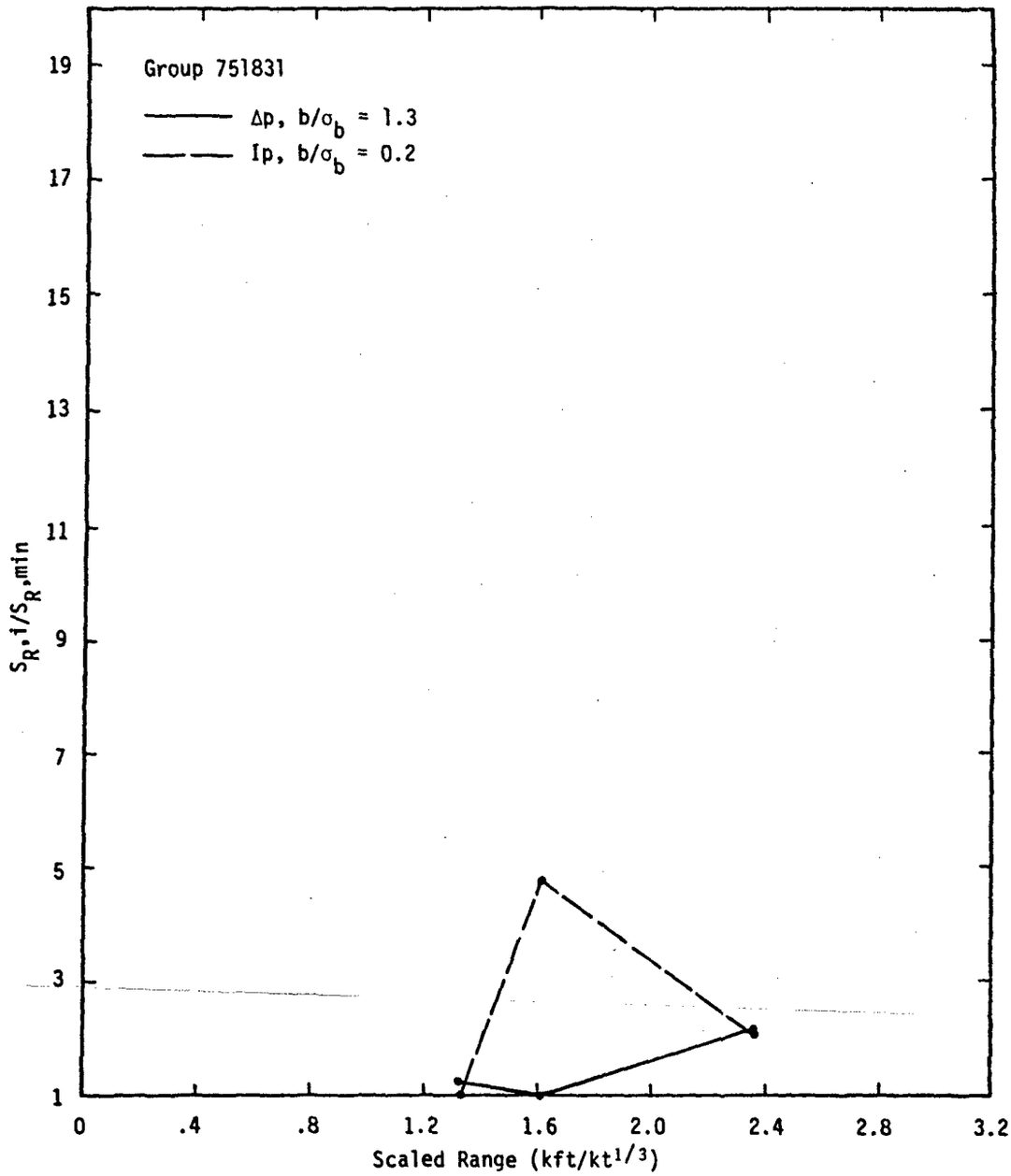

Figure 4.2-18. STANDARD DEVIATION OF RANGE VERSUS RANGE FOR 751 to 831 ft/kt$^{1/3}$ HOB

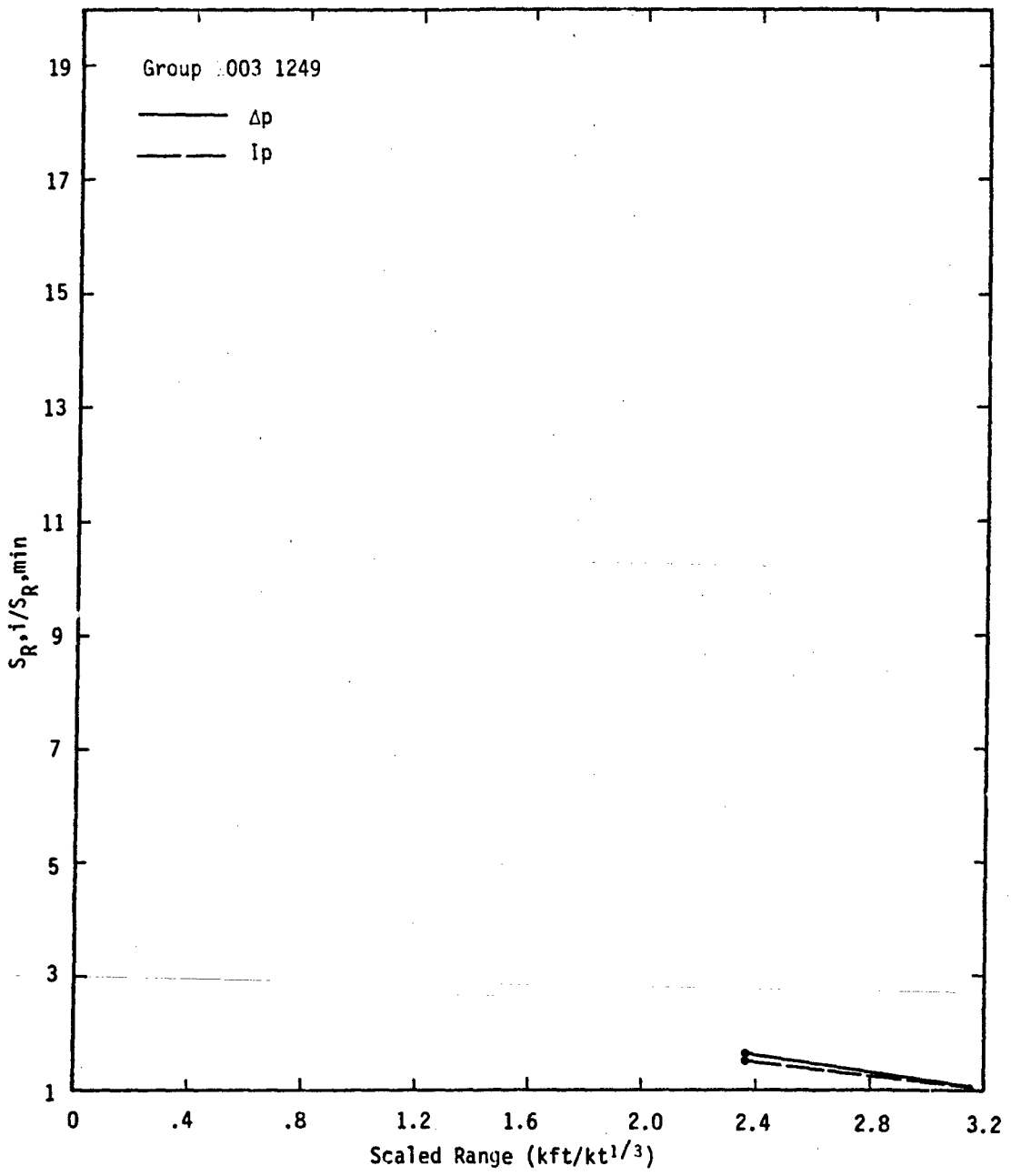

Figure 4.2-19. STANDARD DEVIATION OF RANGE VERSUS RANGE FOR 1003 to 1249 ft/ kt$^{1/3}$ HOB

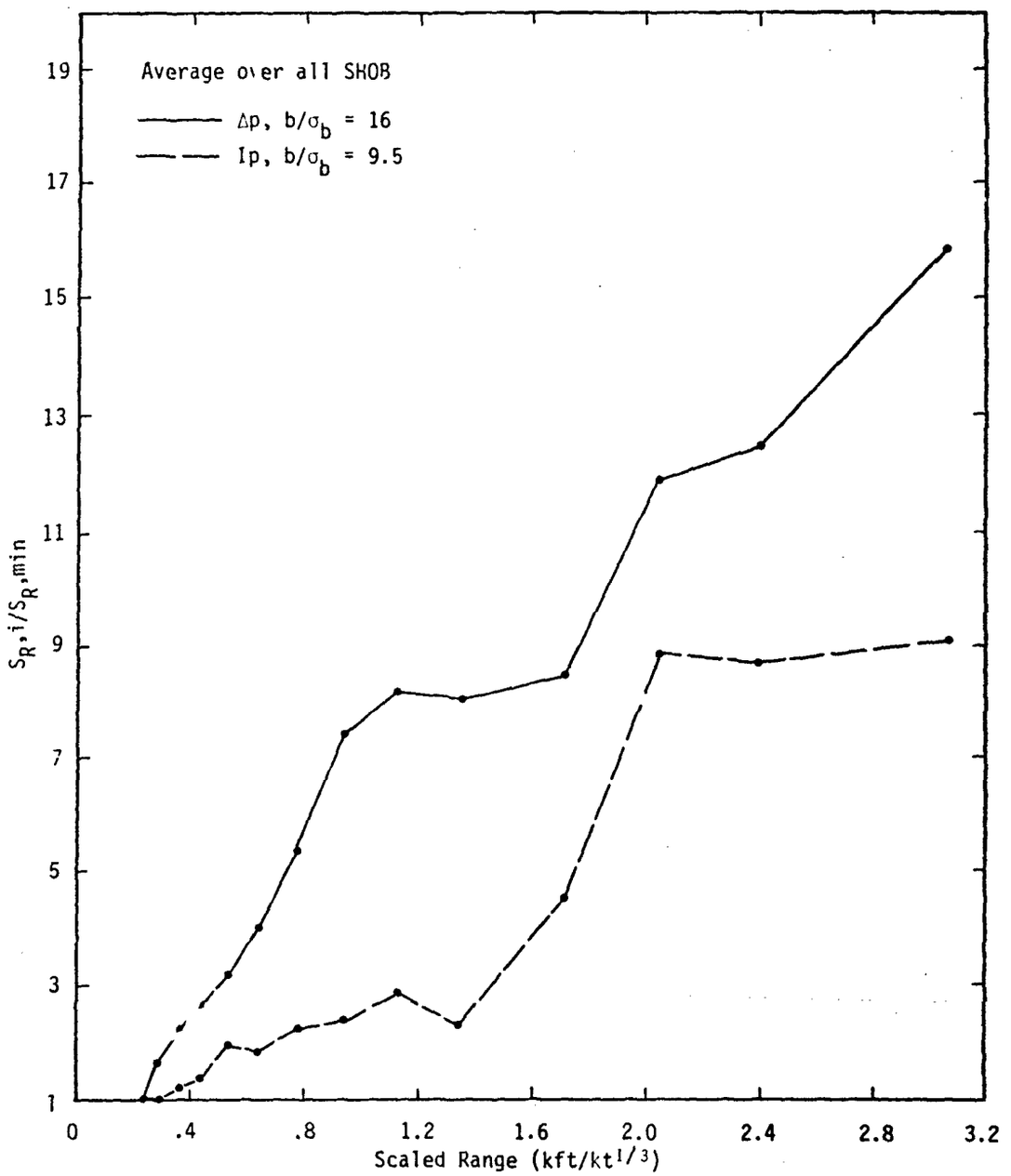

Figure 4.2-20. STANDARD DEVIATION OF RANGE VERSUS RANGE FOR AVERAGED OVER ALL SHOB BINS

Section 5

ANALYSIS FOR BIAS

The potential yield adjustment that could be accomplished by improving the random error variation involves the question of how much one can improve the yield specification if the damage function (e.g., a log normal distribution) were more peaked. The potential yield adjustment from removing systematic biases could result in changing the yield by the range-cubed relationship between yield and range to a specified effect, which is a stronger relationship between yield and range variation than the relationship for the random case. Thus it is important to scrutinize the weapon produced environment data for possible biases, in addition to assessing the effects of random errors.

This section presents the results of analysis of the nuclear test blast data undertaken to ascertain if there are obvious biases in these data. The approach for this analysis was to identify a set of factors that could potentially cause systematic errors and to classify the data according to these factors. An analysis of variance was then conducted on the data to indicate whether any of the effects observed were "significant" (in the statistical sense), or could reasonably have arisen simply by chance. For this analysis, three factors were chosen to discriminate on, namely, instrument type, yield, and waveform type. Three levels of each of the first two factors, and two levels of the third factor were defined:

- Instrument type: SC and SRI gauge recordings; NOL instrumentation recordings; and BRL instrumentation recordings.
- Yield: low yield ($\leq$ 3 Kt); medium yield (3 Kt to 300 Kt); and high yield ($>$300 Kt).
- Waveform type: near-ideal (type V); precursor-associated (non type V).

Only tests for scaled HOB < 11 ft/kt$^{1/3}$ were used.

The analysis was conducted for the scaled ranges to 10, 30, and 100 psi peak overpressure using all the data in Reference 4. A series of four two-factor cross-classified experimental designs were set up and analyzed. Cross-classified designs discriminating on yield and instrumentation type were constructed for scaled range to 10, 30, and 100 psi data, and a cross-classified design discriminating on yield and waveform type was constructed for scaled range to 30 psi data. Designs discriminating on waveform type were not constructed for the scaled range to 10 and 100 psi data, since at these ranges virtually all of these data were of the same waveform type for these low SHOB. In obtaining the ranges to the nuclear produced environments for each shot, an attempt was made to interpolate between data points of a given classification so that the resulting estimated range to each peak overpressure was based on a group of gauge readings rather than on a single reading. In the case where only one instrument type was located in the vicinity of, for instance, the 30 psi range, the range was estimated from the "DASA" curve through these data. In the case where several instrument types obtained recordings in this region, an estimate of the possible bias between the instrument type and the fitted line was obtained. Thus, if an instrument type showed recordings consistently higher or lower than the fitted curve in the region, this bias was accounted for in estimating the range to 30 psi as recorded by that instrument type. Figure 5.1 illustrates this procedure. For the experimental design involving waveform, the waveform type was taken as tabulated in Reference 4.

Table 5.1 shows the cross-classified design discriminating on instrument type and yield for range to 30 psi. The data found to have the appropriate yield/instrument type combinations are shown in each cell, along with the estimated range to 30 psi for that combination. Also shown are the cell means and the column and row means for each factor level. The analysis of variance, showing the partitioning of the total sum of squares among the factors, was performed on these data; the results are presented in Table 5.2. Tables 5.4, 5.5, 5.7, 5.8, 5.10, and 5.11 show the experimental designs and analysis of variance for the

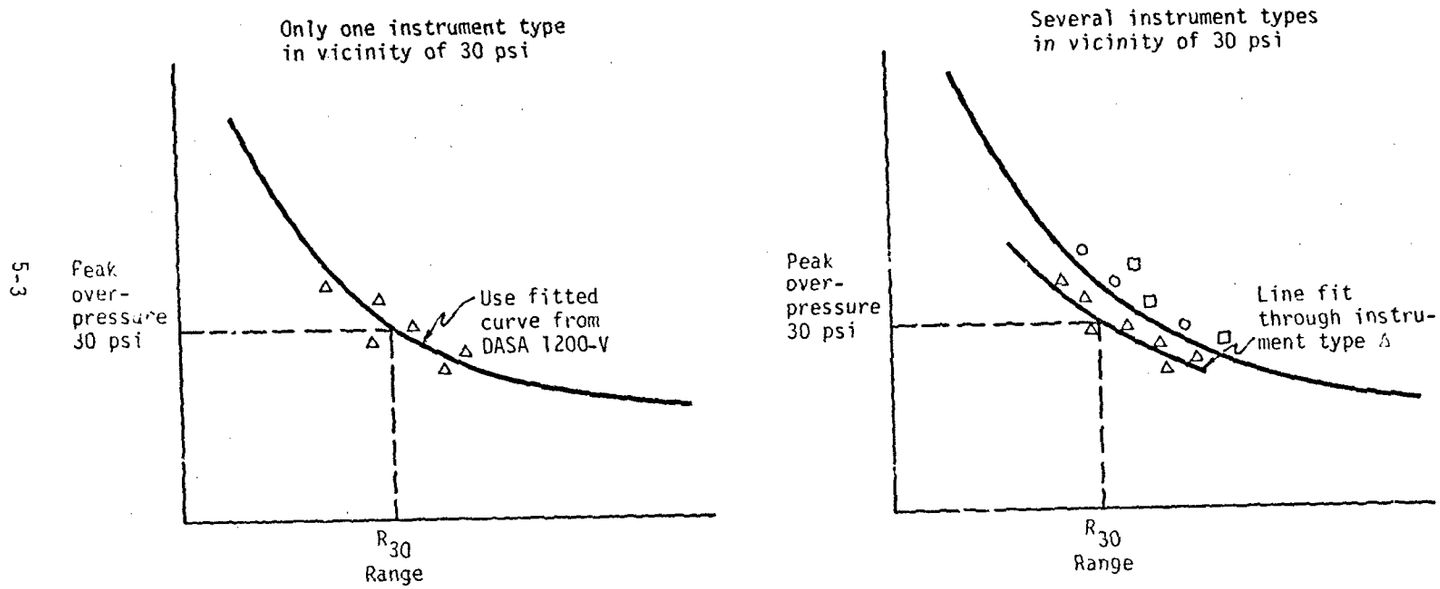

Figure 5.1 Procedure for Obtaining Instrumentation Type Ranges

for the 10 and 100 psi yield versus instrument type experiments, and for the range to 30 psi yield versus waveform type experiment.

To ascertain the significance of the variation ascribed to each factor and the interaction, standard F-tests were performed utilizing the mean squares from the analysis of variance tables. These are presented in four Tables, 5.3, 5.6, 5.9, and 5.12. As can be seen, yield, when compared to the residual variation, appears to make a significant contribution to the total variation for at least 3 of the experimental designs. In fact, for the range to 30 psi data in the design discriminating on yield and instrumentation type, this contribution can be described as "highly significant" since a result like the one observed would occur by chance less than one percent of the time if, in fact, there is no true contribution due to yield. For the range to 10 psi data, however, the result appears to be only marginally significant. In fact, if it were not for the other results, all of which indicate yield as a factor causing a significant amount of variation in the data, the results for the range to 10 psi data would have been dismissed as a "real" effect, since results of this type could be observed a sufficiently large number of times by chance to discount the results as significant.

To ascertain the possible effect on the change in yield suggested by the yield scaling bias, consider the case for the range to 30 psi data:

- The mean of the medium and large yields (computed from Table 5.1) is 575.72 ft/ktl/3 for 30 psi. This represents a systematic bias between small and large yields that corresponds to an error factor of $f_R = 1.08$, which in turn would correspond to a yield mis-specification of about 27 percent if the scaled results of large yields were used to represent small yields. (The same argument applies if the scaled results of small yields are to be used to represent large yields.)
- The scaled range to 30 psi from DASA 2506 is 610 (572 based on using a multiplication factor of only 1.65 for the yield "doubling" expected at the surface). If this

is used to represent low yield environments, a mean bias corresponding to an error factor of f_R=1.15 (1.07 for 1.65 "doubling") is indicated. This corresponds to a mis-specification of yield by approximately 50 percent (24 for 1.65 "doubling").

The above suggests that there might be a relationship between yield and the scaled range to 30 psi for these surface tests. In other words, cube-root scaling may not be appropriate over the entire yield spectrum. Figure 5.2 shows a plot of yield versus scaled range to 30 psi; the line through the points was fit to all 15. Visually, there appears to be a linear relationship between the log of yield and scaled range, i.e., a bias that exists even after the initial scaling for surface shots. Another observation is that Sugar (1.2 kt) and Koon (150 kt) appear to be outliers on this plot. Sugar was an early test conducted with early instrumentation (but it was found that instrumentation did not contribute to the variation), and Koon was a test in which significant instrumentation "failures" were observed (although DASA 1200 reports that the recordings presented are good data). No immediate explanations are available as to why Sugar and Koon should be outliers.

For the present, assume that there is a linear relationship between the log of yield and scaled range to 30 psi, and assume as a tentative hypothesis that this phenomenon is due to a variation in the fraction of total energy that goes into the nuclear produced blast environment that scales with yield. Then the true scaling relationship between yield and range would be the form:

$$\frac{R_W}{R_o} = \left(\frac{g(W)\ W}{g_o\ W_o} \right)^{1/3}$$

where

R_W = True range to 30 psi for arbitrary yield W

R_o = Range to 30 psi for 1 Kt

W_o = 1 Kt

Table 5.1

YIELD VS. INSTRUMENTATION TYPE EXPERIMENTAL DESIGN

SCALED RANGE TO 30 PSI

Instrumentation Type	YIELD: LOW (≤3 kt)			MEDIUM (3 to 300 kt)			HIGH (>300 kt)		
		SCALED RANGE ($ft/kt^{1/3}$)	$\bar{x}_{11} = 500$		SCALED RANGE ($ft/kt^{1/3}$)	$\bar{x}_{12} = 550$		SCALED RANGE ($ft/kt^{1/3}$)	$\bar{x}_{13} = 580.0$
S C/SRI	$\bar{x}_{.1} = 552.5$ $m_1 = 4$		500	$\alpha_{11} = 1$	550	$\alpha_{12} = 1$		585 575	$\alpha_{13} = 2$
NOL	$\bar{x}_{.2} = 570.0$ $m_2 = 4$			$\alpha_{21} = 0$	575	$\bar{x}_{22} = 575$ $\alpha_{22} = 1$		560 585 560	$\bar{x}_{23} = 568.33$ $\alpha_{23} = 3$
BRL	$\bar{x}_{.3} = 568.87$ $m_3 = 15$		520 535 540 565	$\bar{x}_{31} = 540$ $\alpha_{31} = 4$	620 550 630	$\bar{x}_{32} = 600$ $\alpha_{32} = 3$		550 540 598 595 570 570 575 575	$\bar{x}_{33} = 571.63$ $\alpha_{33} = 8$
$\bar{\bar{x}} = 566.22$	$\bar{x}_{1.} = 532.0$ $m_1 = 5$			$\bar{x}_{2.} = 585.0$ $m_2 = 5$			$\bar{x}_{3.} = 572.15$ $m_3 = 13$		

$\bar{x}_{i.}$ = mean value of scaled range for i^{th} column

$\bar{x}_{.j}$ = mean value of scaled range for j^{th} row

α_{ij} = total samples

$\bar{\bar{x}}$ = total mean

m_i = number of samples in i^{th} column

m_j = number of samples in j^{th} row

Table 5.2

ANALYSIS OF VARIANCE

SOURCE OF VARIATION	SUM OF SQUARES	DEGREES OF FREEDOM	MEAN SQUARE (SS/df)	EXPRESSION FOR DEGREES OF FREEDOM
Factor A (Yield)	$\sum_i m_i(\bar{x}_i - \bar{\bar{x}})^2 = 8075.63$	2	4037.82	$df_A = (n - 1)$
Factor B (Gauge)	$\sum_j m_j(\bar{x}_j - \bar{\bar{x}})^2 = 915.44$	2	457.72	$df_B = m - 1$
Interaction	$SS_T - SS_R - SS_A - SS_B = 2748.52$	3	916.17	$df_I = df_T - df_R - df_A - df_B$
Residual (R)	$\sum_i \sum_j \sum_k (x_{ijk} - \bar{x}_{ij})^2 = 8053.73$	15	536.92	$df_R = \sum_i \sum_j (\alpha_{ij} - 1)$
Total (T)	$\sum_i \sum_j \sum_k (x_{ijk} - \bar{\bar{x}})^2$	22		$df_T = (\sum_i \sum_j \alpha_{ij}) - 1$

SS_T = Sum of squares of Total

SS_R = Sum of squares of Residual

SS_A = Sum of squares of Factor A

SS_B = Sum of squares of Factor B

Table 5.3

F-TESTS FOR SIGNIFICANCE

Source of Variation	Mean Square Ratio
Factor A (Yield)	$F_A = \frac{MS_A}{MS_R} = \frac{4037.82}{536.92} = 7.52$
Factor B (Instrumentation)	$F_B = \frac{MS_B}{MS_R} = \frac{457.72}{536.92} = 0.85$
Interaction	$F_I = \frac{MS_I}{MS_R} = \frac{916.17}{536.92} = 1.71$

See 5.6 for text		
%	$F_{2,15}$	$F_{3,15}$
.90	2.70	2.49
.95	3.68	
.99	6.36	
.995	7.70	

- $F_{.99} \leq F_A \leq F_{.995}$ implies yield is a significant source of variation with greater than 99 percent confidence.

- $F_B \leq F_{.9}$ and $F_I < F_{.9}$ implies that instrumentation and the interaction between instrumentation and yield do not contribute significantly to the variation in the data.

Table 5.4

YIELD VS. INSTRUMENTATION TYPE EXPERIMENTAL DESIGN

SCALED RANGE TO 10 PSI

INSTRUMENTATION TYPE		YIELD								
		LOW (≤3 kt)			MEDIUM (3-300 kt)			HIGH (>300 kt)		
			SCALED RANGE $(ft/kt^{1/3})$	CELL STATISTICS		SCALED RANGE $(ft/kt^{1/3})$	CELL STATISTICS		SCALED RANGE $(ft/kt^{1/3})$	CELL STATISTICS
SC/SRI	Row Mean $\bar{x}_{.1} = 1027$ Number in Row $n_1 = 3$		980	$\bar{x}_{11} = 980$ $\alpha_{11} = 1$		1000	$\bar{x}_{12} = 1000$ $\alpha_{12} = 1$		1100	$\bar{x}_{13} = 1100$ $\alpha_{13} = 1$
NOL	Row Mean $\bar{x}_{.2} = 973$ Number in Row $M_2 = 3$					940	$\bar{x}_{22} = 940$ $\alpha_{22} = 1$		980 1000	$\bar{x}_{23} = 99$ $\alpha_{23} = 2$
BRL	Row Mean $\bar{x}_{.3} = 960$ Number in Row $M_3 = 11$		980 920 945 1010	$\bar{x}_{31} = 964$ $\alpha_{31} = 4$		900 960 980	$\bar{x}_{32} = 947$ $\alpha_{32} = 3$		960 920 960 970	$\bar{x}_{33} = 968$ $\alpha_{33} = 4$
Grand Mean $\bar{\bar{x}} = 974$		Column Mean Number in Column		$\bar{x}_{1.} = 967$ $N_1 = 5$	Column Mean Number in Column		$\bar{x}_{2.} = 956$ $N_2 = 5$	Column Mean Number in Column		$\bar{x}_{3.} = 993$ $N_3 = 7$

Table 5.5

YIELD VS. INSTRUMENTATION TYPE ANALYSIS OF VARIANCE

SCALED RANGE TO 10 PSI

SOURCE OF VARIATION	SUM OF SQUARES	DEGREES OF FREEDOM	MEAN SQUARE (SS/df)	EXPRESSION FOR DEGREES OF FREEDOM
Factor A (Yield)	$\sum_i N_i(\bar{x}_{i\cdot} - \bar{\bar{x}})^2 = 4352$	2	2176	$df_A = (n - 1)$
Factor B (Instrumentation)	$\sum_j M_j(\bar{x}_{\cdot j} - \bar{\bar{x}})^2 = 10,339$	2	5169	$df_B = (m - 1)$
Interaction	$SS_T - SS_R - SS_A - SS_B = 6392$	3	2131	$df_I = df_T - df_R - df_A - df_B$
Residual (R)	$\sum_i \sum_j \sum_k (x_{ijk} - \bar{x}_{ij})^2 = 8610$	9	957	$df_R = \sum_i \sum_j (\alpha_{ij} - 1)$
Total (T)	$\sum_i \sum_j \sum_k (x_{ijk} - \bar{\bar{x}})^2 = 29,693$	16		$df_T = \sum_i \sum_j \alpha_{ij} - 1$

Table 5.6

YIELD VS. INSTRUMENTATION TYPE F-TESTS

SCALED RANGE TO 10 PSI

SOURCE OF VARIATION	MEAN SQUARE RATIO
Factor A (Yield)	$F_A = \frac{MS_A}{MS_R} = \frac{2176}{957} = 2.27$
Factor B (Instrumentation)	$F_B = \frac{MS_B}{MS_R} = \frac{5169}{957} = 5.40$
Interaction	$F_I = \frac{MS_I}{MS_R} = \frac{2131}{957} = 2.23$

TABULATED F VALUES: $F_{\alpha,\beta}$ α,β = DEGREES FREEDOM, NUM., DENOM.		
%	$F_{2,9}$	$F_{3,9}$
75	1.62	1.63
90	3.01	2.81
95	4.26	
975	5.71	

- $F_A < F_{.9}$ implies that the factor "yield" is not a significant source of variation (at the 90 percentile level).
- $F_{.95} < F_B < F_{.975}$ implies that the factor "instrumentation type" correlates to a significant source of variation with greater than 95 percent confidence.
- $F_I < F_{.9}$ implies that the interaction term is not a significant source of variation in the data.

Table 5.7

YIELD VS. INSTRUMENTATION TYPE EXPERIMENTAL DESIGN

SCALED RANGE TO 100 PSI

INSTRUMENTATION TYPE		YIELD								
		LOW (≤3 kt)			MEDIUM (3-300 kt)			HIGH (>300 kt)		
			SCALED RANGE ($ft/kt^{1/3}$)	CELL STATISTICS		SCALED RANGE ($ft/kt^{1/3}$)	CELL STATISTICS		SCALED RANGE ($ft/kt^{1/3}$)	CELL STATISTICS
SC/SRI	Row Mean - Number in Row -	←			NO DATA			→		
NOL	Row Mean $\bar{x}_{.1} = 339$ Number in Row $M_1 = 6$		No Data			340	$\bar{x}_{12} = 340$ $\alpha_{12} = 1$		340 320 335 345 355	$\bar{x}_{13} = 339$ $\alpha_{13} = 5$
BRL	Row Mean $\bar{x}_{.2} = 335$ Number in Row $M_2 = 12$		300 280 305 365	$\bar{x}_{21} = 313$ $\alpha_{21} = 4$		340 385	$\bar{x}_{22} = 363$ $\alpha_{22} = 2$		340 360 360 330 325 325	$\bar{x}_{23} = 340$ $\alpha_{23} = 6$
	Grand Mean $\bar{x} = 336$	Column Mean Number in Column		$\bar{x}_{1.} = 313$ $N_1 = 4$	Column Mean Number in Column		$\bar{x}_{2.} = 355$ $N_2 = 3$	Column Mean Number in Column		$\bar{x}_{3.} = 340$ $N_3 = 11$

Table 5.8

YIELD VS. INSTRUMENTATION TYPE ANALYSIS OF VARIANCE

SCALED RANGE TO 100 PSI

SOURCE OF VARIATION	SUM OF SQUARES	DEGREES OF FREEDOM	MEAN SQUARE (SS/df)	EXPRESSION FOR DEGREES OF FREEDOM
Factor A (Yield)	$\sum_i N_i(\bar{x}_{i\cdot} - \bar{\bar{x}})^2 = 3430$	2	1715	$df_A = (n - 1)$
Factor B (Instrumentation)	$\sum_j M_j(\bar{x}_{\cdot j} - \bar{\bar{x}})^2 = 84$	1	84	$df_B = (m - 1)$
Interaction	$SS_T - SS_R - SS_A - SS_B = 257$	1	257	$df_I = df_T - df_R - df_A - df_B$
Residual (R)	$\sum_i \sum_j \sum_k (x_{ijk} - \bar{x}_{ij})^2 = 7056$	13	543	$df_R = \sum_i \sum_j (\alpha_{ij} - 1)$
Total (T)	$\sum_i \sum_j \sum_k (x_{ijk} - \bar{\bar{x}})^2 = 10,827$	17		$df_T = \sum_i \sum_j \alpha_{ij} - 1$

Table 5.9

YIELD VS. INSTRUMENTATION TYPE F-TESTS

SCALED RANGE TO 100 PSI

SOURCE OF VARIATION	MEAN SQUARE RATIO
Factor A (Yield)	$F_A = \frac{MS_A}{MS_R} = \frac{1715}{543} = 3.16$
Factor B (Instrumentation)	$F_B = \frac{MS_B}{MS_R} = \frac{84}{543} = 0.15$
Interaction	$F_I = \frac{MS_T}{MS_R} = \frac{257}{543} = 0.47$

TABULATED F VALUES; $F^{\alpha,\beta}_{\text{NUM.}, \text{DENOM.}}$ = DEGREES FREEDOM;

%	$F_{2,13}$	$F_{1,13}$
90	2.76	3.14
95	3.81	

- $F_{.9} < F_A < F_{.95}$ implies that the factor "yield" correlates to a significant source of variation in the data, with greater than 90 percent confidence.
- $F_B, F_I < F_{.9}$ implies that instrumentation and the interaction do not correlate to significant sources of variation in the data.

Table 5.10

YIELD VS. WAVEFORM TYPE EXPERIMENTAL DESIGN

SCALED RANGE TO 30 PSI

WAVEFORM-TYPE		YIELD: LOW (≤3 kt)	SCALED RANGE ($ft/kt^{1/3}$)	CELL STATISTICS	YIELD: MEDIUM (3-300 kt)	SCALED RANGE ($ft/kt^{1/3}$)	CELL STATISTICS	YIELD: HIGH (<300 kt)	SCALED RANGE ($ft/kt^{1/3}$)	CELL STATISTICS
TYPE V	Row Mean $\bar{x}_{.1} = 555$ Number in Row $M_1 = 6$		520 510	$\bar{x}_{11} = 515$ $\alpha_{11} = 2$		550 580	$\bar{x}_{12} = 565$ $\alpha_{12} = 2$		575 595	$\bar{x}_{13} = 585$ $\alpha_{13} = 2$
NONTYPE V	Row Mean $\bar{x}_{.2} = 569$ Number in Row $M_2 = 6$		540 565	$\bar{x}_{21} = 553$ $\alpha_{21} = 2$		No Data			590 570 598 550	$\bar{x}_{23} = 577$ $\alpha_{23} = 4$
Grand Mean $\bar{\bar{x}} = 562$		Column Mean Number in Column		$\bar{x}_{1.} = 534$ $N_1 = 4$	Column Mean Number in Column		$\bar{x}_{2.} = 565$ $N_2 = 2$	Column Mean Number in Column		$\bar{x}_{3.} = 580$ $N_3 = 6$

Table 5.11

YIELD VS. WAVEFORM TYPE ANALYSIS OF VARIANCE

SCALED RANGE TO 30 PSI

SOURCE OF VARIATION	SUM OF SQUARES	DEGREES OF FREEDOM	MEAN SQUARE (SS/df)	EXPRESSION FOR DEGREES OF FREEDOM
Factor A (Yield)	$\sum_i N_i(\bar{x}_{i\cdot} - \bar{\bar{x}})^2 = 5083$	2	2542	$df_A = (n - 1)$
Factor B (Waveform)	$\sum_j M_j(\bar{x}_{\cdot j} - \bar{\bar{x}})^2 = 574$	1	574	$df_B = (m - 1)$
Interaction	$SS_T - SS_R - SS_A - SS_B - SS_I = 918$	2	459	$df_I = df_T - df_R - df_A - df_B$
Residual (R)	$\sum_i \sum_j \sum_k (x_{ijk} - \bar{x}_{ij})^2 = 2400$	7	343	$df_R = \sum_i \sum_j (\alpha_{ij} - 1)$
Total (T)	$\sum_i \sum_j \sum_k (x_{ijk} - \bar{\bar{x}})^2 = 8975$	12		$df_T = \sum_i \sum_j \alpha_{ij} - 1$

Table 5.12

YIELD VS. WAVEFORM TYPE F-TESTS

SCALED RANGE TO 30 PSI

SOURCE OF VARIATION	MEAN SQUARE RATIO
Factor A (Yield)	$F_A = \frac{MS_A}{MS_R} = \frac{2542}{343} = 7.41$
Factor B (Waveform)	$F_B = \frac{MS_B}{MS_R} = \frac{574}{343} = 1.67$
Interaction	$F_I = \frac{MS_I}{MS_R} = \frac{459}{343} = 1.34$

TABULATED F VALUES; $F_{\alpha,\beta}$ α,β = DEGREES FREEDOM, NUM., DENOM.		
%	$F_{2,7}$	$F_{1,7}$
0.75		1.57
0.9	3.26	3.59
0.975	6.54	
0.99	9.55	

- $F_{.975} < F_A < F_{.99}$ implies that the factor "yield" correlates to a significant source of variation in the data (at the 97.5% level of confidence).
- $F_B < F_{.9}$ implies that the factor "waveform" does not correlate to a significant source of variation in the data.
- $F_I < F_{.9}$ implies that the interaction does not correlate to a significant source variation in the data.

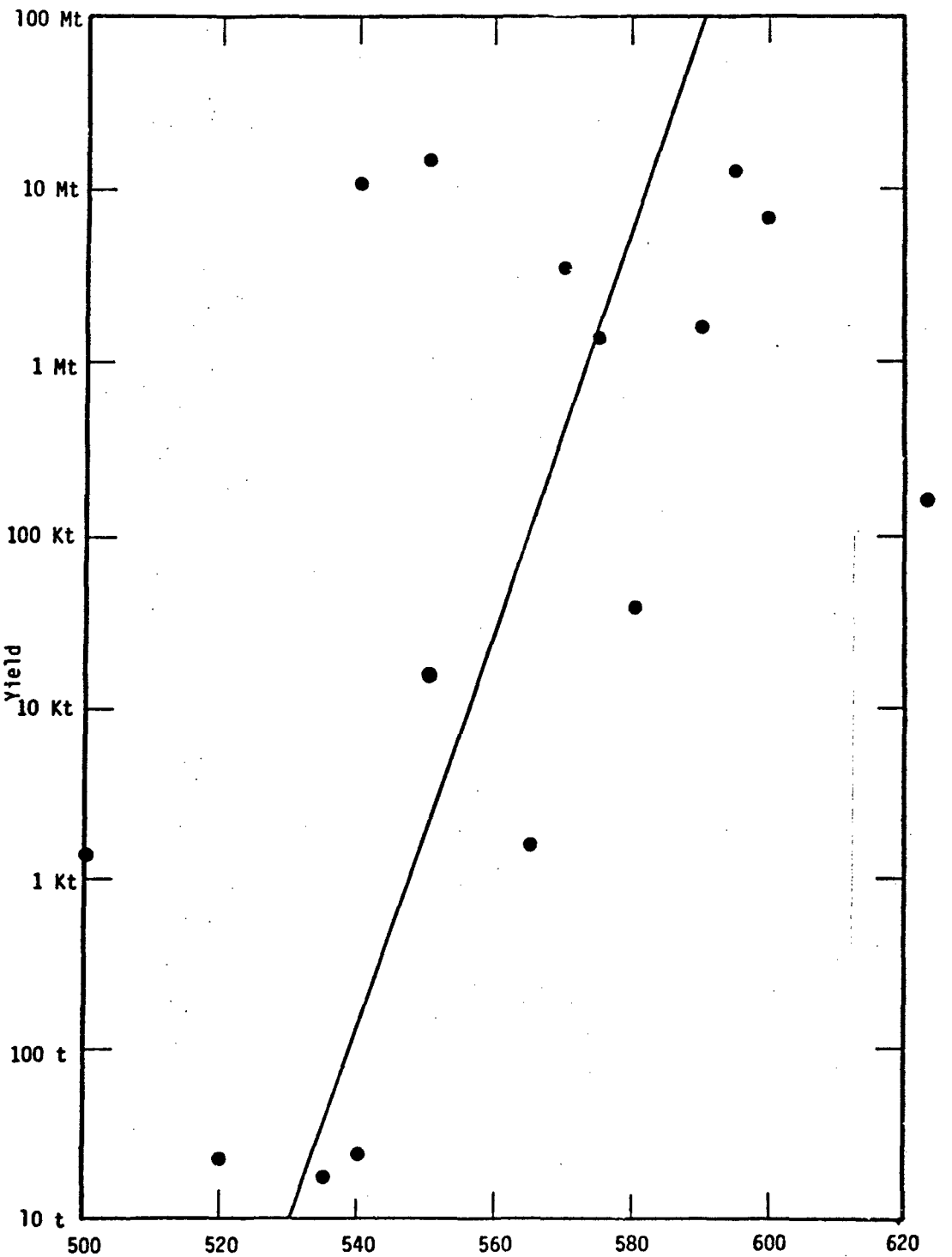

Figure 5.2. Scaled Range to 30 PSI vs. Yield

g_o = Yield multiplicative factor for 1 Kt (proportional to energy coupling into air blast)

$g(W)$ = Yield multiplicative factor for yield W.

From Figure 5.1, the ratio of R_w to R_o should be "corrected" by the factor S_w/R_o, where S_w is the scaled range to 30 psi calculated from the $(W)^{1/3}$ relationship (i.e., the "old" scaled range). Thus:

$$\frac{R_w}{R_o} \cdot \frac{S_w}{R_o} = W^{1/3} \quad ,$$

but

$$S_w = R_o + k \log W \text{ (from Figure 5.1)} \quad .$$

Therefore,

$$\frac{R_o + k \log w}{R_o} \cdot \frac{R_w}{R_o} = W^{1/3}$$

$$\left(\frac{R_o + k \log W}{R_o}\right)^3 \cdot \left(\frac{R_w}{R_o}\right)^3 = W$$

$$\frac{R_w}{R_o} = \left[\frac{W}{(1+k' \log W)^3}\right]^{1/3} \qquad (5\text{-}1)$$

where

$$k' = k/R_o \quad .$$

Therefore, the yield multiplicative factor related to energy coupling, $g(W)$, is:

$$g(W) = 1/(1+k' \log W)^3 \quad .$$

To evaluate k', use the expression for S_w:

$$S_w = R_o + k \log w$$

$$k = \frac{S_w - R_o}{\log W} \quad .$$

Using Figure 5.2 and 20 Kt:

$$k = \frac{566 - 552}{1.301}$$

$$= 10.76$$

$$k' = k/R_o$$

$$= .0195 \quad .$$

The semi-empirical expression, Equation (5-1), can be used to scale low HOB tests and should be adequate between 10 t and 10 Mt. This correction is applicable only for 30 psi from surface bursts.

The potential biases for scaled ranges to 10 and 100 psi are not as pronounced as the bias for the range to 30 psi; in fact, there appears to be no readily discernible bias characterized by the low yield test results being significantly different from the medium and high yield test results for the scaled range to 10 psi data (the analysis of variance indicated a less significant result concerning the amount of variation in the data correlating to the factor yield for this nuclearly produced environment also). The implication is that the effects of blast propagation override any second-order effects that correlate to the factor yield at the scaled range to 10 psi.

For comparison, Figures 5.3 and 5.4 show plots of yield versus scaled range to 10 and 100 psi, respectively.

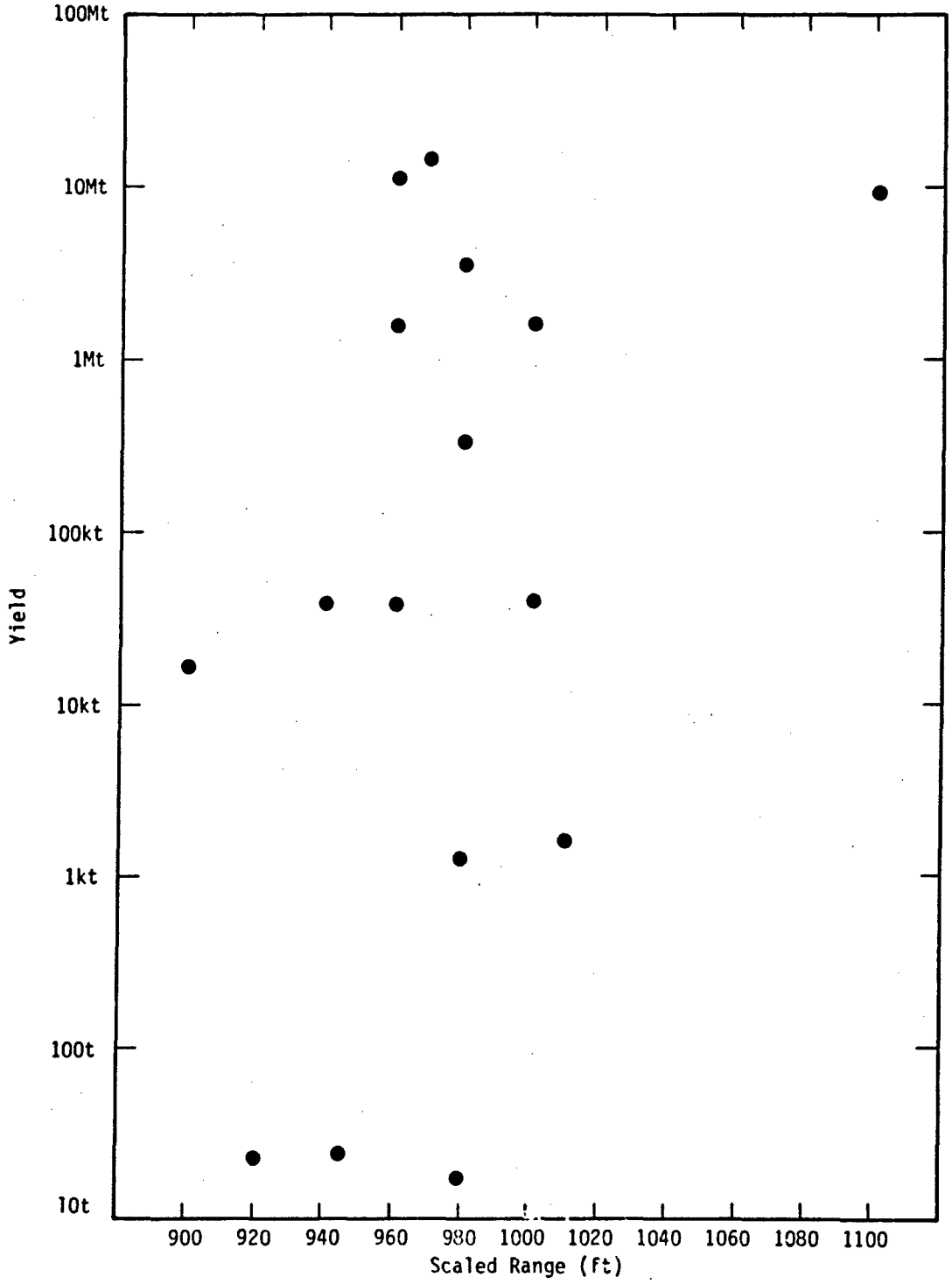

Figure 5.3. Scaled Range to 10 PSI vs. Yield

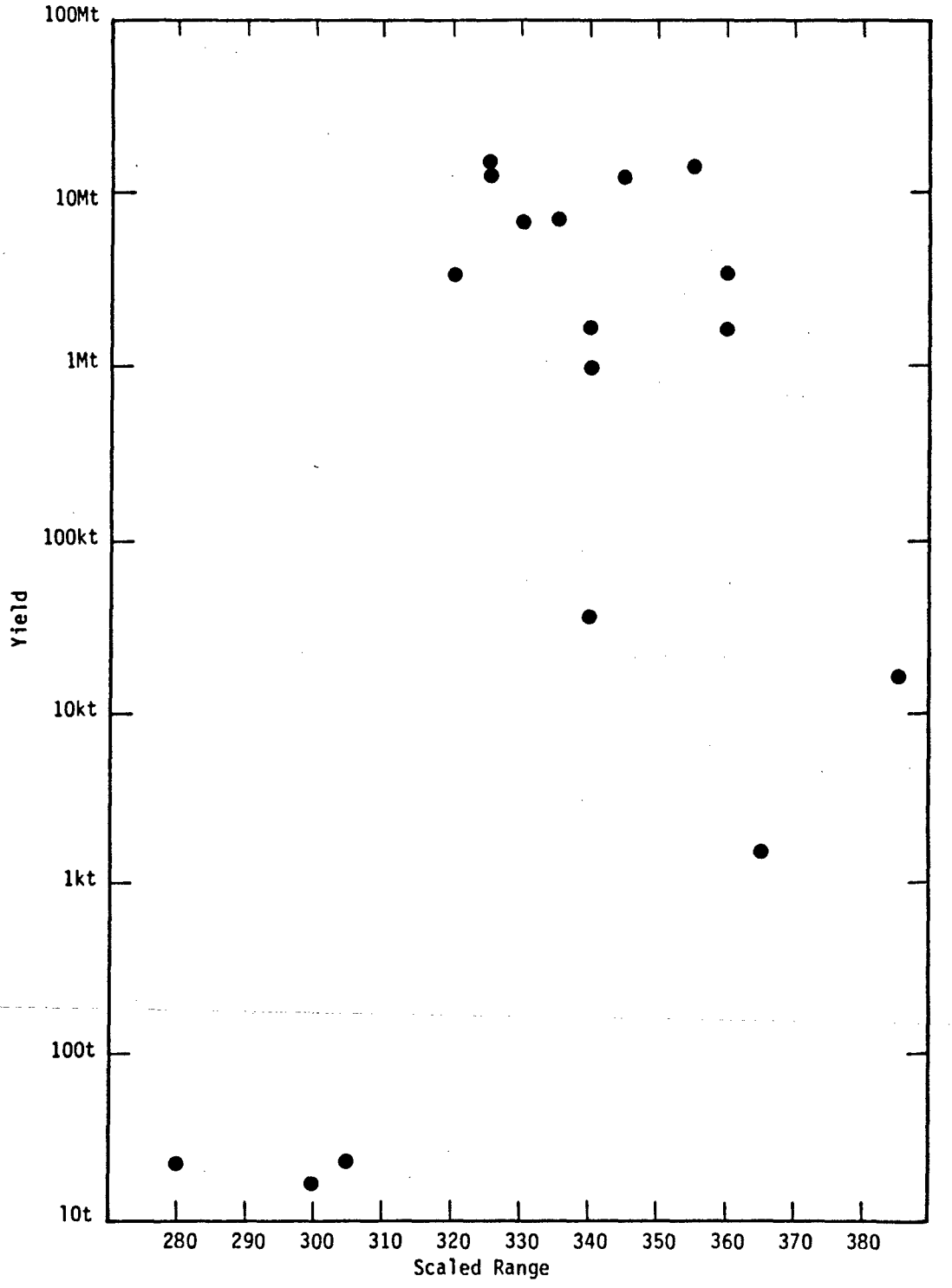

Figure 5.4. Scaled Range to 100 PSI vs. Yield

Section 6

REFERENCES

1. Defense Intelligence Agency, 7 June 1969, Personal Communication.

2. H. L. Brode, Height of Burst Effects at High Overpressures, RAND, DASA 2506, July 1970.

3. C. R. Curran, R. W. Young, and W. F. Davis, "The Performance of Primates Following Exposure to Pulsed Whole-Body Gamma—Neutron Radiation," AFRRI SR 73-1, 1973.

4. C. H. Kingery, et al., October 1971, Personal Communication.

5. C. F. Ksanda, and R. W. Shnider, 16 July 1975, Personal Communication.

6. J. D., Gibbons, Nonparametric Statistical Inference, McGraw-Hill Book Company, 1971.

7. C. E. Needham, et al., Nuclear Blast Standard (1 KT), Air Force Weapons Laboratory, AFWL-TR-73-55 (Rev.), April 1975.

Appendix A
THE LOGNORMAL DISTRIBUTION

A random variable x is said to be lognormally distributed if its logarithm is normally distributed (s^2 = variance of ln x)

$$\frac{dp}{d\ln(x)} = \frac{1}{\sqrt{2\pi s^2}} \exp\left(-\frac{(\ln(x) - \ln(x_o))^2}{2s^2}\right)$$

$$\frac{dp}{dx} = \frac{1}{\sqrt{2\pi s^2}} \frac{1}{x} \exp\left(-\frac{\ln^2(x/x_o)}{2s^2}\right)$$

$$= L\ (x: x_o, s) \text{ and } o<x, x_o, s. \qquad (A1)$$

The lognormal distribution is a natural distribution in that it is appropriate for any random variable which is the product of random variables. In fact, under certain not very restrictive conditions, a Central Limit Theorem can be proved, stating that as N goes to infinity, the product of N independent random variables, no matter how they are individually distributed, is lognormally distributed (References 1, 2). Furthermore, the random variable defined as the sum of lognormal variates is in many cases accurately represented by a lognormal distribution instead of the normal distribution that might be expected on the basis of the Central Limit Theorem (Reference 3). Therefore, if a random variable can be written as the sum of products of random variables, in many cases the appropriate distribution is the lognormal. For very small variance, the region around the mode of the lognormal can be approximated by a normal distribution but the tolerance limits cannot be as easily approximated.

Many properties of the lognormal distribution can be explicitly derived, and will be listed here for use in Section 3.

The cumulative distribution function (CDF) is given in terms of the normal CDF:

$$\int_o^x \frac{dp}{dx}\, dx = F\left(\frac{\ln(x/x_o)}{s}\right) \text{ where } F(z) = \frac{1}{2}\left[1 + \text{erf}\,(z/\sqrt{2})\right| \qquad (A2)$$

The median of the distribution is thus x_o from z=0. Most statistics of interest can be derived from the moments about the origin:

$$\overline{x^n} = \int_0^\infty x^n \frac{dp}{dx}(x)\,dx$$
$$= x_o{}^n \exp\left(\frac{n^2 s^2}{2}\right) \qquad \text{(A3)}$$

so that the mean and variance of x are given by

$$\overline{x} = \overline{x^1} = x_o \exp\left(\frac{s^2}{2}\right)$$
$$\sigma^2 = \overline{x^2} - \overline{x}^2 = \overline{x}^2 \left(\exp(s^2) - 1\right) \qquad \text{(A4)}$$

and s^2, the logarithmic variance, is given by

$$s^2 = \ln\left(1 + (\sigma/\overline{x})^2\right). \qquad \text{(A5)}$$

The lognormal has a very simple expression for the moments of x about the origin; the expression for moments about the mean is more complex. This is just the reverse of the case for the normal distribution.

The mode of the distribution, where dp/dx is maximum, is given by

$$x_{mode} = x_o \exp(-s^2) \qquad \text{(A6)}$$

The lognormal distribution is always skewed, with

$$x_{mode} < x_o < \overline{x} \qquad \text{(A7)}$$

This is illustrated in Figure A-1 for unit median and logarithmic variance.

The percentiles or m-tiles of the lognormal distribution, x_m, are defined as usual

$$\frac{m}{100} = \int_0^{x_m} \frac{dp}{dx}\,dx \qquad \text{(A8)}$$

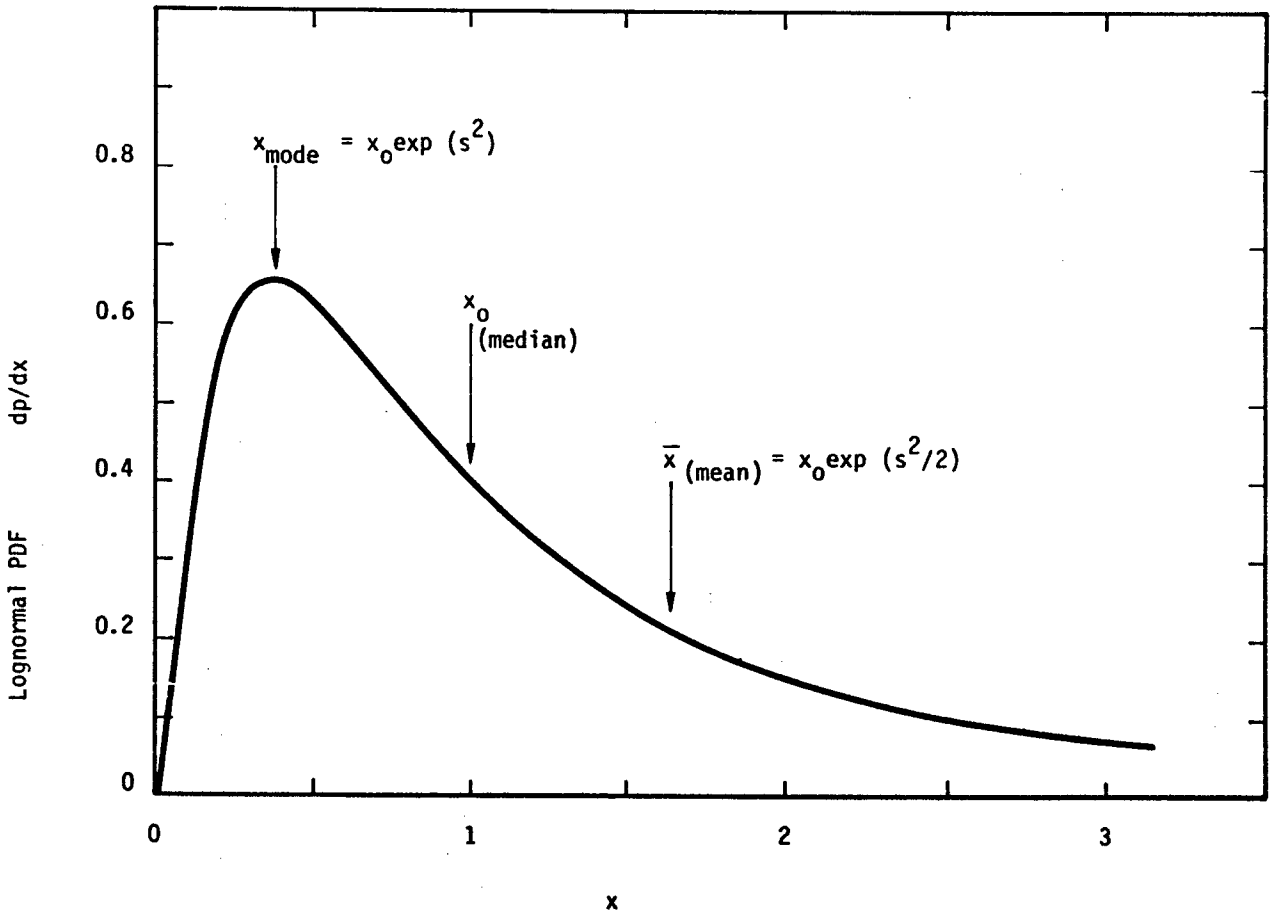

Figure A-1. Lognormal Probability Distribution for Unit Median and Logarithmic Variance.

so that $x_o = x_{50}$. A symmetric p confidence interval is conveniently defined around x_o in terms of a confidence level error factor f_p such that

$$\begin{aligned} x_m &= f_p x_o \quad \text{and} \\ x_{100-m} &= x_o / f_p \quad \text{where} \\ \frac{m}{100} &= (p+1)/2 \,. \end{aligned} \tag{A9}$$

Then it can be seen that

$$\begin{aligned} f_p &= \exp\left(A_{(p)} s\right) \\ A_{(p)} &= F^{-1}\left(\frac{1+p}{2}\right) \end{aligned} \tag{A10}$$

where F is given by Equation (A2). This allows the parameters x_o,s to be determined entirely from the error bounds on the confidence level (CL), i.e., x_m, x_{100-m}. Typically this is done for a 90 percent CL: p=0.9, m=95. For this choice the notation in this report omits the subscript p=0.9 from f_p:

$$f^2 = x_{95}/x_5 \qquad (90\%\text{CL})$$

$$x_o = \sqrt{x_{95} x_5} \tag{A11}$$

Two important theorems about the lognormal distribution are used in this report. The first is:

Theorem 1: If x is a lognormal variate with parameters x_o,s, then $z = ax^b$ is a lognormal variate with parameters $ax_o{}^b$, bs.

Theorem 1 is proved by direct substitution.

Theorem 2: If x, y are lognormal variates with x_o, s_x and y_o, s_y, then $z = x^p y^q$ is a lognormal variate with $z_o = x_o^p y_o^q$, $s_z^2 = p^2 s_x^2 + q^2 s_y^2$.

Theorem 2 is a standard theorem proved many places, e.g., Reference 4, p. 278 ff. However, the proof is illustrative of some of the manipulations required in this study, so will be briefly outlined here. From Theorem 1, x^p and y^q are lognormal variates, so Theorem 2 is similar to the theorem that the sum of two normal variates is a normal variate. For this purpose define normal variates u,v with means u_o, v_o and variances σ_u, σ_v, and a random variable w, with mean w_o, σ_w. Then the probability that the sum of u and v is less than some particular value w is given by the probability of occurrence of a particular u, together with the probability that v is less than or equal to w-u for all u less than w. This relationship may be expressed

$$\int^w \frac{dp}{dw}\, dw = \int^w \frac{dp}{du} \int^{w-u} \frac{dp}{dv}\, dv \quad du \tag{A12}$$

or

$$p_w(w) = \int^w \frac{dp}{du}\; p_v(w-u)\; du \tag{A13}$$

It is convenient to define the Laplace transform

$$\mathcal{L}\left(\frac{dp}{du}, s\right) = \int e^{-su} \frac{dp}{du}\, du \tag{A14}$$

where $\mathcal{L}$ is the Laplace operator and not the PDF of Equation (A1). Then using the common properties of the Laplace transform, the convolution in Equation (A13) becomes

$$\mathcal{L}(p_w, s) = \mathcal{L}\left(\frac{dp}{du}, s\right) \mathcal{L}(p_v, s) \tag{A15}$$

and the relation

$$s\,\mathcal{L}(p_w,s) = \mathcal{L}\left(\frac{dp}{dw},\ s\right) \tag{A16}$$

gives the result

$$\mathcal{L}\left(\frac{dp}{dw}\ ,\ s\right) = \mathcal{L}\left(\frac{dp}{du}\ ,\ s\right)\mathcal{L}\left(\frac{dp}{dv}\ ,\ s\right) \tag{A17}$$

It is easy to see that for the normal distributions, Equation (A14) gives

$$\mathcal{L}\left(\frac{dp}{du}\ ,\ s\right) = \frac{1}{\sqrt{2\pi\sigma_u^2}} \int e^{-su} \exp\left[- \frac{(u-u_o)^2}{2\sigma_u^2}\right]du$$

$$= \exp\ (-\ u_o s + \sigma_u^2 s^2/2). \tag{A18}$$

As a result the unknown dp/dw has the Laplace transform

$$\mathcal{L}\left(\frac{dp}{dw}\ ,\ s\right) = \exp\ (-\ (u_o+v_o)s + (\ \sigma_u^2 + \sigma_v^2)s/2), \tag{A19}$$

which is the Laplace transform of a normal distribution with mean $w_o = u_o + v_o$ and variance $\sigma_w^2 = \sigma_u^2 + \sigma_v^2$. For the present case $u=\ell n(x^p)$, $\sigma_u = ps_x$, with similar relations for v. This substitution proves the theorem. Theorem 2 can obviously be expanded to include random variates that are the products of any number of lognormal variates.

Appendix A

REFERENCES

1. J. Aitchison and J. A. C. Brown, The Lognormal Distribution, University Press, Cambridge, 1963.

2. W. Feller, An Introduction to Probability Theory and Its Applications, 2nd Edition, Volume 1, John Wiley and Sons, New York, 1957.

3. R. L. Mitchell, "Permanence of the Log-Normal Distribution," J. of Opt. Soc. Am., Vol. 58, p. 1267, September 1968.

4. A. E. Green and A. J. Bourne, Reliability Technology, Wiley-Interscience, London, 1972.

DISTRIBUTION LIST

DEPARTMENT OF DEFENSE

Defense Documentation Center
Cameron Station
12 cy ATTN: TC

Director
Defense Nuclear Agency
ATTN: TISI, Archives
ATTN: RATN
ATTN: SPTD, Major Skarupa
ATTN: STRA
3 cy ATTN: TITL, Tech. Library
ATTN: DDST
ATTN: SPAS
ATTN: SPSS

Commander
Field Command
Defense Nuclear Agency
ATTN: FCPR

Director
Interservice Nuclear Weapons School
ATTN: Document Control

Chief
Livermore Division, Field Command, DNA
Lawrence Livermore Laboratory
ATTN: FCPRL

Dir. of Defense Research & Engineering
Department of Defense
ATTN: S&SS (OS)

DEPARTMENT OF THE ARMY

Director
BMD Advanced Tech. Center
Huntsville Office
ATTN: ATC-T, Melvin T. Capps

Dep. Chief of Staff for Rsch. Dev. & Acq.
Department of the Army
ATTN: DAMA-CSM-N, LTC G. Ogden

Commander
Harry Diamond Laboratories
ATTN: DRXDO-NP, Francis N. Wimenitz
ATTN: DRXDO-TI, Tech. Lib.
ATTN: DRXDO-NP, Jim Gwaltney

Commander
Picatinny Arsenal
ATTN: Technical Library

Director
US Army Ballistic Rsch. Labs.
ATTN: DRXBR-TE, John Keefer
ATTN: DRXBR-TE, William Taylor

Deputy Commander
US Army Nuclear Agency
ATTN: MONA-WE, COL Arthur Deverill

DEPARTMENT OF THE NAVY

Superintendent (Code 1424)
Naval Postgraduate School
ATTN: Code 2124, Tech. Rpts. Librarian

Officer-in-Charge
Naval Surface Weapons Center
ATTN: Code WA501, Navy Nuc. Prgms. Off.

DEPARTMENT OF THE AIR FORCE

AF Weapons Laboratory, AFSC
ATTN: SUL

Hq. USAF/RD
ATTN: RDQSM

ENERGY RESEARCH & DEVELOPMENT ADMINISTRATION

University of California
Lawrence Livermore Laboratory
ATTN: Tech. Info. Dept. L-3

Los Alamos Scientific Laboratory
ATTN: Doc. Con. for Reports Lib.

Sandia Laboratories
ATTN: Doc. Con. for 3141, Sandia Rpt. Coll.

DEPARTMENT OF DEFENSE CONTRACTORS

General Electric Company
TEMPO-Center for Advanced Studies
ATTN: DASIAC

R & D Associates
ATTN: Cyrus P. Knowles
ATTN: Technical Library

Science Applications, Inc.
ATTN: R. I. Miller

Science Applications, Inc.
ATTN: William Layson
ATTN: J. E. Cockayne
ATTN: E. V. Lofgren

Systems, Science & Software, Inc.
ATTN: Charles R. Dismukes

Science Applications, Inc.
ATTN: Duane Hove

Kaman Sciences Corp.
ATTN: Dan Sachs

SRI International
ATTN: George Abrahamson

TRW Defense & Space Sys. Group
ATTN: Tech. Lib.